2014

Synthesis of biologically active polycyclic natural products and multifunctional imaging probes

Tezcan Guney
Iowa State University

Synthesis of biologically active polycyclic natural products and multifunctional imaging probes

by

Tezcan Guney

A dissertation submitted to the graduate faculty

in partial fulfillment of the requirements for the degree of

DOCTOR OF PHILOSOPHY

Major: Organic Chemistry

Program of Study Committee:
George A. Kraus, Major Professor
Aaron D. Sadow
Emily A. Smith
Arthur H. Winter
Yan Zhao

Iowa State University

Ames, Iowa

2014

In memory of my grandfather,

Mehmet Güney

TABLE OF CONTENTS

LIST OF ABBREVIATIONS

Å	angstrom
Ac	acetyl
APCI	atmospheric-pressure chemical ionization
aq.	aqueous
Ar	aryl
BINAP	2,2′-bis(diphenylphosphino)-1,1′-binaphthalene
Bn	benzyl
BODIPY	boron dipyrromethene
^{o}C	degrees centigrade
calcd	calculated
Cbz	benzyloxycarbonyl
CDC	cell division cycle
CDy1	compound of designation yellow 1
Cy	cyanine
δ	NMR chemical shift in ppm downfield from tetramethylsilane
d	doublet
DBU	1,8-diazabicyclo[5.4.0]undec-7-ene
DCM	dichloromethane
dd	doublet of doublets
ddd	doublet of doublet of doublets

DMF	*N*,*N*-dimethylformamide
dt	doublet of triplets
EI	electron ionization
equiv	equivalent
ESI	electrospray ionization
Et	ethyl
Et_3N	triethylamine
g	gram
GC/MS	gas chromatography/mass spectrometry
h	hour
HRMS	high-resolution mass spectrometry
IC_{50}	50% inhibitory concentration
J	coupling constant
L	liter
LDA	lithium diisopropylamide
LiTMP	lithium tetramethylpiperidide
µ	micron
M	molarity
m	multiplet
m-CPBA	*meta*-chloroperoxybenzoic acid
Me	methyl
MeCN	acetonitrile

$MeNO_2$	nitromethane
mg	milligram
MHz	megahertz
min	minute
mL	milliliter
MMPP	magnesium monoperoxyphthalate hexahydrate
mm	millimeter
mmol	millimole
mol %	mole percent
MOM	methoxymethyl
m.p.	melting point
Ms	methanesulfonyl
n-Bu	normal butyl
NCS	*N*-chlorosuccinimide
NMR	nuclear magnetic resonance
OTf	trifluoromethanesulfonate
p	para
PCC	pyridinium chlorochromate
Ph	phenyl
pH	$-\log_{10} H^+$ concentration
ppm	parts per million
py	pyridine

q	quartet
quant.	quantitative
rac	racemic
R_f	retention factor
RNA	ribonucleic acid
s	singlet
sat.	saturated
t	triplet
TBAF	tetrabutylammonium fluoride
TBS	*tert*-butyldimethlsilyl
t-BuOK	potassium *tert*-butoxide
Tf_2O	trifluoromethanesulfonic anhydride
THF	tetrahydrofuran
TIPS	triisopropylsilyl
TLC	thin-layer chromatography
TMS	trimethylsilyl
TOF	time of flight
Ts	toluenesulfonyl
UV	ultraviolet

ACKNOWLEDGMENTS

I would like to express my sincere gratefulness to Professor George Kraus for his continuous support and encouragement throughout my graduate education, and for sharing his immense wisdom in synthetic organic chemistry. I have always felt very privileged to work with him as he provided many great opportunities to build the essential skills that I needed to move onto the next stage of my career as a scientist. I will always remember his love and passion for chemistry, creativity in problem solving, and fairness in leadership, all of which he has instilled in me.

In addition, I would like to thank my program of study committee members: Professors Aaron Sadow, Emily Smith, Arthur Winter, and Yan Zhao for their guidance and helpful suggestions. I appreciate the discussions with other knowledgeable faculty members at Iowa State University, especially Professors Jason Chen, Richard Larock, and Thomas Barton. I have enjoyed the collaborative research opportunities I have had with Professor Marit Nilsen-Hamilton and Dr. Bahram Parvin.

I thank former and present Kraus group members for their support; in particular, I am very thankful to my colleague Jennifer Lee, whom I have very much enjoyed working with and having valuable discussions on a regular basis. Her contributions to the carbazole project both at the design and execution stages of the experiments were very critical in the rapid completion and publication of the impactful work.

I am very grateful to the Department of Chemistry and the NSF-funded Center for Biorenewable Chemicals at Iowa State University for providing partial financial support

during my graduate studies; especially the former for awarding me the 2013 Noble Hines Endowed Graduate Fellowship. I would also like to genuinely acknowledge the Society of Chemical Industry for awarding me the 2013 Perkin Medal Scholarship.

My graduate research would not have been completed had the instrumentation facility not been run and maintained by the very knowledgeable and helpful team of Drs. Kamel Harrata, David Scott, Shu Xu, Sarah Cady, and Steve Veysey.

There are a few other extremely special and inspiring individuals in my life that provided unwavering support, motivation and encouragement since the beginning of my undergraduate days. Foremost among these are Professor H. Riza Guven and Ms. Asuman Guven. I will be forever grateful to them. I am also very thankful to have received training as an undergraduate by two great mentors, Professor Mehmet Kandaz and Professor Erol Ercag, as they further nurtured my interest in chemistry research.

I would like to express my thanks to many friends from my hometown Buyukada, Sakarya University, especially Emre Taner, and the US for all their support. I owe special gratitude to very generous and wonderful friends from Los Angeles: Deniz, Panos, and their bright children (Constantin, Ada, and Olympia), Banu, Ece, and Robert (Bob) for their extremely warm welcome and their immense support for my smooth transition to the US.

Finally, I am deeply indebted to my parents, Tuncay and Hatice and my brother Burak, and my extended family who have always been proud of me and fully supported my career decisions, even though I had to spend many years away from them. They have contributed so much to help me become who I am today and I will never forget their sacrifices for my education.

ABSTRACT

Natural products with their ever-growing potential applications in the drug discovery process have influenced many researchers to devise flexible and concise synthetic strategies towards these biologically active substances. As more complex and structurally unique natural products are isolated from plants or microorganisms, developing innovative synthetic tools become highly desirable to obtain them in sufficient quantities. Synthetic organic chemistry allows a thorough investigation of their biological properties and the endeavor enhances the dynamic evolution process of the field. With this in mind, we have developed new synthetic methodologies to synthesize meroterpenoid paracaseolide A and an important class of 3-methylcarbazole alkaloids. In addition, the same approach enabled a direct synthesis of fluorescent rosamine probes with practical applications.

The first chapter of the dissertation describes the total synthesis of potential anti-cancer agent (±)-paracaseolide A, which possesses a unique tetracyclic framework with concave and convex faces. The facile synthesis of the natural product was accomplished in 8 steps in 6.6% overall yield, utilizing multiple sulfoxide eliminations and a key tandem 1,4-conjugate addition/aldol reaction to introduce the necessary functional groups onto the tetracyclic bis-lactone scaffold. The synthetic strategy allows diverse analogue development through a common advanced intermediate.

The second chapter reveals a novel inverse electron-demand Diels–Alder (IEDDA) methodology to access biologically active and naturally-occurring 3-methylcarbazoles as

well as synthetic derivatives using 3-chloroindoles and the 2-pyrone methyl coumalate. The transformation constitutes the first successful example of its kind; consequently extending the scope of indole dienophiles in the IEDDA reactions. The application of the single-pot Diels–Alder/decarboxylation/elimination domino sequence resulted in the metal-free generation of carbazole alkaloids with exclusive regioselectivity in up to 90% yield.

The last chapter focuses on the synthesis of rosamine probes to capitalize on a new strategy of an organolithium addition to a benzophenone imine-substituted xanthone. Subsequent acid-catalyzed deprotection and dehydration resulted in an efficient four-step synthesis from 3,6-dihydroxyxanthone. The condensed synthetic approach provides rapid access to desirable primary amine-functionalized multifunctional rosamine analogues in good yields for applications in live-cell imaging.

CHAPTER 1.

TOTAL SYNTHESIS OF (±)-PARACASEOLIDE A[†]

1.1. Introduction

Natural products, mainly produced by plants and microorganisms, have played a vital role in providing a wide spectrum of therapeutics for the treatment and prevention of many diseases.[1] Terpenoids are not only the largest family of natural products with approximately 40,000 reported structures[2], but they also perhaps offer some of the most difficult synthetic challenges for organic chemists to overcome.[3] Structurally diverse and rare terpenoids are continually isolated from nature; as a result, advancements in synthetic organic chemistry to access these biologically-active targets are desired in order to build an extensive structure-activity relationship database.[4]

One unique subset of terpenoids that are formed through mixed biosynthetic pathways is called "meroterpenoids" (partial terpenoids)[5] has become one of the most promising source of lead drug candidates in medicinal research today.[6] These hybrid natural products contain both terpenoid and non-terpenoid components, and are mainly classified as polyketide–terpenoids and non-polyketide–terpenoids.[7] A few prominent examples of the polyketide-derived meroterpenoids include pyripyropene A (**1**)[8], the strongest known cholesterol-lowering natural product to date, territrem B (**2**)[9], a promising

[†] Adapted with permission from Guney, T.; Kraus, G. A., *Org. Lett.* **2013**, *15*, 613-615. Copyright © 2013 American Chemical Society.

lead drug candidate for the treatment of Alzheimer's disease, and anticancer agent tropolactone B (**3**)[10] as shown in Figure 1.

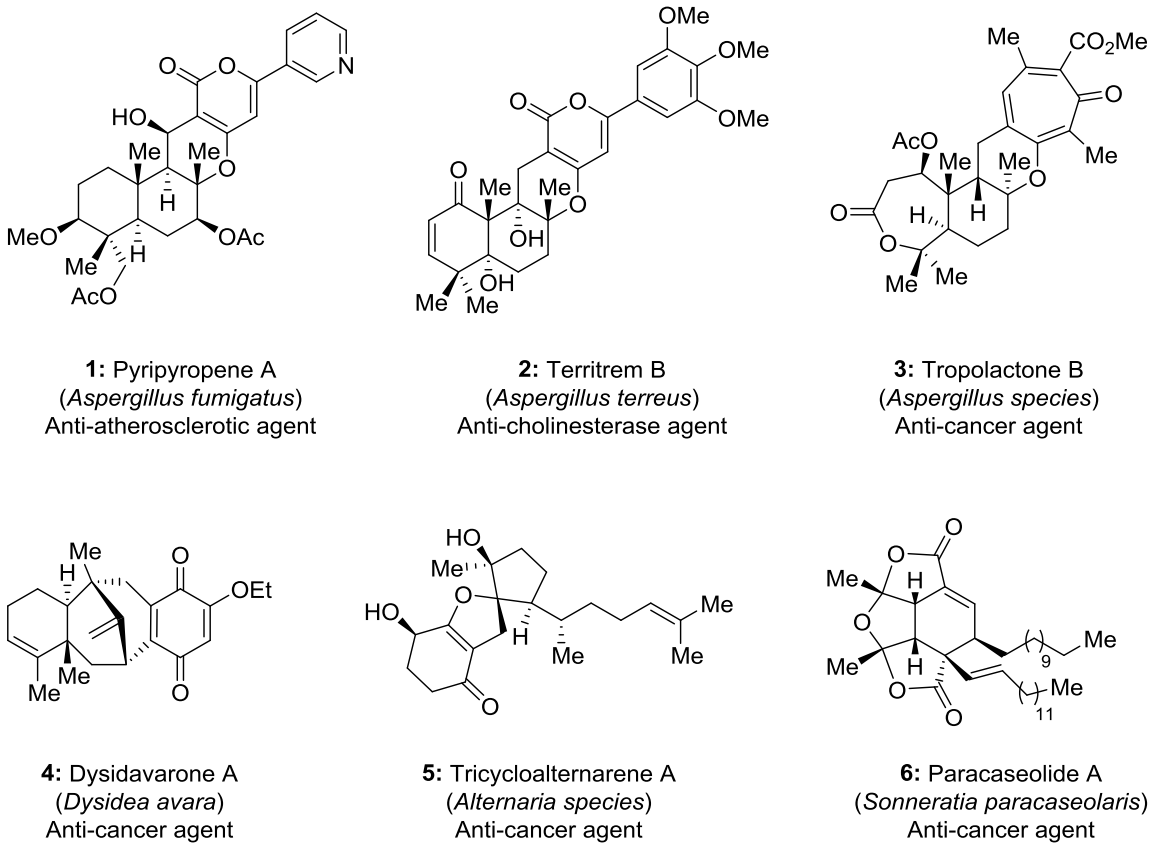

Figure 1. Representative meroterpenoids and their biological activities.

In addition, architecturally diverse non-polyketide meroterpenoids such as dysidavarone A (**4**)[11], tricycloalternarene A (**5**)[12], and paracaseolide A (**6**)[13] similarly display anti-cancer activities (Figure 1). Although these natural materials potentially offer great value in treating human diseases, their scarce quantities often create problems obtaining sufficient amounts from biological sources. Moreover, these natural products

may not necessarily be the most active form of the structural framework to exhibit their biological activity. Thus, they frequently require functional group modifications to achieve the optimal bioactivity.

Designing a diverted total synthesis strategy[14] to efficiently synthesize diverse natural product analogues would lead to a comprehensive bioactivity profile of the resultant derivatives. Ultimately, the compilation of the bioactivity would lead to overall insights on the mechanism of action at the cellular level.[15] Recognizing the critical need for synthetic campaigns to unlock the therapeutic potential of meroterpenoids, synthetic chemists have devised creative strategies and tactics in their total syntheses.[16] Developing routes to some of the formidable targets prompted both the development of novel synthetic methods and the expansion of the chemical synthesis toolbox. With this in mind, we focused our studies on crafting a novel platform strategy for the synthesis of paracaseolide A (**6**).

Paracaseolide A (**6**) was isolated from the stem bark of a Chinese mangrove plant *Sonneratia paracaseolaris* by Guo and co-workers in 2011.[13] Their thorough structure elucidation revealed a unique tetracyclic molecular architecture. They postulated that the distinct tetraquinane oxa-cage bislactone system conceivably originated from a Diels–Alder [4+2] dimerization of an α-alkylbutenolide (Scheme 1).

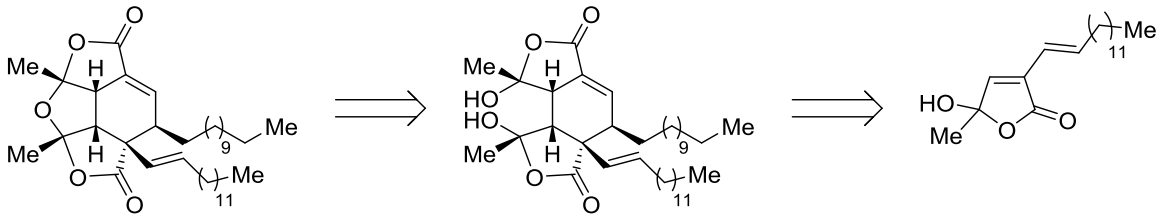

6 **7** **8**

Scheme 1. Proposed retrosynthetic pathway for paracaseolide A (**6**) by Guo.[13]

The α-alkylbutenolide structural motif is expressed in a range of natural products that reflects the moiety's wide range of therapeutic activities as represented in an antimicrobial substance ancepsenolide (**9**)[17], an effective antitumor agent annomolon A (**10**)[18], an anti-leukemic and neuroprotective terpenoid pinusolide (**11**)[19], and an anti-malarial agent gomphostinin (**12**)[20] (Figure 2).

Not surprisingly, paracaseolide A (**6**), the first known example of an α-alkylbutenolide dimer, was also proven to be an active substance. It showed significant inhibitory activity against dual specificity phosphates CDC25B with an IC_{50} value of 6.44 μM. Cell division cycle 25 (CDC25) phosphatases serve as key regulators of cell cycle progression.[21] Recent studies showed the involvement of CDC25A and B in various human cancer lines such as breast[22] and prostate[23] cancer associated with tumor aggressiveness and poor prognosis.

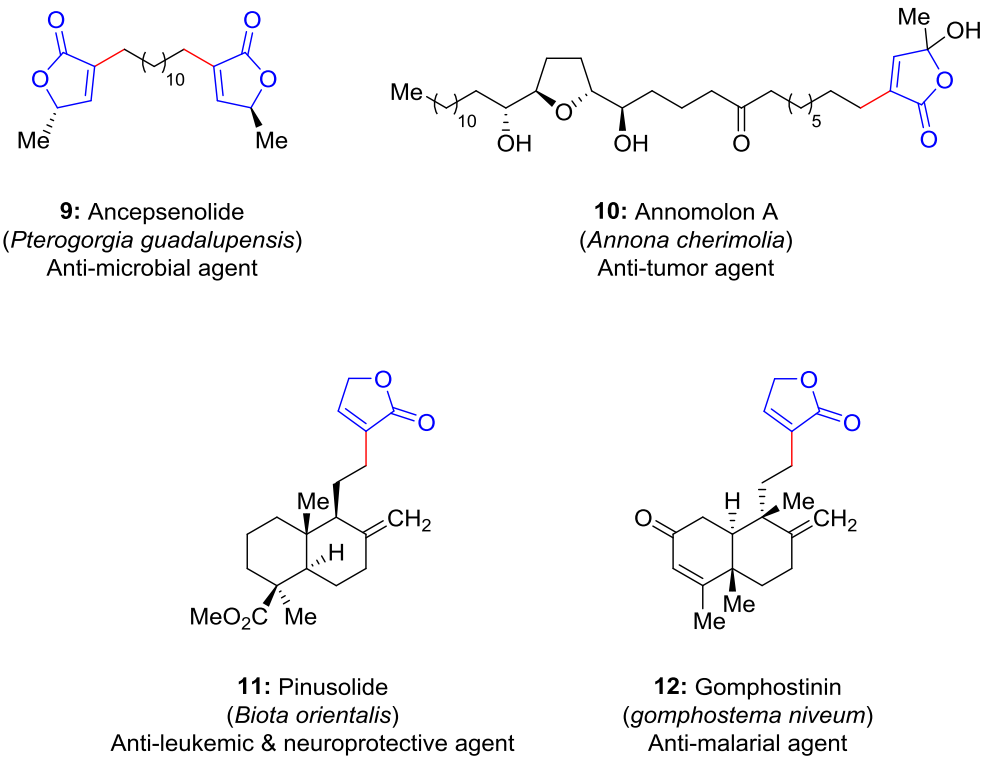

Figure 2. Representative α-alkylbutenolides and their biological activities.

Given the importance of inhibiting the cell cycle regulatory enzymes that are linked to carcinogenesis, many efforts have been devoted to the total synthesis of **6** and its potential analogues. The Vassilikogiannakis group[24] was the first to successfully tackle the synthetic problem. In agreement with the initially proposed biosynthetic pathway[13], they set out to accomplishing a Diels–Alder-dimerization of the α-alkenyl-γ-hydroxybutenolide **8** to access the tetracyclic core of **6**. It was predicted that the concerted [4+2] cycloaddition would generate the diastereomer of paracaseolide A (**14**), which would be readily epimerized to **6** since having both alkyl chains on the convex face of the molecule would be thermodynamically more stable as shown in Scheme 2.

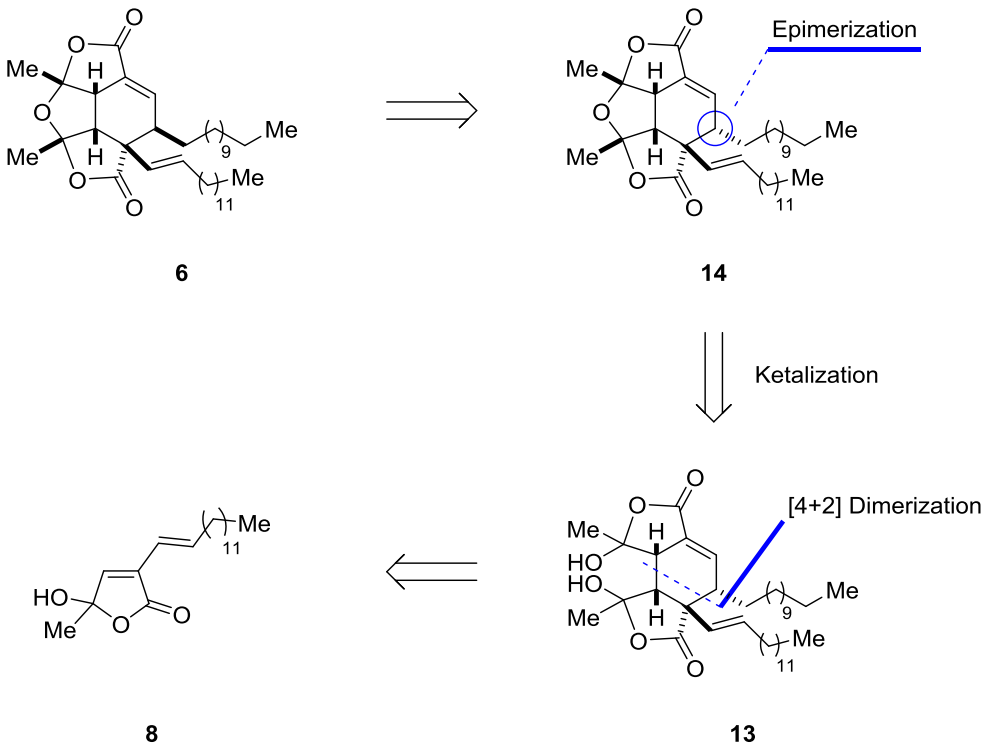

Scheme 2. Retrosynthetic analysis of paracaseolide A (**6**) by Vassilikogiannakis. [24]

Vassilikogiannakis's synthesis started by transforming readily available 1-tridecanol (**15**) to the corresponding iodide **16**, which was then lithiated and combined with 3-furaldehyde to form furanol **17** in 96% yield. The resulting hydroxyl group was then TBS protected under standard reaction conditions, furnishing silyloxyalkylfuran **18** in 84% yield. [1,4] O→C silyl migration upon treatment of **18** with *n*-BuLi was smoothly achieved, producing 2-trialkylsilyl-3-(α-hydroxy)alkylfuran **19** in 96% yield. Acid-catalyzed dehydration of **19** followed by methylation of the furan gave the photooxygenation precursor **21** in 65% yield. Regioselective oxidation of the furan with singlet oxygen ($^1O_2$) was aided by the TBS group to afford **8** in 52% yield.

Lastly, the key step involving their hypothesized bio-inspired Diels–Alder-dimerization/ketalization occurred under thermal conditions and in the absence of solvent in 59% yield, to provide **6** (Scheme 3). In summary, the first synthetic approach described by Vassilikogiannakis and his colleague featured a bio-inspired cycloadditive dimerization strategy to form paracaseolide A in 8 steps with 15% overall yield.[24]

Although this creative synthetic method efficiently provides access to the natural product, it still could benefit from improvements in several dimensions. Primarily, given the potentially significant anti-cancer activity of the natural product, a diversity-oriented synthetic approach would be useful for analogue development. Lacking the diversification platform, at least 7 steps to must be carried out to reach the desired α-alkenyl-γ-hydroxybutenolide before its crucial dimerization to generate a single tetracyclic analogue of the natural substance. In addition, as outlined in their manuscript, the key dimerization reaction required in solvent-free conditions at high temperature. This might be another potential disadvantage if temperature-sensitive functional groups were incorporated on the skeleton of paracaseolide derivatives. Therefore, we developed a novel diverted total synthesis of paracaseolide A to address the raised concerns.[25]

Even though we reported the second synthesis of the aforementioned natural product (in a strategically different way) a few months after the appearance of the initial synthesis in the literature, paracaseolide A has since been attracted many synthetic groups around the globe. Thus, a summary of recent reported paracaseolide A syntheses will preface the discussion of our unique methodology to the target.

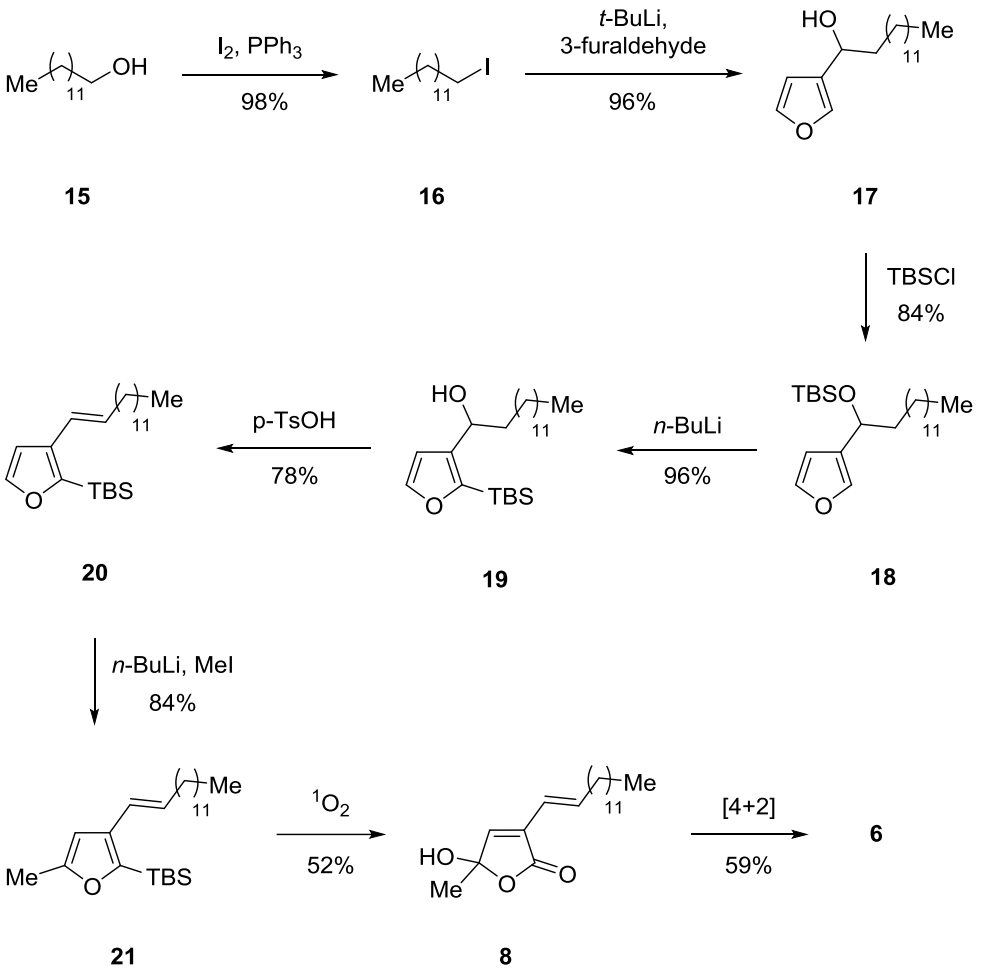

Scheme 3. Synthesis of paracaseolide A (**6**) by Vassilikogiannakis.[24]

In 2013, Mehta[26] and his colleagues reported a very similar synthetic plan for paracaseolide A *via* the presumed biomimetic pathway described by Guo and co-workers.[13] In my view, their contribution not only shortened the number of steps to butenolide **8**, but they also elucidated the dimerization mechanism. In contrast to Vassilikogiannakis's[24] proposed concerted cycloaddition mechanism which was outlined in Scheme 2, Mehta's experimental results showed that the thermally-induced dimerization produced the

diastereomers of paracaseolide A (**6** and **14**) and a ring-opening by-product in a ratio of 4.9:1:2.4 with 66% yield under essentially the same conditions as previously reported. Prolonging the thermal activation did not result in the interconversion of the diastereomers. Moreover, dimerization of an analogous butenolide **22** generated non-interconvertible diastereomers of tetracyclic analogues **23** and **24** in a ratio of 2:3 in 52% yield presented in Scheme 4. They concluded that the dimerization route may involve a step-wise [4+2] mechanism, rather than a concerted one, which essentially contradicts Vassilikogiannakis's observations.[24]

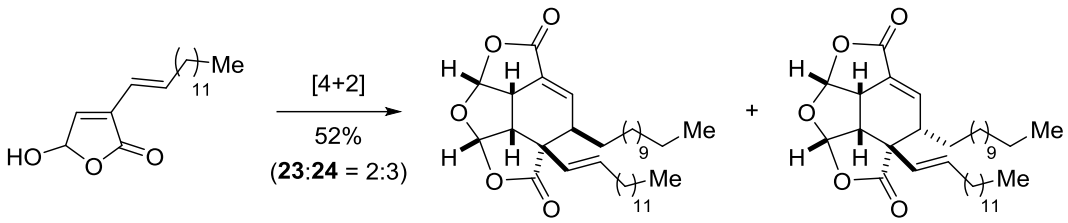

Scheme 4. Non-interconvertible diastereomeric paracaseolide analogues **23** and **24**.[26]

Subsequently, Stark and his co-workers[27] posed an interesting hypothesis to investigate the possibility of an early step ketalization reaction of an α-alkenyl-γ-hydroxybutenolide followed by a subsequent intramolecular Diels–Alder reaction under Lewis acidic conditions. On the way to test their idea, they also improved the synthesis of the common butenolide intermediate **8**, accessing it *via* a 4-step sequence. As outlined in Scheme 5, α-angelica lactone **25** was first acyloxylated using a catalytic amount of palladium acetate, sodium perborate and excess acetic anhydride to yield butenolide **26**. α-

Iodination of **26** was problematic; however, after many trials they were able to improve the yield of α-iodination to form **27**. Palladium-catalyzed Suzuki cross-coupling of **27** with vinyl boronic acid **28** provided **29**, which was then hydrolyzed under basic conditions giving access to butenolide **8** in good yield. Lewis acids such as Me_3Al, Me_2AlCl, $AlCl_3$, and $FeCl_3$ were employed but unfortunately did not promote the cycloaddition. Only the Lewis acids $ZnBr_2$ and $FeBr_3$ exclusively gave rise to the epimer **14** in 20% and 13% yields, respectively. Overall, they were able to synthesize paracaseolide A **6** in 5 steps with 25% yield, featuring the identical thermally-induced bio-inspired dimerization technology.

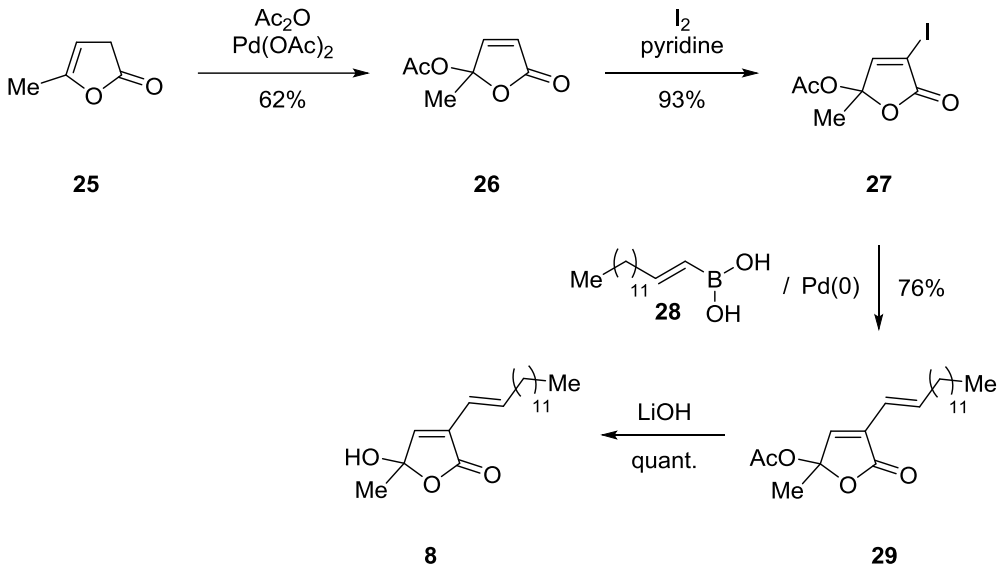

Scheme 5. Improved synthesis of α-alkenyl-γ-hydroxybutenolide **8** by Stark.[27]

The most recent synthesis of paracaseolide A to date was described by Boukouvalas et al. in 2014.[28] Even though their synthesis once again hinged on the pre-existent dimerization strategy, they uncovered a new route for the hydroxybutenolide **8** as shown in Scheme 6. They planned an aldol reaction between α-angelica lactone **25** and tetradecanal **30** mediated by dibutylboron triflate to afford butenolide **31** as a diastereomeric mixture. Crude **31** was dehydrated with the help of alumina in boiling pyridine to produce the dehydrobutenolide isomers **32** and **33** in 38% and 28% yield, respectively. The silylation of both isomers under their newly developed conditions successfully generated 2-silyloxyfuran **34** in excellent yield. The oxidation of **34** into silyl ketoester **35** was quantitatively occurred in the presence of dimethyldioxirane. The acid-catalyzed ring-closing of **35** furnished hydroxybutenolide **8** which was readily dimerized to the final product **6**.

To date, there are a total of five reports on the total synthesis of paracaseolide A (**6**) following its isolation. In contrast to our work[25], the other four research groups utilized Guo's proposal of [4+2] dimerization strategy as their key step. Following Vassilikogiannakis's 7-step butenolide **8** synthesis, other research groups became interested in improving the efficiency of the approach by shortening the route to the same butenolide building block.

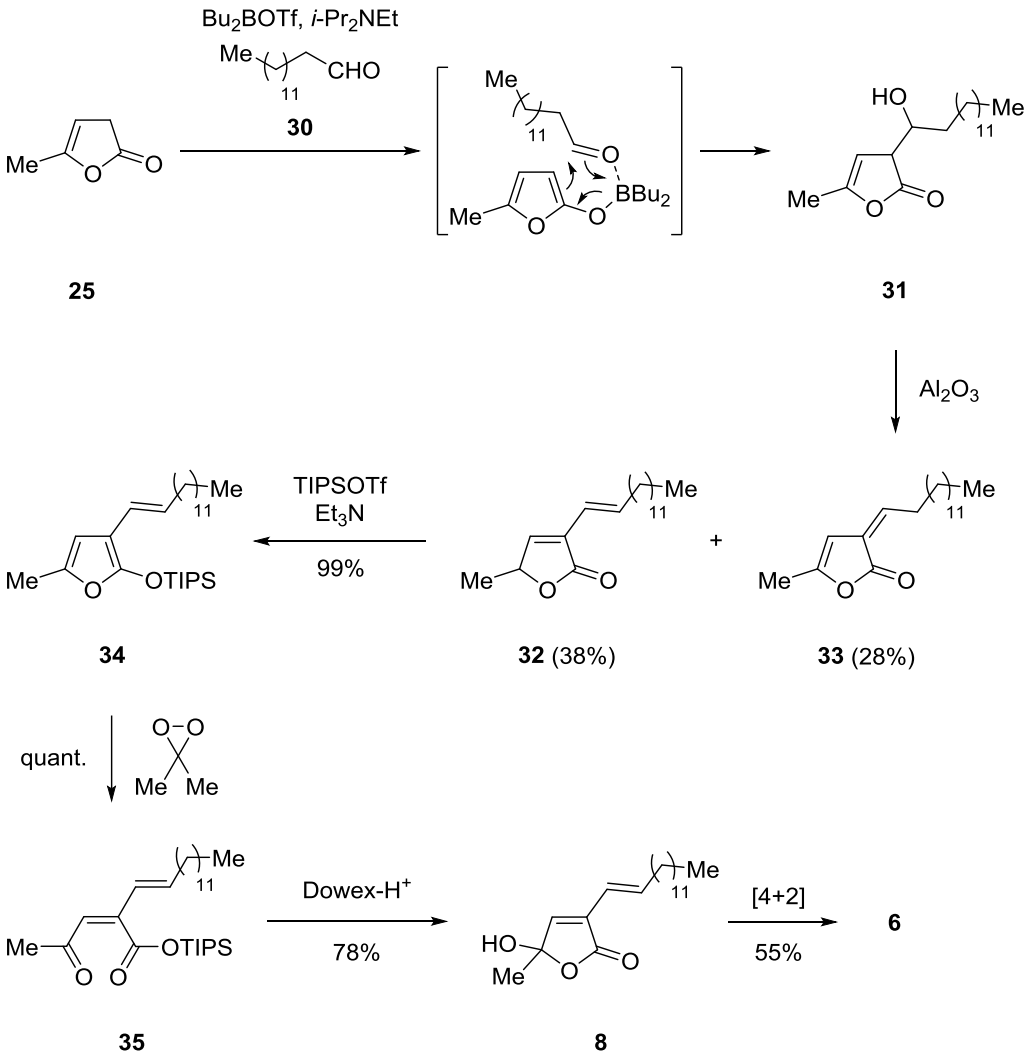

Scheme 6. Alternate synthesis of α-alkenyl-γ-hydroxybutenolide **8** by Boukouvalas.[28]

1.2. Results and Discussion

Recognizing its great therapeutic potential and impressed by its very unusual structural framework, paracaseolide A (**6**) attracted our attention as a synthetic challenge shortly after its discovery published by Guo and co-workers. After carefully analyzing the

three-dimensional fused ring system of the molecule, we constructed our strategy based on its concave and convex geometry to introduce the essential functional groups in a stereocontrolled fashion.

Our first generation retrosynthetic approach to natural product **6** proposed a last-step installation of the α,β-unsaturated lactone through a sulfoxide elimination from advanced intermediate **36**, which would be generated *via* a key vicinal difunctionalization methodology of the α,β-unsaturated lactone **37**. Accessing substrate of the conjugate addition **37** was predicted through the sequential sulfenylation, oxidation, and elimination reactions from tetracyclic symmetrical bislactone **38**. To our advantage, the synthesis of **38** was reported by Lin and Wu[29], employing a Diels–Alder reaction between the building blocks (*Z*)-3-hexene-2,5-dione **40** and 1,3-cylohexadiene **41** to provide the cycloaddition adduct **39**, followed by ozonolysis and oxidation as shown in Scheme 7.

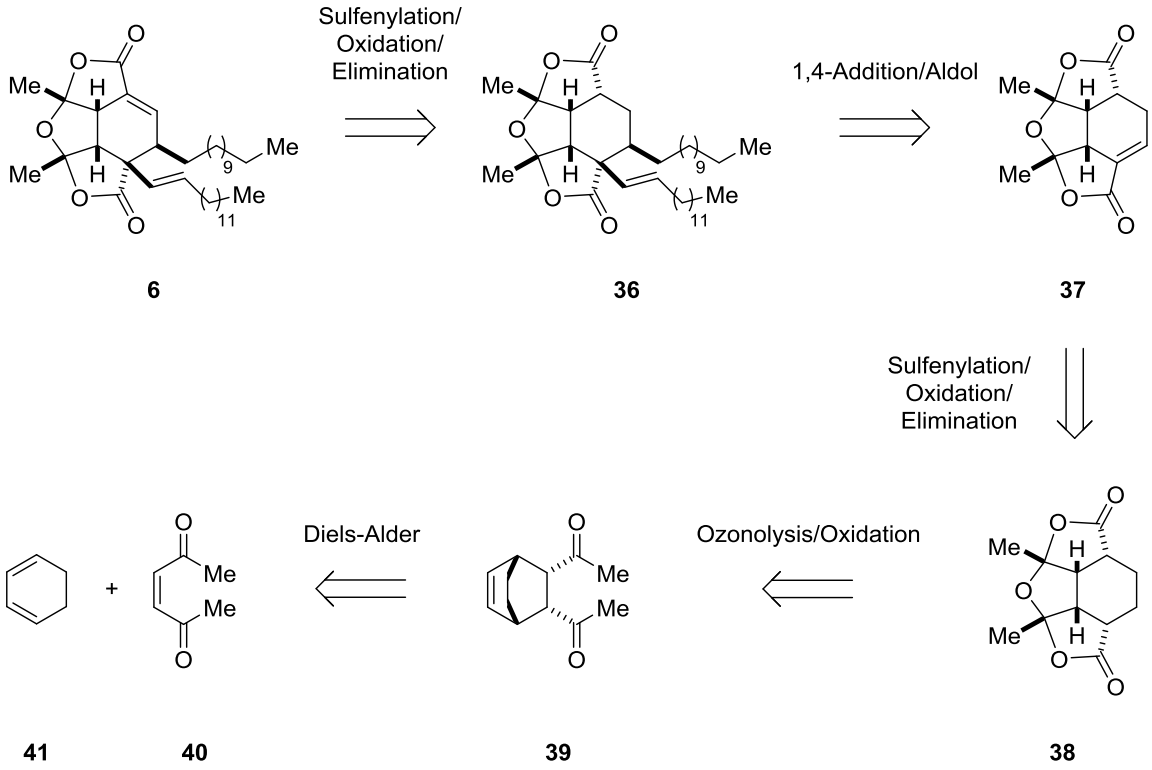

Scheme 7. First generation retrosynthetic analysis.

Our total synthesis began with the realization of tetracyclic core **38** (Scheme 8), utilizing the known method developed by Wu, who made many valuable contributions in synthesizing novel heterocyclic cage compounds. Diels–Alder reaction of the *cis*-enedione **40**, readily prepared by oxidation[30] of 2,5-dimethylfuran, and commercially available 1,3-cyclohexadiene **41** in a sealable tube at 100 ^{o}C in dichloromethane resulted in bicyclo[2.2.2]octene **39** in 75% yield. Subjecting purified **39** to ozonolysis in dichloromethane at -78 ^{o}C, followed by treatment with triethylamine provided tetracylic hemiacetal **42** in 36% yield. Subsequent PCC oxidation then furnished tetracyclic bislactone **38** in 75% yield.[29]

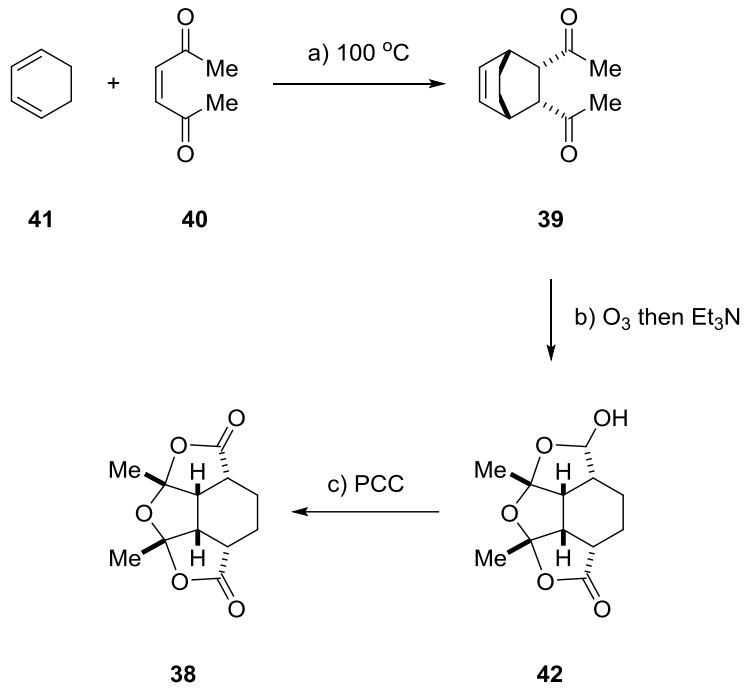

Scheme 8. Synthesis of tetracyclic symmetrical bislactone **38**[a].

[a] Reagents and conditions: a) CH_2Cl_2, 100 °C, 24 h, 75%; b) O_3, CH_2Cl_2, -78 °C, 40 min; then Et_3N (1.0 equiv), -78 °C to 23 °C, 3 h, 36%; c) PCC, CH_2Cl_2, 23 °C, 4 h, 75%.

With the core structure of paracaseolide A in hand, the stage was set for the α-functionalization of **38**. We envisaged a mono-sulfenylation followed by an oxidative elimination reaction to incorporate the unsaturation. To test the feasibility of the proposed idea, we first considered using a more simple electrophile such as methyl iodide for α-functionalization (Scheme 9). Contrary to our expectations, initial attempts to generate the key enolate intermediate **43** was problematic. The poor solubility of **38** in ethereal solvents was likely the main contributing factor to the unsuccessful results obtained with LDA, LiTMP and *t*-BuOK. Alternatively, formation of enol silyl ether of **38** in the presence of

TMSOTf gave complex product distribution observed by ^{1}H NMR, attributed to the decomposition of the silylated intermediate.

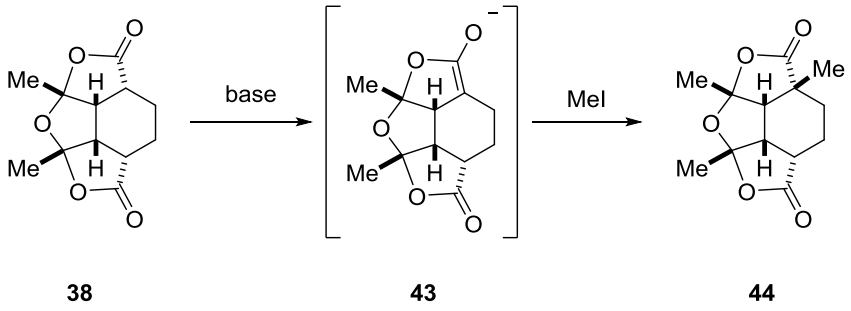

38 **43** **44**

Scheme 9. Model study towards α,β-unsaturated lactone *via* the enolate intermediate.

Pleasingly, after screening many polar organic solvents and compatible bases, we found conditions to access enolate **43** using sodium hydride (1.0 equiv) and DMF at 0 ^{o}C. Even though the newly developed conditions were very promising, careful examination of the ^{1}H NMR spectrum revealed that the obtained crude material was comprised primarily of the starting material **38** as shown in Scheme 10.

The most surprising phenomenon was that in the presence of one equivalent of methyl iodide, the doubly methylated product **45** occurred preferentially over the desired singly methylated product **44**. Changing the electrophile to the more reactive allyl iodide did not change the trend. The crude mixture contained starting material **38**, singly allylated product **46**, and fully allylated product **47** in a 3 : 1 : 1.5 ratio**.** The unexpected preferential reactivity pattern uncovered through the model study led us to reevaluate our synthetic strategy to paracaseolide A. Instead of spending time to optimize the reaction conditions

for single α-functionalization of **38**, we decided to postpone the desymmetrization operation by one step.

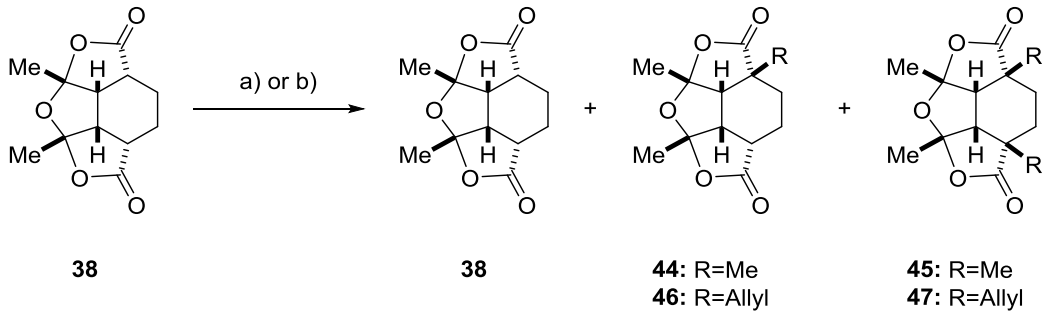

Scheme 10. Successful alkylations of **38** with sodium hydride in DMF[a,b].
[a] Reagents and conditions: a) NaH (1.0 equiv), MeI (1.1 equiv), DMF, 0 °C, 45 min, **38**:**44**:**45** = 26:1:23; b) NaH (1.0 equiv), allyl iodide (1.1 equiv), DMF, 0 °C, 45 min, **38**:**46**:**47** = 3:1:1.5. [b] Ratios determined by integration of crude ^{1}H NMR.

Our second generation approach entailed a final sulfoxide elimination to form the natural product **6**, which in turn was accessed from the sulfide intermediate **48**. Achieving subtarget **48** was envisioned *via* the key tandem 1,4-addition and aldol reaction from the α,β-unsaturated lactone **49**. Advantageously lactone **49** can potentially serve as a diversification platform which could be prepared through the mono-oxidation of a phenyl sulfide followed by elimination of the ensuing sulfoxide from the symmetrical bis-sulfide **50**. Desired building block **50** was proposed to arise by the double-sulfenylation of the tetracylic core **38,** as outlined in Scheme 11.

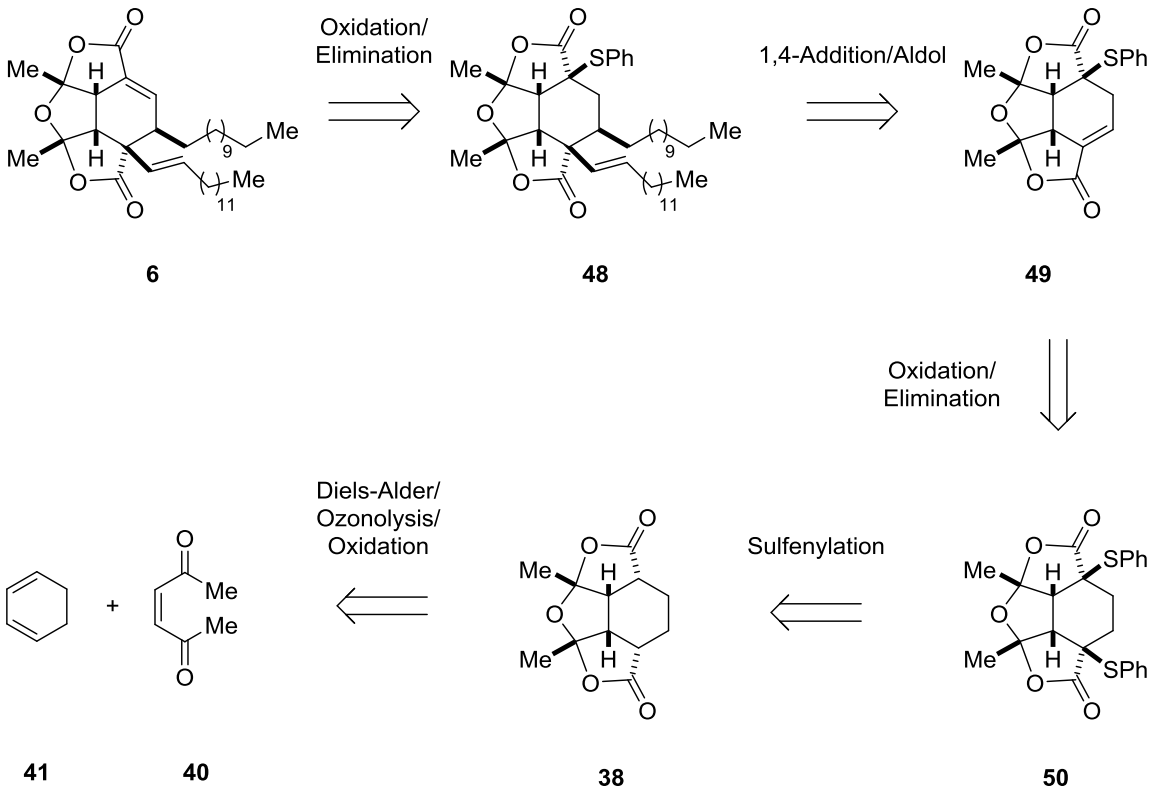

Scheme 11. Second generation retrosynthetic analysis.

Following the restructured retrosynthesis, the first synthetic subtarget bis-sulfide **38** was sulfenylated by the action of excess diphenyl disulfide in the presence of sodium hydride in DMF at 0 ^{o}C in excellent yield. Once bis-sulfide **50** was in hand, it was ready for the subsequent oxidation (Scheme 12).

Given the complexity of the substrate, we first utilized a milder oxidant, sodium periodate. Standard oxidation conditions[31] with this reagent only returned starting material, even after prolonging the reaction time. We then turned our attention to another oxidant, *m*-CPBA. Our first trial with this reagent was successful, but the reaction conditions needed to be optimized since over-oxidation of a single sulfide to sulfone could have

prevented the ensuing elimination. Fortunately, the single sulfide oxidation proceeded smoothly in the presence of one equivalent *m*-CPBA at room temperature, providing access to intermediate **51** as shown in Scheme 12.

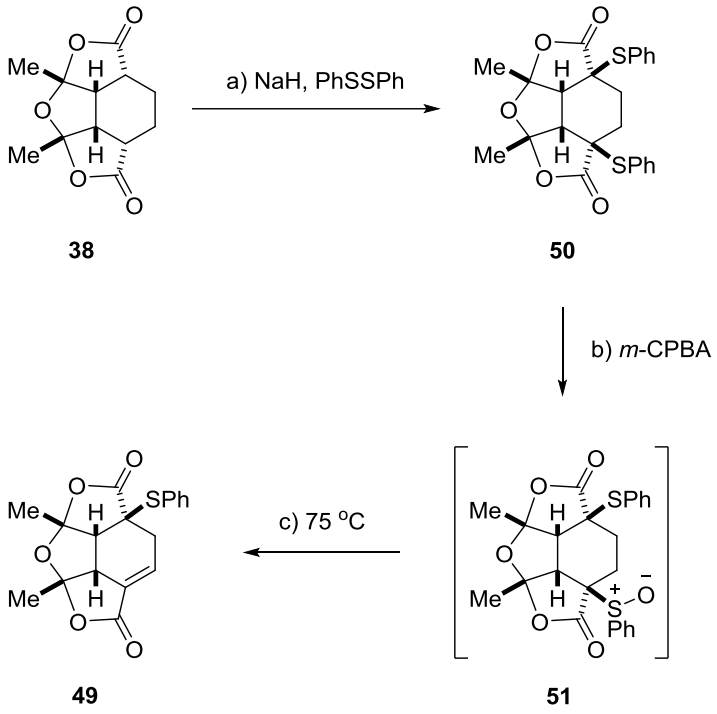

Scheme 12. Synthesis of α,β-unsaturated lactone **49**[a].
[a] Reagents and conditions: a) NaH (3.0 equiv), PhSSPh (3.0 equiv), CH_2Cl_2, 0 °C, 3 h, 92%; b) *m*-CPBA (1.15 equiv), CH_2Cl_2, rt, 2 h; c) $CHCl_3$, 75 °C, 5 min, 85%.

Initially, we intended to eliminate the sulfoxide in a separate step following its isolation, as the literature precedent suggested that elimination traditionally occurs under thermal conditions between 80 °C and 120 °C. Surprisingly, we found that the sulfoxide elimination was partially achieved at room temperature, observed by TLC and ^{1}H NMR. After observing the tendency of the resulting sulfoxide for elimination, we aimed to

combine the overall transformation into a one-pot procedure. Heating the sulfoxide after the workup at 75 °C for 5 min was sufficient to furnish **49** in 85% yield (Scheme 12).

We then set out to investigate the pivotal vicinal difunctionalization[32] strategy to construct the alkyl and alkenyl chain units of the natural product. Since copper-promoted conjugate additions of hydrocarbons to α,β-unsaturated carbonyl compounds are one of the most well-established reactions in organic chemistry, adopting the methodology as our key step would be a valuable avenue for diversification of the tetracyclic scaffold **49**.

We began by studying the conjugate addition of either stoichiometric or catalytic organocopper reagents to the α,β-unsaturated lactone **49** before combining the addition in a postulated tandem process with an aldol reaction. The viability of the key step was again tested on a model system. The conjugate addition of lithium dibutylcuprate (**52**), readily prepared from n-butyllithium (2.0 equiv) and copper iodide (1.0 equiv), smoothly provided access to Michael (1,4) adduct **53** in 86% yield as shown in Scheme 13.

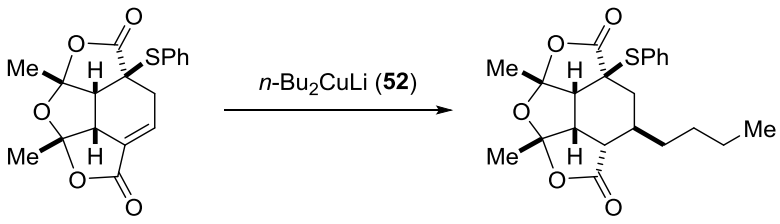

49 **53**

Scheme 13. 1,4-Addition of lithium dibutylcuprate to the α,β-unsaturated lactone **49**[a].
[a] Reagents and conditions: **49** (1.0 equiv), *n*-BuLi (2.4 equiv), CuI (1.2 equiv), THF, -78 °C, 1 h, 86%.

Although the conjugate addition of stoichiometric organocopper reagents was successfully demonstrated, the preparation of the requisite lithium dodecylcuprate was considered to be inconvenient. Moreover, decreasing the amount of copper salt usage would be beneficial in terms of the scale-up potential of the reaction. Thus, we focused our attention on the conjugate addition of readily available organomagnesium reagents in the presence of a catalytic amount of a copper salt. Treating the lactone **49** with dodecylmagnesium bromide (**54**) and copper(I) bromide dimethyl sulfide (12 mol %) through normal addition resulted in a complex mixture of products. The key to success in our system was the application of the inverse addition protocol as also utilized by other researchers.[33] Thereby, the addition of dodecylmagnesim bromide to the solution of **49** and the copper salt gave 1,4-adduct **55** in 92% yield (Scheme 14).

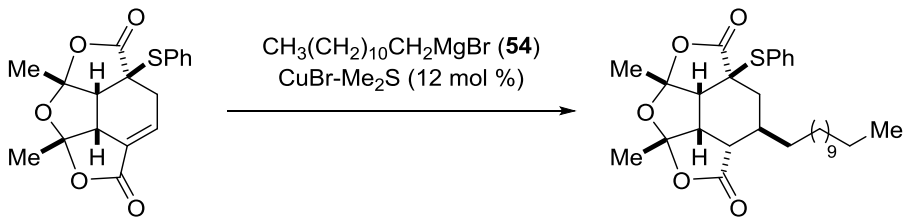

49 **55**

Scheme 14. 1,4-Addition of dodecylmagnesium bromide to the lactone **49**[a].
[a] Reagents and conditions: **49** (1.0 equiv), **54** (1.3 equiv, 1.0 M in Et_2O), CuBr-Me_2S (12 mol%), THF, -78 °C, 1 h, 92%.

Once the optimized conditions for the conjugate addition were in place, the stage was set for trapping the subsequent enolate with with tetradecanal (**56**)[34] in a tandem fashion. Cannulation of a freshly prepared solution of **56** into the solution of magnesium

enolate **57** at 0 ^{o}C yielded aldol product **58** in 72% yield as shown in Scheme 15. The dehydration of **58** was not as trivial as we expected to effect the one-pot measylation-elimination. Attempts with standard conditions employed excess triethylamine (10 equiv) at 0 ^{o}C followed by the addition of mesyl chloride (5 equiv) with subsequent heating at 40 ^{o}C in dichloromethane. The *trans*-olefin **48** resulted in 42% yield, along with a diastereomeric mixtures of mesylates. Furthermore, the ^{1}H NMR spectrum of the crude mixture indicated the presence of decomposition byproducts, which conceivably may have resulted from retro aldol reaction of **58** in basic media. After several trials, we found that the addition of Et_3N (4.0 equiv) and mesyl chloride (4.0 equiv) to the solution of **58** in dichloromethane at -78 ^{o}C was critically important to preclude byproduct formation. Prompting the elimination of the mesylates **59** by the action of DBU (4.0 equiv) at 80 ^{o}C in a single-pot process generated the *trans* olefin **48** in 65% yield.

The final transformation of the synthesis involved the second simultaneous sulfide oxidation and elimination reaction. Implementing the previously established *m*-CPBA conditions followed by the thermally induced sulfoxide elimination at 75 ^{o}C smoothly generated paracaseolide A (**6**) in 90% yield. The identity of **6** was in complete agreement with the isolated and synthetic natural product previously reported confirmed by the ^{1}H NMR, ^{13}C NMR, and mass spectral data. In summary, the total synthesis of **6** was accomplished in 8 steps and 6.6% overall yield.

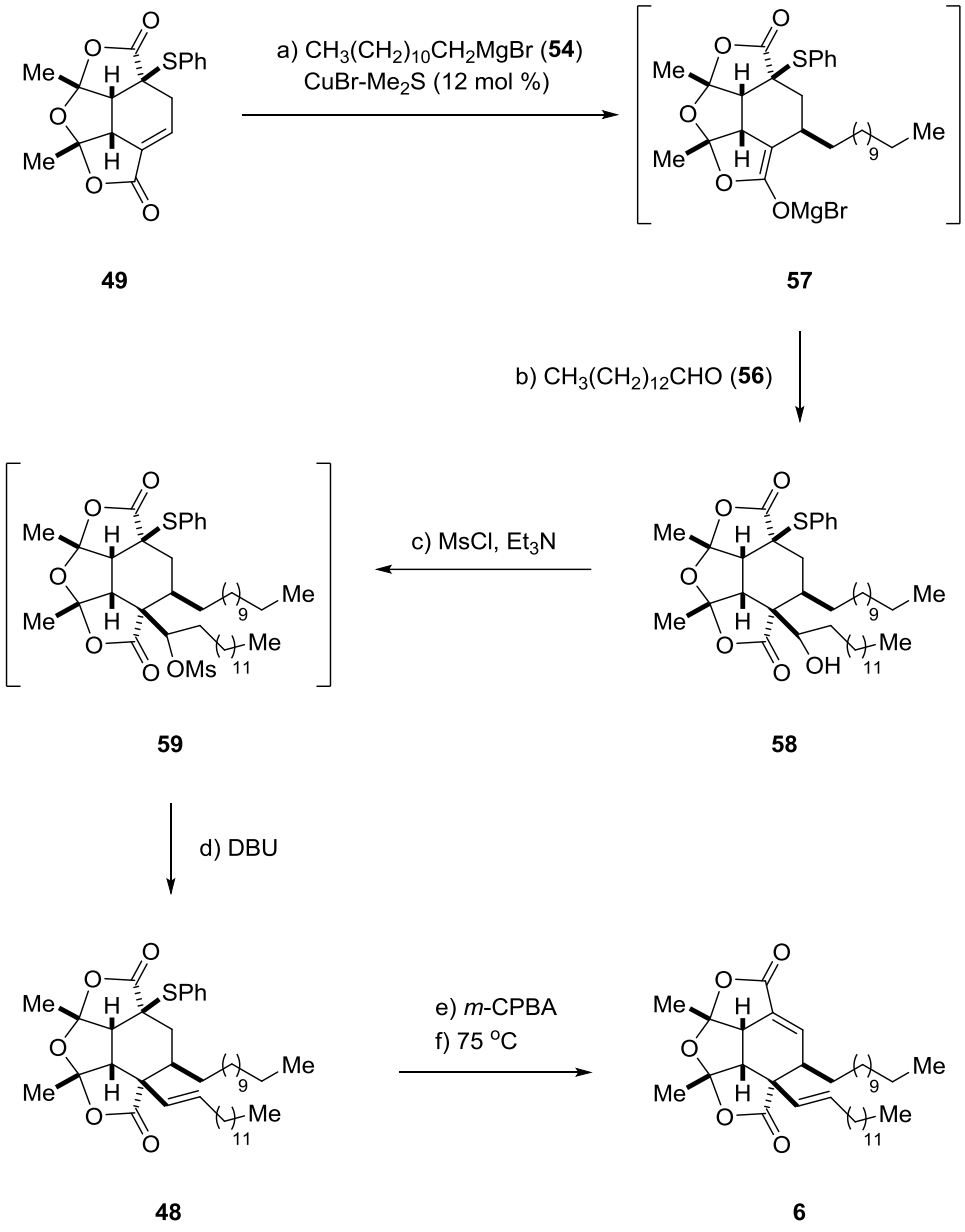

Scheme 15. Synthesis of paracaseolide A (**6**)[a].

[a] Reagents and conditions: a) **49** (1.0 equiv), **54** (1.3 equiv, 1.0 M in Et_2O), CuBr-Me_2S (12 mol%), THF, -78 °C, 1 h; b) **56** (5.0 equiv), 0 °C, 30 min, 72%; c) Et_3N (4.0 equiv), MsCl (4.0 equiv), CH_2Cl_2, -78 °C to 23 °C, 2 h; d) DBU (4.0 equiv), 80 °C, 8 h, 65%; e) *m*-CPBA (1.15 equiv), CH_2Cl_2, 23 °C, 2 h; f) $CHCl_3$, 75 °C, 5 min, 90%.

1.3. Conclusions

Upon its isolation from the bark of a Chinese mangrove plant *Sonneratia paracaseolaris* by Guo and co-workers in 2011, paracaseolide A (**6**) attracted our attention as a structurally unique and biologically valuable target. Our concise synthetic route to the natural product **6** hinged on a series of controlled sulfoxide eliminations from its tetracylic core framework and the key tandem 1,4-addition followed by the aldol reaction. Designing the synthetic steps to take advantage of the inherent reactivity patterns as well as recognizing the concave and convex geometry of the molecule to control the stereochemistry resulted in our direct realization of the target. Moreover, combining the transformations in single-pot procedures decreased the number of steps and avoided multiple purifications. Potential future work to further optimize the synthesis would involve the steps leading to Wu's tetracylic bislactone **38** to increase the overall yield of **6**.

Overall, in comparison to the four other synthetic approaches, all of which applied the same dimerization pathway to paracaseolide A, our synthesis is novel and still the only one that flexibly allows diverse functionalization of analogues rather than being specifically constrained to the target.

1.4. Experimental

General Procedures

All starting materials were purchased from Sigma-Aldrich; solvents were purchased from Fisher Scientific and used without further purification. Sodium hydride (60% in mineral oil) was purchased from TCI America. All reactions were carried out in flame-dried glassware under argon with dry solvents under anhydrous conditions. All yields refer to chromatographically isolated products. Reactions were monitored by thin-layer chromatography (TLC) carried out on 0.20 mm silica gel plates using UV light as a visualizing agent and either potassium permanganate or 5% sulfuric acid in methanol with heat as developing agents. Silica gel 60Å, particle size 0.032 – 0.063 mm, was used for flash column chromatography. Preparative thin-layer chromatography (PTLC) separations were carried out on 1.00 mm silica gel plates. ^{1}H and ^{13}C NMR spectra were acquired in $CDCl_3$ on a Varian MR-400 or Bruker Avance III 600 MHz spectrometer. ^{1}H and ^{13}C chemical shifts (δ) are given in ppm relative to the residual protonated chloroform peak ($CDCl_3$: $_{\delta}H$ = 7.26 ppm, $_{\delta}C$ = 77.0 ppm) as an internal reference. High-resolution mass spectra (HRMS) were recorded on an Agilent 6540 QTOF (quadrupole time of flight) mass spectrometer using ESI (electrospray ionization) or APCI (atmospheric-pressure chemical ionization). Melting points are uncorrected and were analyzed on a Melt-Temp II capillary melting point apparatus.

Selected Experimental, Physical, and Spectral Data

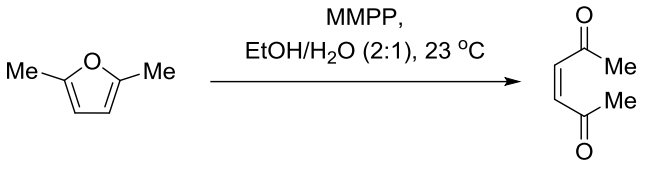

60 **40**

(*Z*)-3-hexene-2,5-dione (40).[30,35] To a solution of 2,5-dimethylfuran (5.00 g, 52.0 mmol) in EtOH (156 mL) at room temperature was added a solution of magnesium monoperoxyphthalate hexahydrate (MMPP, 80%, 16.1 g, 26.0 mmol) in water (78 mL), dropwise via addition funnel over 10 minutes. The resulting reaction mixture was stirred for 15 minutes at room temperature, monitored by TLC. The reaction was quenched by $NaHCO_3$ (sat. aq., 85 mL) and extracted with CH_2Cl_2 (4 x 50 mL). No peroxide was detected testing the solution with potassium iodide starch paper. The combined organic layers were then washed with brine (50 mL), dried over $MgSO_4$, and concentrated *in vacuo* to afford 5 (5.77 g, 99% yield) as a yellow liquid, which was used without purification. **40:** R_f = 0.40 (silica gel, EtOAc:hexanes 1:1); ^{1}H NMR ($CDCl_3$, 600 MHz) δ = 6.29 (s, 2H), 2.29 (s, 6H) ppm; ^{13}C NMR ($CDCl_3$, 150 MHz) δ = 200.4 (2C), 135.7 (2C), 29.8 (2C) ppm.

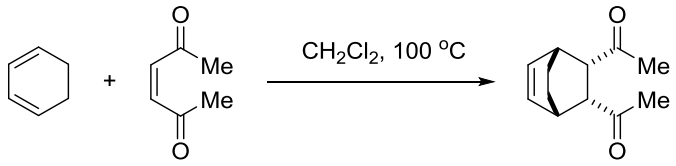

41 **40** **39**

Bicyclo[2.2.2]octene 39.[29] To a solution of **40** (5.00 g, 44.6 mmol) in CH_2Cl_2 (25 mL) in a sealable flask was added 1,3-cyclohexadiene (4.47 g, 55.75 mmol). After sealing the flask, the reaction mixture was heated to 100 °C for 24 h. The reaction mixture was first cooled to room temperature then concentrated *in vacuo* to afford the crude product, which was purified by flash column chromatography (silica gel, EtOAc:hexanes 0:1 to 1:2) to afford **39** (6.43 g, 75% yield) as a colorless crystalline solid. Subsequent larger scale reactions were conveniently purified by recrystallization from EtOAc:hexanes 1:2 and seeding the crude solution with pure crystals obtained from column chromatography. **8:** m.p. 56-57 °C; R_f = 0.20 (silica gel, EtOAc:hexanes 1:1); ^{1}H NMR ($CDCl_3$, 600 MHz) δ = 6.25 (dd, *J* = 4.6, 3.2 Hz, 2H), 3.06 (s, 2H), 2.94 (s, 2H), 2.07 (s, 6H), 1.60–1.55 (m, 2H), 1.37–1.30 (m, 2H) ppm; ^{13}C NMR ($CDCl_3$, 150 MHz) δ = 207.7 (2C), 132.3 (2C), 56.6 (2C), 32.5 (2C), 29.6 (2C), 25.0 (2C) ppm.

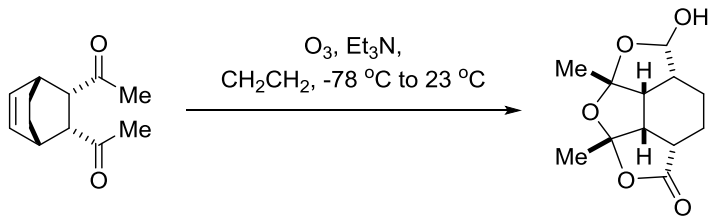

39 **42**

Oxa-cage tetraquinane 42.[29] To a solution of **39** (5.00 g, 26.0 mmol) in CH_2Cl_2 (200 mL) was bubbled O_3 at -78 °C. The solution turned blue in color after approximately 40 minutes after which Et_3N (2.63 g, 26.0 mmol) was added dropwise. The reaction mixture was slowly warmed to room temperature and stirred for an additional 3 hours. The reaction mixture was concentrated *in vacuo* and purified by flash chromatography (silica gel, EtOAc:hexanes 1:1 to 3:1) to afford **42** (2.25 g, 36% yield) as a white solid. **42:** R_f = 0.20 (silica gel, EtOAc:hexanes 3:1); ^{1}H NMR ($CDCl_3$, 600 MHz) δ = 5.21 (d, *J* = 4.4 Hz, 1H), 3.11 (s, 1H), 3.09–3.04 (m, 1H), 2.99 (t, *J* = 10.9 Hz, 1H), 2.77 (t, *J* = 10.9 Hz, 1H), 2.45–2.37 (m, 1H), 2.15–2.08 (m, 1H), 1.91–1.82 (m, 1H), 1.66 (s, 3H), 1.63 (s, 3H), 1.61–1.54 (m, 2H), 1.47–1.38 (m, 1H) ppm; ^{13}C NMR ($CDCl_3$, 150 MHz) δ = 176.7, 119.3, 116.1, 104.4, 44.8, 44.7, 41.8, 38.4, 27.3, 25.9, 19.7, 19.2 ppm.

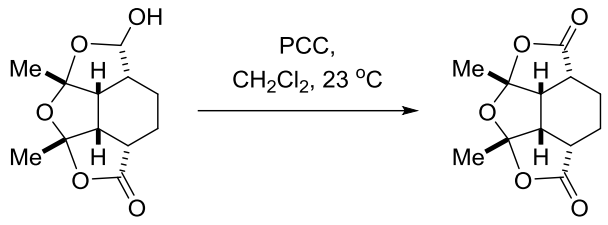

42 **38**

Bis-lactone 38.[29] To a solution of **42** (2.00 g, 8.32 mmol) in CH_2Cl_2 (120 mL) was added Celite (12.6 g) and pyridinium chlorochromate (3.59 g, 16.6 mmol) sequentially and the reaction mixture was stirred at room temperature for 4 hours. The reaction mixture was filtered through Celite, concentrated *in vacuo*, and purified by flash chromatography (silica gel, EtOAc:hexanes 1:1 to 3:1) to afford **38** (1.48 g, 75% yield) as a slightly brown-white solid. **38:** R_f = 0.10 (silica gel, EtOAc:hexanes 3:1); ^{1}H NMR ($CDCl_3$, 400 MHz) δ = 3.11 (s, 2H), 3.05–2.94 (m, 2H), 2.16–2.00 (m, 2H), 1.92–1.76 (m, 2H), 1.70 (s, 6H). ppm; ^{13}C NMR ($CDCl_3$, 150 MHz) δ = 175.1 (2C), 116.4 (2C), 43.6 (2C), 37.2 (2C), 24.8 (2C), 18.0 (2C) ppm.

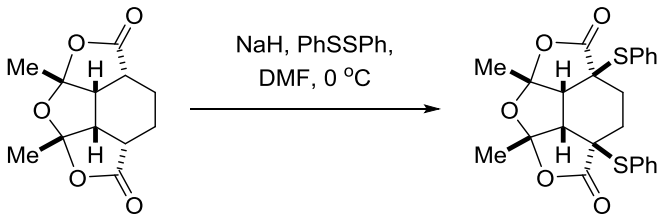

38 **50**

Bis-sulfide 50. To a suspension of NaH (0.17 g, 7.10 mmol) in DMF (4 mL) at 0 °C was added a solution of **38** (0.54 g, 2.27 mmol) in DMF (4 mL) dropwise over 5 minutes which was stirred for an additional 5 minutes. Diphenyl disulfide (1.55 g, 7.10 mmol) in DMF

(4 mL) was brought to 0 °C and added dropwise over 5 minutes to the sodium hydride solution. The resulting reaction mixture was stirred for 3 h at 0 °C, monitored by TLC. The reaction was quenched by ice-cold water (10 mL) and partitioned between EtOAc (100 mL). The organic layer was washed with water (4 x 40 mL) and brine (40 mL), dried over $MgSO_4$, and concentrated *in vacuo*. The crude product was purified by flash column chromatography (silica gel, EtOAc:hexanes 0:1 to 2:1) to afford **50** (0.95 g, 92% yield) as a white crystalline solid. **50:** m.p. 193-195 °C; R_f = 0.90 (silica gel, EtOAc:hexanes 3:1); ^{1}H NMR ($CDCl_3$, 600 MHz) δ = 7.57 (d, *J* = 7.1 Hz, 4H), 7.48 (t, *J* = 7.5 Hz, 2H), 7.40 (t, *J* = 7.6 Hz, 4H), 3.08 (s, 2H), 2.10–2.01 (m, 2H), 1.89–1.81 (m, 2H), 1.38 (s, 6H) ppm; ^{13}C NMR ($CDCl_3$, 150 MHz) δ = 173.5 (2C), 137.5 (4C), 130.9 (2C), 129.4 (4C), 128.7 (2C), 114.3 (2C), 53.1 (2C), 51.5 (2C), 28.1 (2C), 25.9 (2C) ppm; HRMS (APCI-TOF) calcd for $C_{24}H_{23}O_5S_2$ $[M + H]^+$ 455.0981, found 455.0982.

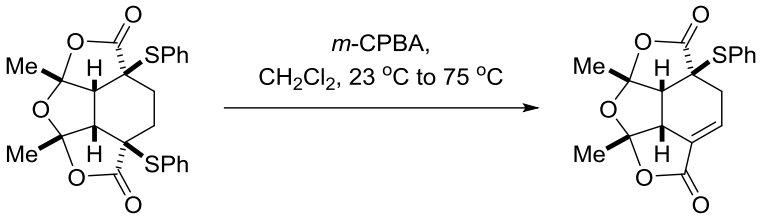

50 **49**

α,β-Unsaturated lactone 49. To a solution of bis-sulfide **50** (0.70 g, 1.54 mmol) in CH_2Cl_2 (60 mL) at room temperature was added a solution of *m*-CPBA (77%, 0.33 g, 1.77 mmol) in CH_2Cl_2 (60 mL), dropwise over 15 minutes. The reaction was monitored by TLC and after 2 h, the reaction was quenched by $NaHCO_3$ (sat. aq., 50 mL). The combined organic phases were washed with water (2 x 30 mL) and brine (30 mL), dried over $MgSO_4$, and

concentrated *in vacuo*. To complete the elimination of any remaining sulfoxide, anhydrous $CHCl_3$ (50 mL) was added and the heating bath on the rotary evaporator was maintained at 75 °C as the $CHCl_3$ slowly evaporated without vacuum for 5 minutes. The remaining $CHCl_3$ was concentrated *in vacuo*. The crude product was purified by flash column chromatography (silica gel, EtOAc:hexanes 1:2) to afford **49** (0.45 g, 85% yield) as a white crystalline solid. **49:** m.p. 145-146 °C; R_f = 0.50 (silica gel, EtOAc:hexanes 2:1); ^{1}H NMR ($CDCl_3$, 400 MHz) δ = 7.57 (d, *J* = 6.9 Hz, 2H), 7.50 (t, *J* = 7.4 Hz, 1H), 7.41 (t, *J* = 7.4 Hz, 2H), 6.96 (dt, *J* = 7.8, 3.5 Hz, 1H), 3.33 (dt, *J* = 9.7, 2.8 Hz, 1H), 3.28 (d, *J* = 9.7 Hz, 1H), 2.92 (dd, *J* = 15.0, 7.9 Hz, 1H), 2.36 (ddd, *J* = 15.1, 3.7, 2.5 Hz, 1H), 1.77 (s, 3H), 1.74 (s, 3H) ppm; ^{13}C NMR ($CDCl_3$, 150 MHz) δ = 172.2, 165.3, 137.8, 137.6 (2C), 131.51, 130.9, 129.3 (2C), 127.7, 114.5, 113.2, 56.2, 53.7, 47.3, 33.5, 26.9, 25.4 ppm; HRMS (APCI-TOF) calcd for $C_{18}H_{17}O_5S$ $[M + H]^+$ 345.0791, found 345.0792.

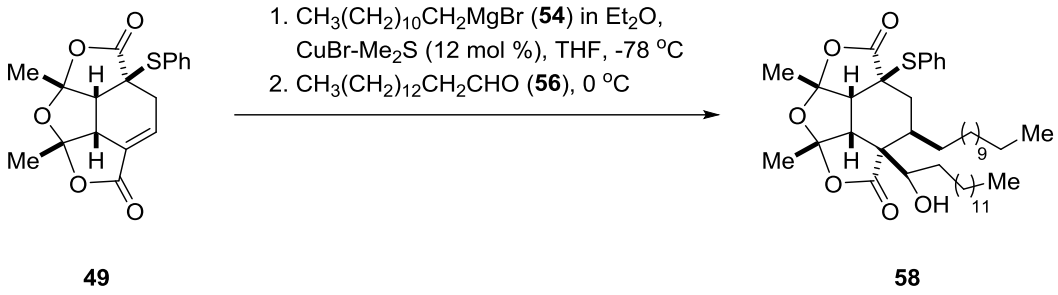

49 **58**

Alcohol 58. To a cloudy, pale yellow solution of α,β-unsaturated lactone **49** (250 mg, 0.73 mmol) and CuBr-Me_2S (24 mg, 0.11 mmol) in THF (25 mL) at -78 °C was added dodecyl magnesium bromide (1.0 M in Et_2O, 0.95 mL, 0.95 mmol) dropwise over 5 min, after which the solution became bright yellow-green in color. After 30 min, a TLC analysis showed complete consumption of starting material and formation of the 1,4-adduct. At

that time, the -78 °C bath was replaced by an ice bath and stirred for an additional 5 min. To the reaction mixture, an ice-cold solution of freshly prepared anhydrous tetradecanal[34] (775 mg, 3.65 mmol) in THF (10 mL) was transferred by cannula over 5 min, during which the reaction mixture changed from a cloudy yellow to a clear, pale yellow solution. Complete consumption of the 1,4-enolate intermediate and formation of the tandem aldol product as a single diastereomer was observed by TLC after 15-20 minutes. The reaction was quenched by slowly adding cold NH_4Cl solution (sat. aq., 10 mL) at 0 °C, during which time the solution became blue in color. The reaction mixture was poured into a separatory funnel, diluted with CH_2Cl_2 (200 mL) and washed with water (2 x 50 mL) and brine (50 mL). The combined organic layers were dried over $MgSO_4$ and concentrated *in vacuo* with a water bath temperature maintained at 35 °C. The crude product was purified by flash column chromatography (silica gel, EtOAc:hexanes 1:9 to 1:2) to afford **58** (380 mg, 72% yield) as a colorless oil. **58:** R_f = 0.80 (silica gel, EtOAc:hexanes 2:1); ^{1}H NMR ($CDCl_3$, 400 MHz) δ = 7.56 (d, *J* = 7.2 Hz, 2H), 7.47 (t, *J* = 7.3 Hz, 1H), 7.40 (t, *J* = 7.3 Hz, 2H), 4.17 (dd, *J* = 10.3, 3.0 Hz, 1H), 3.18 (d, *J* = 12.1 Hz, 1H), 3.11 (d, *J* = 12.6 Hz, 1H), 2.23–2.09 (m, 2H), 2.05 (d, *J* = 4.6 Hz, 1H), 1.69 (s, 3H), 1.65 (s, 3H), 1.44–1.13 (m, 46H), 0.88 (t, *J* = 6.8 Hz, 6H) ppm; ^{13}C NMR ($CDCl_3$, 150 MHz) δ = 177.9, 172.9, 137.4 (2C), 130.6, 129.2 (2C), 128.7, 115.9, 115.1, 72.2, 55.0, 54.8, 51.5, 45.9, 38.2, 33.7, 32.4, 31.9 (2C), 29.6 (9C), 29.6, 29.4 (2C), 29.4 (4C), 28.3, 27.4, 26.8, 26.5, 25.6, 22.7 (2C), 14.1 (2C) ppm; HRMS (APCI-TOF) calcd for $C_{44}H_{71}O_6S$ $[M + H]^+$ 727.4966, found 727.4971.

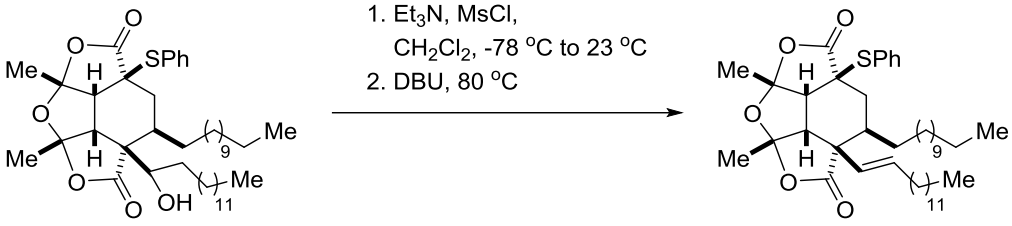

Trans olefin 48. To a solution of **58** (250 mg, 0.34 mmol) in CH_2Cl_2 (8 mL) in a sealable tube at -78 °C was added Et_3N (0.19 mL, 1.36 mmol) and MsCl (0.11 mL, 1.36 mmol) sequentially and the reaction mixture was slowly warmed to room temperature and stirred for 2 h. DBU (0.20 mL, 1.36 mmol) was added and the reaction mixture was heated to 80 °C for 8 h, after which the reaction was cooled to room temperature, diluted with CH_2Cl_2 (50 mL), quenched with NH_4Cl (sat. aq., 15 mL), and washed with water (2 x 30 mL) and brine (30 mL). The combined organic layers were dried over $MgSO_4$ and concentrated *in vacuo*. The crude product was purified by flash column chromatography (silica gel, EtOAc:hexanes 0:1 to 1:4) to afford **48** (160 mg, 65% yield) as a colorless oil. **48:** R_f = 0.60 (silica gel, EtOAc:hexanes 1:4); ^{1}H NMR ($CDCl_3$, 400 MHz) δ = 7.58 (d, *J* = 7.1 Hz, 2H), 7.47 (t, *J* = 7.4 Hz, 1H), 7.39 (t, *J* = 7.5 Hz, 2H), 5.75 (dt, *J* = 15.4, 6.8 Hz, 1H), 5.47 (d, *J* = 15.8 Hz, 1H), 3.10 (d, *J* = 11.7 Hz, 1H), 3.03 (d, *J* = 11.7 Hz, 1H), 2.17–2.00 (m, 4H), 1.99–1.93 (m, 1H), 1.60 (s, 3H), 1.36–1.22 (m, 42H + 3H), 0.88 (t, *J* = 6.2 Hz, 6H) ppm; ^{13}C NMR ($CDCl_3$, 100 MHz) δ = 174.8, 174.4, 137.4 (2C), 134.6, 130.9, 129.5 (2C), 129.3, 128.2, 115.0, 114.8, 53.9, 51.7, 51.2, 49.8, 39.3, 32.6, 31.9 (2C), 29.8, 29.6 (8C), 29.5 (2C), 29.4 (3C) 29.2, 29.0, 27.7, 27.4, 25.5, 25.3, 22.7 (2C), 14.1 (2C) ppm; HRMS (ESI-TOF) calcd for $C_{44}H_{69}O_5S$ $[M + H]^+$ 709.4859, found 709.4841.

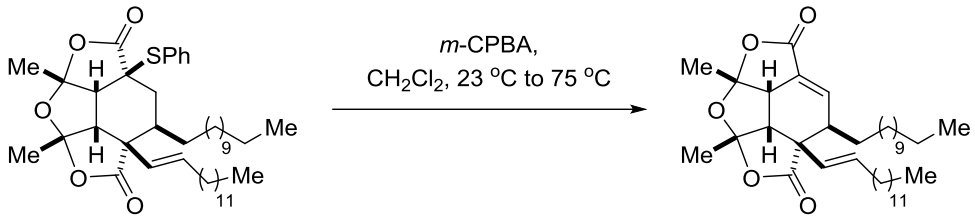

48 **6:** Paraceseolide A

Paracaseolide A (6). To a solution of **48** (66 mg, 0.093 mmol) in CH_2Cl_2 (4 mL) at room temperature was added a solution of *m*-CPBA (77%, 17 mg, 0.10 mmol) in CH_2Cl_2 (3 mL), dropwise over 5 minutes. The reaction was monitored by TLC and after 2 h, the reaction was quenched by $NaHCO_3$ (sat. aq., 5 mL) and diluted with CH_2Cl_2 (5 mL). The combined organic phases were washed with water (2 x 5 mL) and brine (5 mL), dried over $MgSO_4$, and concentrated *in vacuo*. To complete the elimination of any remaining sulfoxide, anhydrous $CHCl_3$ (10 mL) was added and the heating bath on the rotary evaporator was maintained at 75 °C as the $CHCl_3$ slowly evaporated without vacuum for 5 minutes. The remaining $CHCl_3$ was concentrated *in vacuo*. The crude product was purified by preparative TLC (silica gel, EtOAc:hexanes 1:4) to afford **6** as a white crystalline solid (50 mg, 90% yield). **6:** R_f = 0.40 (silica gel, EtOAc:hexanes 1:4); ^{1}H NMR ($CDCl_3$, 400 MHz) δ = 7.24 (dd, *J* = 7.4, 3.0 Hz, 1H), 5.83 (dt, *J* = 14.5, 6.8 Hz, 1H), 5.49 (d, *J* = 15.9 Hz, 1H), 3.36 (dd, *J* = 9.5, 2.9 Hz, 1H), 3.30 (d, *J* = 9.6 Hz, 1H), 3.04 (ddd, *J* = 11.6, 7.7, 3.5 Hz, 1H), 2.14–2.09 (m, 2H), 1.76 (s, 3H), 1.72–1.65 (m, 1H), 1.62 (s, 3H), 1.48–1.03 (m, 41H), 0.88 (t, *J* = 6.6 Hz, 6H) ppm; ^{13}C NMR ($CDCl_3$, 100 MHz) δ =175.0, 166.2, 144.7, 135.1, 129.3, 126.2, 115.4, 113.8, 58.3, 50.2, 46.7, 45.0, 32.7, 31.9 (2C), 29.6 (8C), 29.5, 29.4 (2C), 29.3 (2C), 29.1, 29.0, 28.2, 28.0, 26.6, 25.7, 22.7 (2C), 14.1 (2C) ppm; HRMS (ESI-TOF) calcd for $C_{38}H_{63}O_5$ $[M + H]^+$ 599.467, found 599.4669.

1.5. References

1. (a) Cragg, G. M.; Grothaus, P. G.; Newman, D. J., *J. Nat. Prod.* **2014,** *77*, 703-723. (b) Dias, D. A.; Urban, S.; Roessner, U., *Metabolites* **2012,** *2*, 303-336. (c) Newman, D. J.; Cragg, G. M., *J. Nat. Prod.* **2012,** *75*, 311-335. (d) Newman, D. J.; Cragg, G. M., *J. Nat. Prod.* **2007,** *70*, 461-477. (e) Clardy, J.; Fischbach, M. A.; Walsh, C. T., *Nat. Biotechnol.* **2006,** *24*, 1541-1550. (f) Butler, M. S., *Nat. Prod. Rep.* **2005,** *22*, 162-195. (g) Clardy, J.; Walsh, C., *Nature* **2004,** *432*, 829-837. (h) Butler, M. S., *J. Nat. Prod.* **2004,** *67*, 2141-2153.

2. Bohlmann, J.; Keeling, C. I., *Plant J.* **2008,** *54*, 656-669.

3. (a) Gershenzon, J.; Dudareva, N., *Nat. Chem. Biol.* **2007,** *3*, 408-414. (b) Wang, G.; Tang, W.; Bidigare, R. R. In *Terpenoids as therapeutic drugs and pharmaceutical agents*, Humana Press: New Jersey, 2005; pp 197-227.

4. (a) Guimaraes, A. G.; Serafini, M. R.; Quintans-Junior, L. J., *Expert Opin. Ther. Pat.* **2014,** *24*, 243-265. (b) Gonzalez-Burgos, E.; Gomez-Serranillos, M. P., *Curr. Med. Chem.* **2012,** *19*, 5319-5341. (c) Kuttan, G.; Pratheeshkumar, P.; Manu, K. A.; Kuttan, R., *Pharm. Biol.* **2011,** *49*, 995-1007. (d) Cohen, E.; Koch, L.; Thu, K. M.; Rahamim, Y.; Aluma, Y.; Ilan, M.; Yarden, O.; Carmeli, S., *Bioorg. Med. Chem.* **2011,** *19*, 6587-6593; (e) Stierle, D. B.; Stierle, A. A.; Patacini, B.; McIntyre, K.; Girtsman, T.; Bolstad, E., *J. Nat. Prod.* **2011,** *74*, 2273-2277.

5. Cornforth, J. W., *Chem. Brit.* **1968,** *4*, 102-106.

6. (a) Hale, K. J., *Org. Lett.* **2013,** *15*, 3181-3198. (b) Itoh, T.; Tokunaga, K.; Matsuda, Y.; Fujii, I.; Abe, I.; Ebizuka, Y.; Kushiro, T., *Nat. Chem.* **2010,** *2*, 858-864.

7. Geris, R.; Simpson, T. J., *Nat. Prod. Rep.* **2009,** *26*, 1063-1094.

8. (a) Tomoda, H.; Kim, Y. K.; Nishida, H.; Masuma, R.; Omura, S., *J. Antibiot.* **1994,** *47*, 148-153. (b) Nagamitsu, T.; Sunazuka, T.; Obata, R.; Tomoda, H.; Tanaka, H.; Harigaya, Y.; Omura, S.; Smith, A. B., III, *J. Org. Chem.* **1995,** *60*, 8126-8127. (c) Kim, Y. K.; Tomoda, H.; Nishida, H.; Sunazuka, T.; Obata, R.; Omura, S., *J. Antibiot.* **1994,** *47*, 154-162.

9. (a) Chen, J.-W.; Luo, Y.-L.; Hwang, M.-J.; Peng, F.-C.; Ling, K.-H., *J. Biol. Chem.* **1999,** *274*, 34916-34923. (b) Peng, F.-C., *J. Nat. Prod.* **1995,** *58*, 857-862.

10. Cueto, M.; MacMillan, J. B.; Jensen, P. R.; Fenical, W., *Phytochemistry* **2006,** *67*, 1826-1831.

11. (a) Fukui, Y.; Narita, K.; Katoh, T., *Chem. Eur. J.* **2014,** *20*, 2436-2439. (b) Jiao, W.-H.; Huang, X.-J.; Yang, J.-S.; Yang, F.; Piao, S.-J.; Gao, H.; Li, J.; Ye, W.-C.; Yao, X.-S.; Chen, W.-S.; Lin, H.-W., *Org. Lett.* **2012,** *14*, 202-205. (c) Schmalzbauer, B.; Herrmann, J.; Mueller, R.; Menche, D., *Org. Lett.* **2013,** *15*, 964-967.

12. (a) Yuan, L.; Zhao, P.-J.; Ma, J.; Li, G.-H.; Shen, Y.-M., *Helv. Chim. Acta* **2008,** *91*, 1588-1594. (b) Zhang, G.; Wu, G.; Zhu, T.; Kurtan, T.; Mandi, A.; Jiao, J.; Li, J.; Qi, X.; Gu, Q.; Li, D., *J. Nat. Prod.* **2013,** *76*, 1946-1957.

13. Chen, X.-L.; Liu, H.-L.; Li, J.; Xin, G.-R.; Guo, Y.-W., *Org. Lett.* **2011,** *13*, 5032-5035.

14. Njardarson, J. T.; Gaul, C.; Shan, D.; Huang, X.-Y.; Danishefsky, S. J., *J. Am. Chem. Soc.* **2004,** *126*, 1038-1040.

15. Schreiber, S. L., *Science* **2000,** *287*, 1964-1969.

16. (a) Dixon, D. D.; Lockner, J. W.; Zhou, Q.; Baran, P. S., *J. Am. Chem. Soc.* **2012,** *134*, 8432-8435. (b) Kuan, K. K. W.; Pepper, H. P.; Bloch, W. M.; George, J. H., *Org. Lett.* **2012,** *14*, 4710-4713. (c) Alvarez-Manzaneda, E.; Chahboun, R.; Alvarez, E.; Cano, M. J.; Haidour, A.; Alvarez-Manzaneda, R., *Org. Lett.* **2010,** *12*, 4450-4453.

17. Rodriguez, A. D.; Ramirez, C., *J. Nat. Prod.* **1994,** *57*, 339-347.

18. Son, J. K.; Kim, D. H.; Woo, M. H., *J. Nat. Prod.* **2003,** *66*, 1369-1372.

19. Yang, H. O.; Suh, D.-Y.; Han, B. H., *Planta Med.* **1995,** *61*, 37-40.

20. Sathe, M.; Kaushik, M. P., *Bioorg. Med. Chem. Lett.* **2010,** *20*, 1312-1314.

21. (a) Lavecchia, A.; Di Giovanni, C.; Novellino, E., *Mini-Rev. Med. Chem.* **2012,** *12*, 62-73. (b) Boutros, R.; Lobjois, V.; Ducommun, B., *Nat. Rev. Cancer* **2007,** *7*, 495-507.

22. Ito, Y.; Yoshida, H.; Uruno, T.; Takamura, Y.; Miya, A.; Kuma, K.; Miyauchi, A., *Breast Cancer* **2004,** *11*, 295-300.

23. Ngan, E. S. W.; Hashimoto, Y.; Ma, Z.-Q.; Tsai, M.-J.; Tsai, S. Y., *Oncogene* **2003,** *22*, 734-739.

24. Noutsias, D.; Vassilikogiannakis, G., *Org. Lett.* **2012,** *14*, 3565-3567.

25. Guney, T.; Kraus, G. A., *Org. Lett.* **2013,** *15*, 613-615.

26. Vasamsetty, L.; Khan, F. A.; Mehta, G., *Tetrahedron Lett.* **2013,** *54*, 3522-3525.

27. Giera, D. S.; Stark, C. B. W., *RSC Adv.* **2013,** *3*, 21280-21284.

28. Boukouvalas, J.; Jean, M.-A., *Tetrahedron Lett*. **2014,** *55*, 4248-4250.

29. Lin, C.-C.; Wu, H.-J., *J. Chin. Chem. Soc.* **1995,** *42*, 815-820.

30. Dominguez, C.; Csaky, A. G.; Plumet, J., *Tetrahedron Lett.* **1990,** *31*, 7669-7670.

31. (a) Leonard, N. J.; Johnson, C. R., *J. Org. Chem.* **1962,** *27*, 282-284. (b) Hiskey, R. G.; Harpold, M. A., *J. Org. Chem.* **1967,** *32*, 3191-3194.

32. (a) Chapdelaine, M. J.; Hulce, M., *Org. React.* **1990,** *38*, 225-653. (b) Taylor, R. J. K., *Synthesis* **1985,** 364-92. (c) Han, Y.-K.; Paquette, L. A., *J. Org. Chem.* **1979,** *44* , 3731-3733. (d) Zoretic, P. A.; Yu, B. C.; Biggers, M. S.; Caspar, M. L., *J. Org. Chem.* **1990,** *55*, 3954-3957.

33. (a) Posner, G. H., *Org. React.* **1972,** *19*, 1-113. (b) Nielsen, E. B.; Munch-Petersen, J.; Joergensen, P. M.; Refn, S., *Acta Chem. Scand.* **1959,** *13*, 1943-1954. (c) Munch-Petersen, J., *Bull. Soc. Chim. Fr.* **1966,** 471-480.

34. Chen, J.; Li, Y.; Cao, X.-P., *Tetrahedron: Asymmetry* **2006,** *17*, 933-941.

35. Soorukram, D.; Knochel, P., *Org. Lett.* **2007,** *9*, 1021-1023.

CHAPTER 2.

FIRST DIELS–ALDER STRATEGY OF INDOLES AND METHYL COUMALATE TO CARBAZOLE ALKALOIDS[†]

2.1. Introduction

Cycloaddition reactions[1] have become one of the most powerful synthetic tools for the synthesis of complex polycyclic molecules as they often provide numerous advantages in controlling the desired chemo-, regio-, diastereo-, and enantioselectivity. Among the top versatile cycloaddition technologies includes the [4+2]-cycloaddition or the Diels–Alder reaction[2], which has been successfully applied as a key step in the construction of the bicyclic moieties of natural products and biologically active substances, ever since its discovery by Otto Diels and Kurt Alder in 1928.[3] Moreover, because of its efficiency at forming two new σ bonds by the reorganization of the π-electron system, the Diels–Alder reaction has been showcased as an ideal synthetic method in the context of atom economy advanced by Trost.[4]

Based on the electronic properties of the substituents present on the diene and the dieophile, Diels–Alder reactions can be categorized into two main groups:

(i) The normal electron-demand Diels–Alder reaction

(ii) The inverse electron-demand Diels–Alder (IEDDA) reaction

---

[†] Adapted with permission from Guney, T.; Lee, J. J.; Kraus, G. A., *Org. Lett.* **2014**, *16*, 1124-1127. Copyright © 2014 American Chemical Society.

Contrary to the normal electron-demand Diels–Alder reaction, the IEDDA reaction takes place between electron-poor dienes and electron-rich dienophiles, as first demonstrated in 1959 by Carboni and co-workers[5] between 3,6-bis-(polyfluoroalkyl)-1,2,4,5-tetrazines as electron-poor dienes and various olefins as electron-rich dienophiles to form pyridazines.

As discoveries of structurally diverse alkaloids containing the indole moiety appeared, efficient methodologies featuring indole chemistry have since been generated. Given its potential tunability through electron-rich or electron-withdrawing substituents, utilizing the 2,3-carbon–carbon double bond of the indole offered advantages when applied to cycloaddition reactions. In this regard, the [4+2]-cycloaddition has been one of the most appealing pericyclic concepts for the indole building blocks.[6] The enamine substructure of the indole has served in both normal electron-demand Diels–Alder and IEDDA reactions as the dienophile for the assembly of heterocyclic natural products. Some of the most notable and successful cycloaddition methodologies were discovered after the first IEDDA reaction of indoles pioneered independently by both Seitz[7] and Takahashi[8] in 1976 employing 1,2,4,5-tetrazines.

In his studies, Seitz reported that 1-methylindole (**1**) underwent a [4+2] cycloaddition with methyl 1,2,4,5-tetrazine-3,6-dicarboxylate (**2**) followed by release of nitrogen to produce cycloadduct **3**. Rapid rearrangement of intermediate **3** *via* the ring-opening of the pyrrole component and its subsequent amidation resulted in pyridazinoquinolone **5** in 45% yield as shown in Scheme 1.

Similarly, Takahashi and co-workers revealed that refluxing the solution of indole (**6**) and 3,6-di-(2-pyridyl)-1,2,4,5-tetrazine (**7**) in toluene gave 5*H*-pyridazino[4,5-*b*]indole

8 in 35% yield as shown in Scheme 2. They described this as an unexpected result since the cycloadduct intermediate further aromatized to **8**, which was not observed by Seitz in his analogous system. The initial success obtained with 1,2,4,5-tetrazines was then expanded to other azadienes such as 1,2,4-triazines and 1,2-diazines (pyridazines). More examples are comprehensively provided in the recent reviews by Snyder[9] and Berthel.[10]

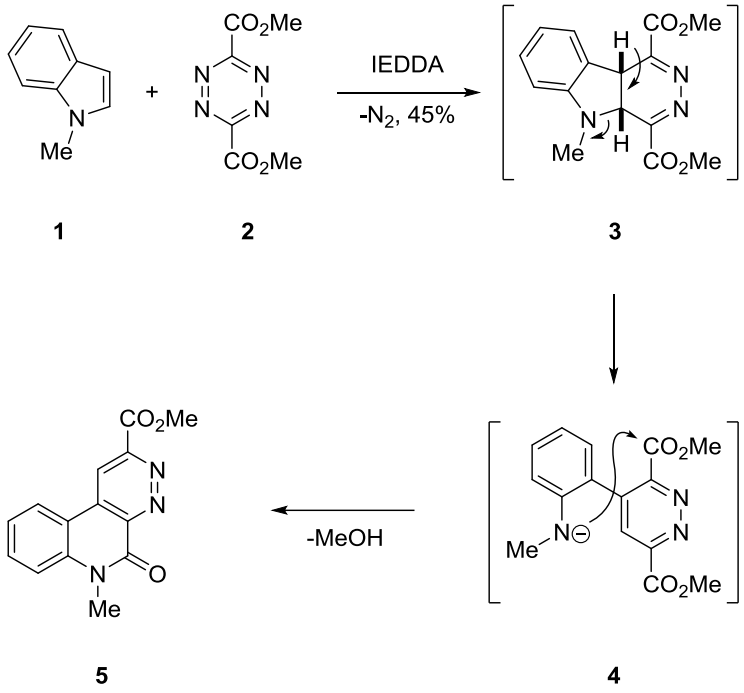

Scheme 1. Reaction of 1-methylindole (**1**) and tetrazine **2** to obtain quinolone **5** by Seitz.[7]

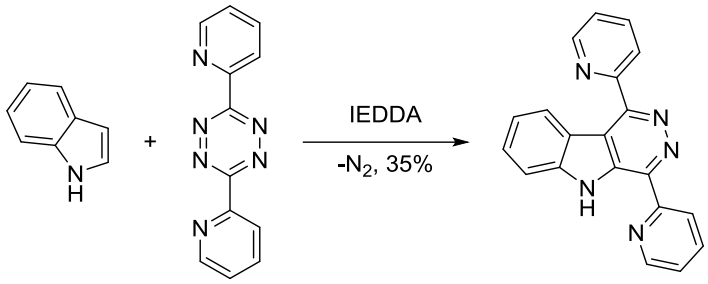

6 **7** **8**

Scheme 2. Reaction of indole (**6**) and tetrazine **7** to form pyridazinoindole **8** by Takahashi.[8]

Several years later, another breakthrough in [4+2]-cycloaddition reactions of indoles was achieved by our group. Kraus and co-workers[11] demonstrated the first example of an intramolecular Diels–Alder reaction using an indole as the dienophile, where highly functionalized dihydroindoles were prepared in the presence of amide or urea tethered dienes attached to the indole moiety. For example, methyl indole-3-carboxylate and the diene acid were coupled to afford amide **9**, which was then subjected to thermal conditions to furnish dihydroindole **10** in 93% yield as shown in Scheme 3.

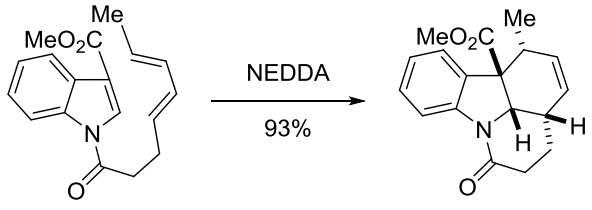

9 **10**

Scheme 3. Synthesis of dihydroindoles *via* intramolecular Diels–Alder strategy by Kraus.[11]

Additionally, Stoltz and co-workers[12] described a novel route to the indoline alkaloid communesin B based on a key IEDDA reaction between the indole derivative **11** and an *o*-azaxylylene generated in situ from chloroaniline **12** through base-induced hydrogen chloride elimination developed by Corey.[13] The cycloaddition reaction took place smoothly at -78 ^{o}C to give the adduct **13** in 99% yield as a 1:1 diastereomeric mixture as shown in Scheme 4. The cycloadduct **13** was then further advanced to a potential intermediate for communesin B.

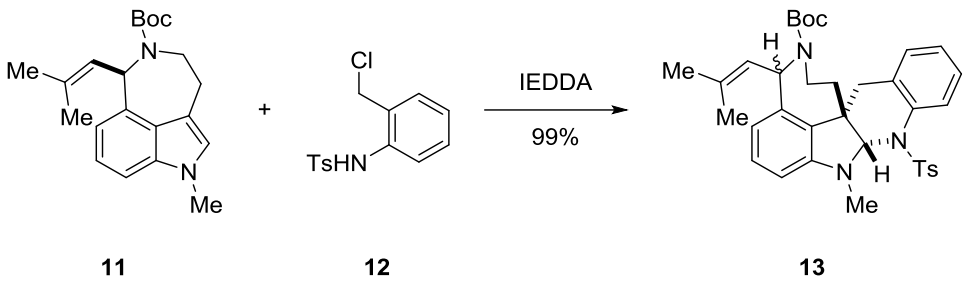

11 **12** **13**

Scheme 4. Synthesis of pentacylic potential communesin B precursor by Stoltz.[12]

More recently, three very innovative strategies for the construction of the polycyclic core of strychnine (**14**) were designed by the Bodwell[14], Padwa[15], and Vanderwal[16] labs. Although each group envisioned strategically different sets of functional group manipulations to obtain the natural product, they all had a common [4+2]-cycloaddition key step.

Padwa chose an intramolecular Diels–Alder approach. The tetracyclic intermediate **15** was achieved in 95% yield when furanylindole **16** was subjected to thermal conditions in a microwave reactor in the presence of catalytic magnesium iodide. Subsequent

transformations of the tetracycle **15** afforded the natural alkaloid, strychnine (**14**) as shown in Scheme 5.[15]

On the other hand, Bodwell focused on an IEDDA route utilizing the cyclophane **17** which was rapidly accessed from tryptamine. Inducing the cycloaddition of **17** by heat provided the pentacyclic product **18** in quantitative yield. Stereospecific installation of the key quaternary stereogenic center was an attractive feature of Bodwell's synthesis.[14]

Most recently, Vanderwal's group disclosed their elegant work on the total synthesis of strychnine (**14**) in six linear steps, the shortest route to date. Their assembly of the core framework featured a pivotal IEDDA reaction of tryptamine-derived Zincke aldehyde **19** under base-mediated conditions. They were able to form the tetracyclic moiety **20** in 64% yield.[16]

As witnessed by the short literature review described herein, the Diels–Alder reaction has been the subject of stimulating research in the field of synthetic organic chemistry. The flexibility of the indole 2,3-carbon–carbon double bond in either normal electron-demand Diels–Alder or IEDDA reactions has been encountered on numerous occasions. In particular, the three highlighted routes to strychnine impressively displayed the exceptional tunability of the indole in [4+2]-cycloaddition reactions in the formation of complex targets.

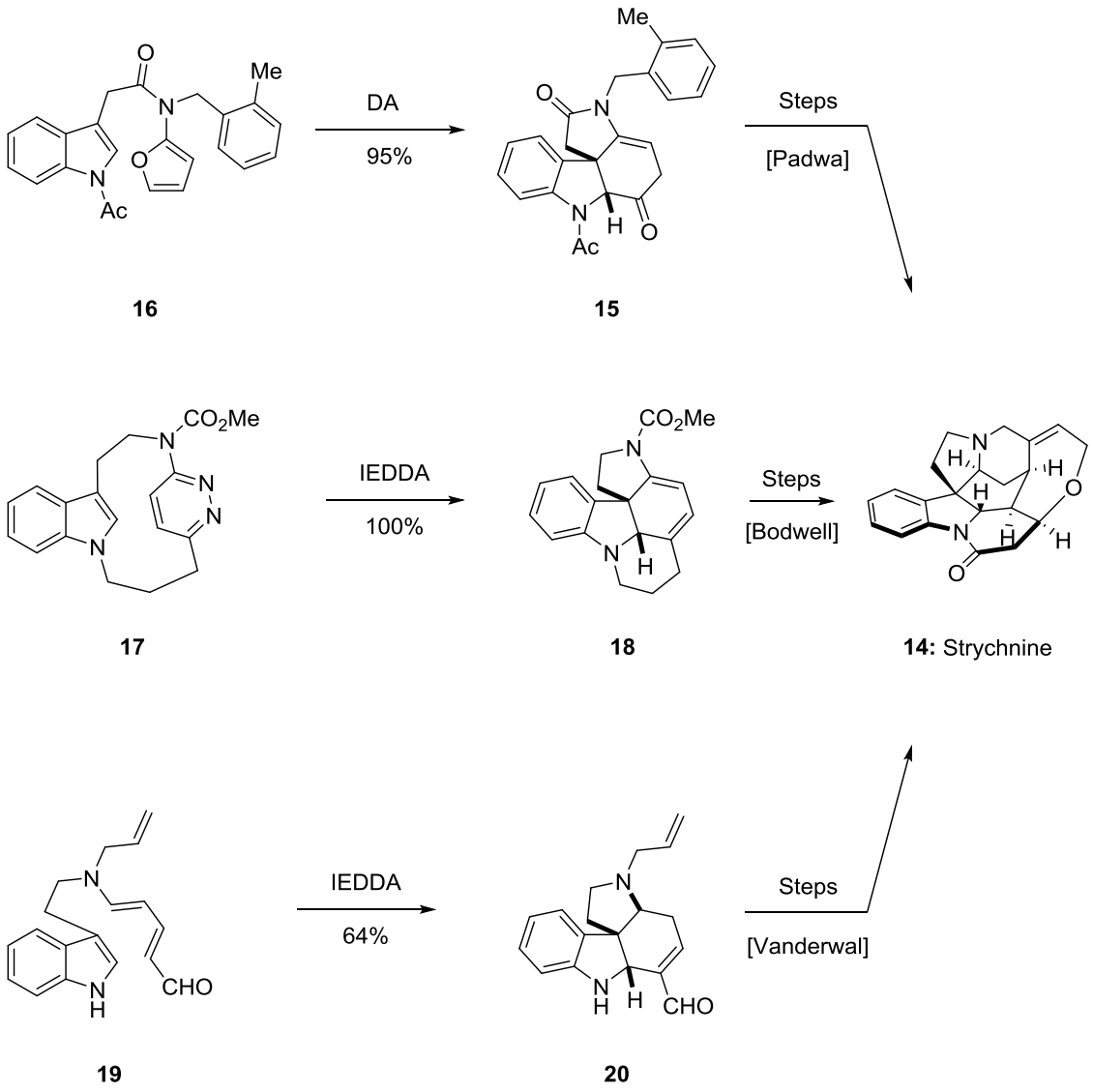

Scheme 5. [4+2]-cycloaddition strategies to the complex natural alkaloid strychnine (**14**).

The scope of the IEDDA reaction in the context of indoles as dienophiles has been limited to electron-deficient heteroaromatic azadienes such as 1,2,4,5-tetrazines, 1,2,4-triazines and 1,2-diazines.[9,10] Furthermore, 2-nitrovinyl-substituted quinones[17], *o*-azaquinones[18], and aza-*ortho*-xylylenes[19] have been successful. However, the restricted

scope of the indoles in the IEDDA reaction can be attributed to the greater challenge of breaking its aromaticity compared to enamines. The nucleophilicity of the 3-position can additionally hinder the desired IEDDA reaction, which has led researchers to apply an intramolecular approach to circumvent the issues.

One noticeable obstacle for the indole Diels–Alder reactions has been electron-deficient pyrones. Although pyrones have been very effective in many [4+2]-cycloadditions[20], Snyder's early work recognized that methyl coumalate (**21**) was unreactive towards substituted indoles under his reaction conditions.[21] He discovered that the pyrones instead underwent nucleophilic additions to generate 3-substituted indole adducts.

The intriguing question of whether an IEDDA reaction can be accomplished between an indole and a pyrone empowered our research to invent a new methodology to naturally-occurring carbazole alkaloids (**22**). Our research group has been investigating green platform technologies to access a diverse array of functionalized aromatics.[22,23] We recognized that the 2-pyrone methyl coumalate (**21**), which can be obtained through the dimerization of malic acid, could be one such sustainable synthon as shown in Figure 1.

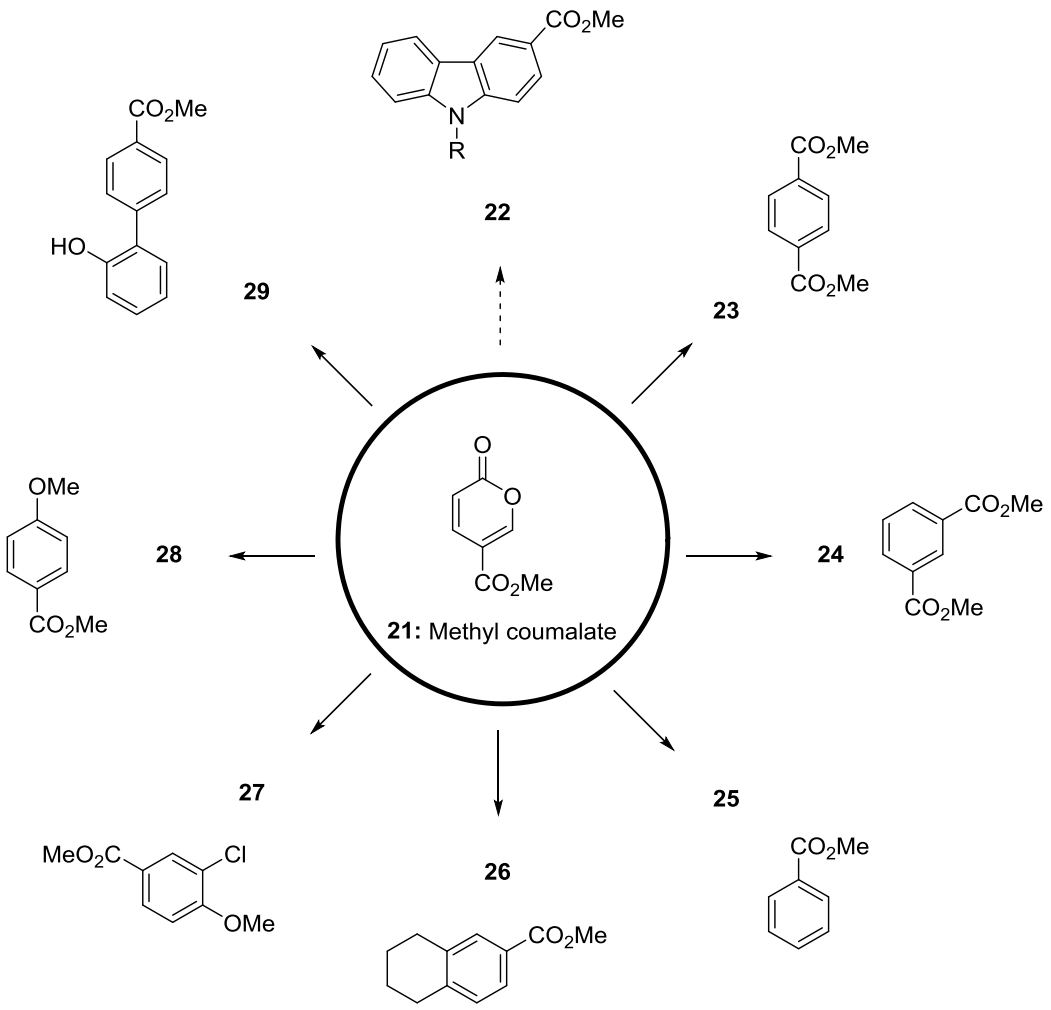

Figure 1. Functionalized aromatics accessible *via* the methyl coumalate platform.

Recently, Lee and Kraus reported an efficient biorenewable approach to commodity and specialty aromatic building blocks *via* a one-pot IEDDA/decarboxylation/elimination cascade.[24] Through this methodology, methyl coumalate (**21**) was paired with readily accessible vinyl ethers, ketals, orthoesters and captodative dienophiles to produce green aromatics **23-29** in good to excellent yields with in exclusive regioselectivity.

In light of our laboratory's successful prior work, extension of the coumalate platform to natural and synthetic carbazole alkaloids became our new challenging synthetic endeavor. Carbazoles are a class of aromatic heterocycles that display a wide range of useful properties from therapeutic activities to applications in materials science as dyes, optoelectronics, and conducting polymers. Consequently, synthetic developments in the area of carbazole alkaloids have intensified as seen by the comprehensive reviews and numerous research articles in recent years.[25]

Carbazoles are mainly classified in two large groups based on their biogenesis. The group of alkaloids isolated from plants contains a methyl unit or its oxygenated analogues at the 3-position of the carbazole skeleton. On the other hand, the second group of carbazoles lacks the carbon substitution on the 3-position and are primarily isolated from microorganisms. The vast majority of biologically active 3-methylcarbazole alkaloids are isolated from the *Murraya*, *Clausena*, and *Glycomis* species of the same plant from the family Rutaceae.[26] These natural alkaloids exhibit antiviral, antimalarial, and antitumor activities as representative structures are shown in Figure 2.[26,27,28]

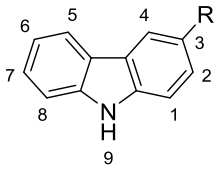

30: 3-Methylcarbazole, R=Me
31: Methyl carbazole-3-carboxylate, R=CO_2Me

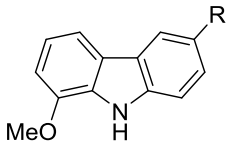

32: Glycozolicine, R=Me
33: Mukoline, R=CH_2OH
34: Mukolidine, R=CHO

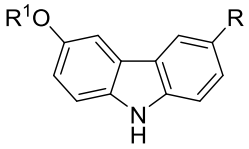

35: Glycozoline, R=R^1=Me
36: Glycozolinol, R=Me, R^1=H
37: 3-Formyl-6-methoxycarbazole, R=CHO, R^1=Me
38: Methyl 6-methoxycarbazole-3-carboxylate, R=CO_2Me, R^1=Me

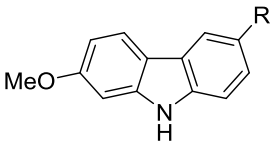

39: Clauszoline K, R=CHO
40: Clausine C, R=CO_2Me
41: Clausine N, R=CO_2H

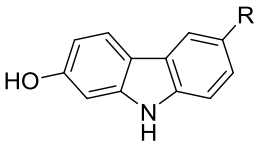

42: 3-Formyl-7-hydroxycarbazole, R=CHO
43: Clausine M, R=CO_2Me

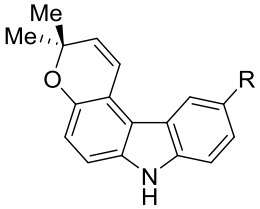

44: Glycomaurin, R=Me
45: Clauraila C, R=CO_2Me

Figure 2. Representative structures of the 3-methylcarbazole family and its analogues.

Given the increasing importance of carbazole alkaloids, a broad array of synthetic strategies has been reported. In recent years, the transition metal-catalyzed systems have been established as a general trend. Some of the latest methods to construct the family of 3-methylcarbazole or its higher oxidation state analogues **46** include Witulski's [2+2+2] cycloaddition of diynes **47** and alkynes **48** in the presence of Wilkinson's catalyst.[29] Subsequently, Back et al. described a Lewis acid-catalyzed Diels–Alder reaction between the vinylogous 2-(phenylthio)indole **49** and methyl propiolate (**50**) to form the desired carbazoles.[30] In addition, Larock and co-workers designed an elegant pathway that featured *in situ* generation of an aryne intermediate from the silylaryl triflate **51** to first react with the 2-iodoanilines **52** to form the C–N bond, followed by palladium-catalyzed annulation to yield the aromatic heterocycles.[31] In 2013, Itami and Lei reported a Pd-Cu-Ag trimetallic protocol that coupled substituted indoles **53** and methyl acrylate (**54**) via a tandem C–H functionalization/Diels–Alder reaction as shown in Scheme 6.[32]

Although these well-designed methods were able to generate targeted 3-methylcarbazoles, they come with some practical challenges. For example, the complete removal of transition-metal catalysts is important since the presence of metals could affect the bioactivity evaluation process. Particularly, the Itami and Lei protocol[32] employs multiple metal catalysts, some of which are present in greater than stoichiometric amounts. In addition, highly substituted aromatic systems require multi-step preparations, which reduces the overall efficiency of the route. Furthermore, the formation of regioisomeric mixtures is a potential risk if an unsymmetrical alkyne is chosen in Witulski's method.[29]

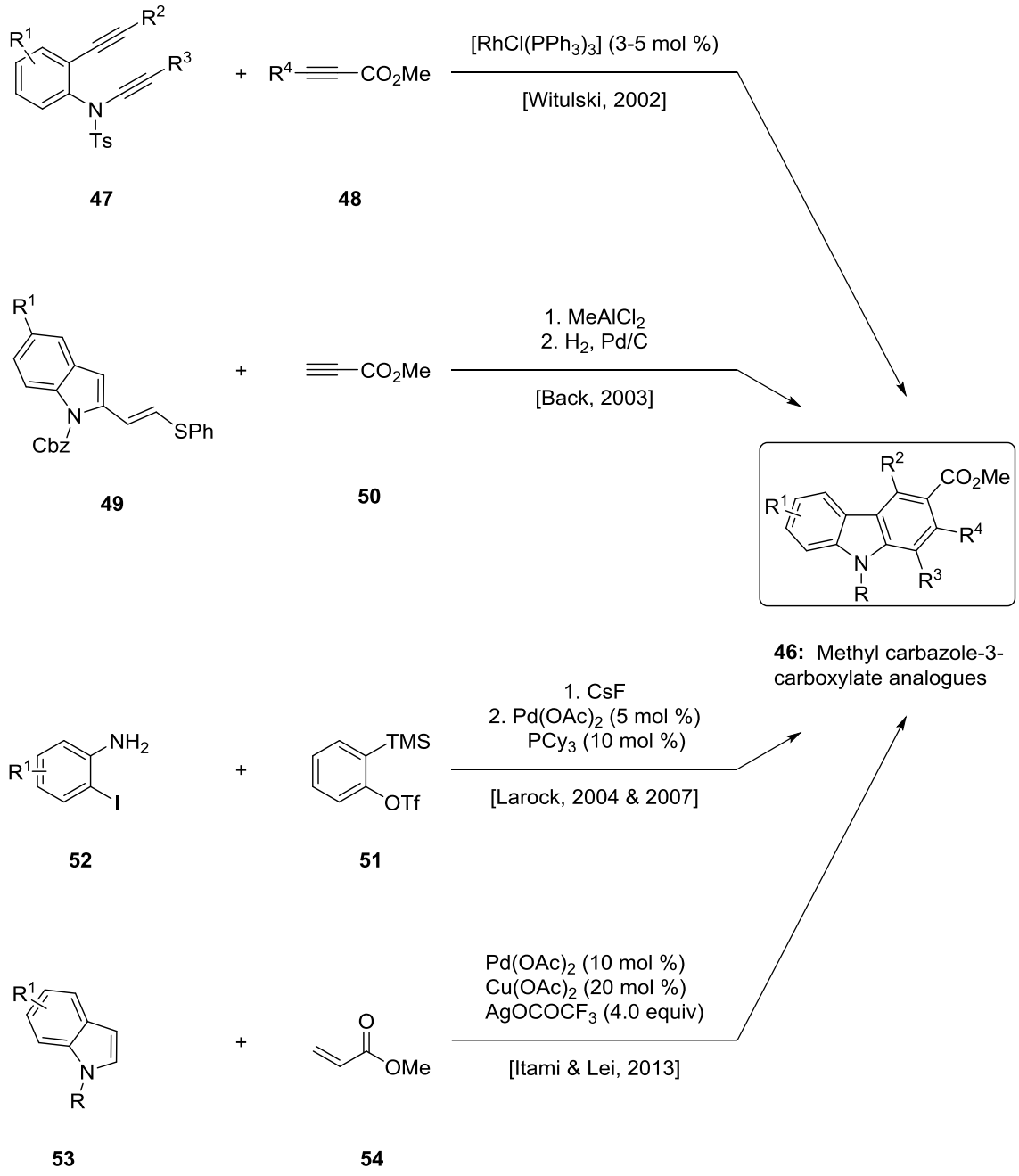

Scheme 6. General approaches to carbazole alkaloids **46**.

2.2. Results and Discussion

We endeavored to design direct access to the family of naturally-occurring carbazole alkaloids **30-45** using the IEDDA methodology between indoles and methyl coumalate (**21**). We recognized that two major potential challenges associated with electron-rich indole dienophiles needed to be addressed: (i) the nucleophilicity of the 3-position of the indole and (ii) the ring-opening of the pyrrole component after the formation of the cycloadduct.

First, the inherent reactivity pattern of indoles toward electrophilic nucleophilic substitutions has been one of the most well-characterized phenomena of indole chemistry. Significant delocalization of electron density from nitrogen to the C-3 postion of the indole was projected by molecular orbital calculations, and supported by experimental evidence. Halogenation, nitration, formylation, and sulfonation are just a few examples where the 3-position of the indole was functionalized.[33] More specifically, Snyder and co-workers reported that nucleophilic substitution reactions of indoles with methyl coumalate (**21**) occurred at the 3-position.[21]

Secondly, the ring fragmentation of the pyrrole moiety of the Diels–Alder adduct *via* aromatization was first witnessed by Seitz (Scheme 1).[7] Furthermore, Lee and Kraus exploited the one-pot Diels–Alder/decarboxylation/elimination pathway to obtain *para*-substituted biphenyl alcohol **29** in 77% yield with benzofuran (**55**) and methyl coumalate (**21**) as shown in Scheme 7.[24] Extrapolating the evidence to the targeted carbazoles, facile ring-opening was predicted to occur.

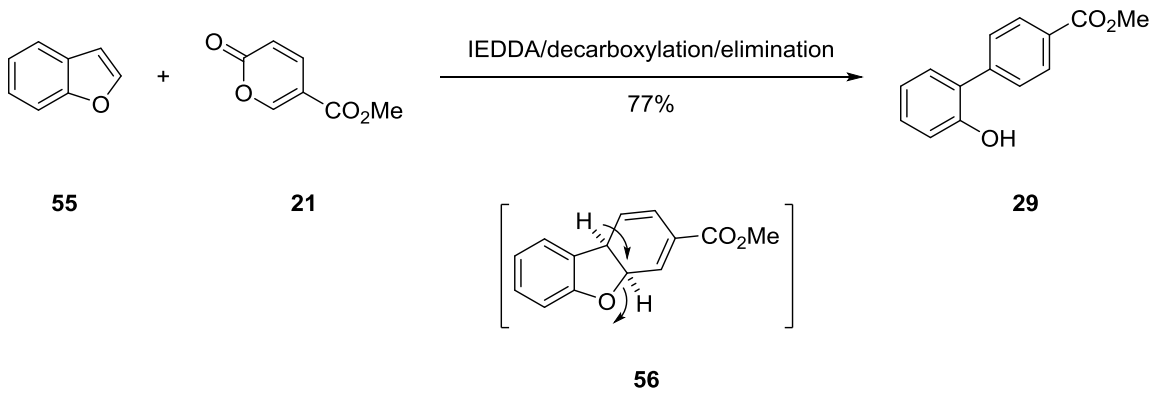

Scheme 7. Synthesis of biphenyl alcohol **29** by Lee and Kraus.

After careful thinking we imagined functionalizing the 3-position of the indole with an activating group to depress its localized electron density and prevent detrimental nucleophilic additions. Functionalization would also facilitate aromatization through elimination to efficiently construct the 3-methylcarbazole family without the need for transition metal-mediated oxidation. Consequently, the activating group had to be mildly electron-withdrawing in nature to build a unidirectional dipole, which would ultimately assist in controlling the regioselectivity of the cycloaddition. Selection of halides as activating groups was advantageous since the selective halogenation of the indole 3-position was a well-established operation. Additionally, their electronegativity would empower the regiospecificity of the intermolecular IEDDA reaction. Overall, our proposed methodology hinged on the IEDDA-initiated cascade aromatization reaction between substituted 3-chloroindoles as dienophiles and methyl coumalate as the diene to reveal carbazole alkaloids, which was the first reaction of its kind.[34]

As shown in Scheme 8, we expected that 3-chloroindoles **57** would undergo an IEDDA reaction with methyl coumalate (**21**) to furnish the cycloadduct **58**. Afterwards, carbon dioxide extrusion from **58** was envisioned to occur, giving rise to the intermediate **59**, which would quickly aromatize by the elimination of hydrogen chloride to provide methyl carbazole-3-carboxylates **60**.

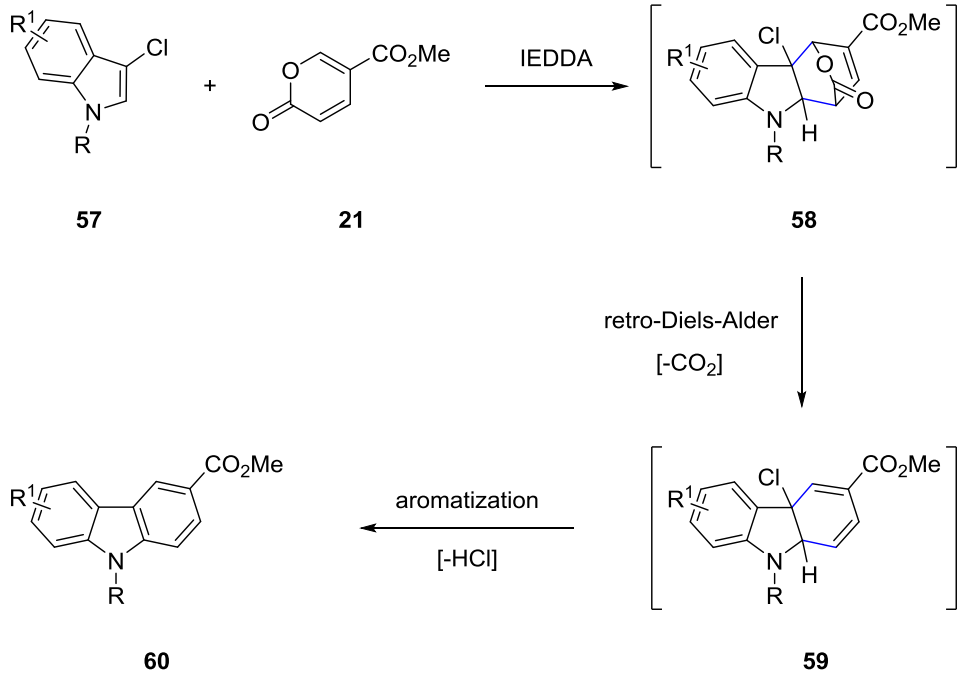

Scheme 8. Proposed mechanism to carbazoles by IEDDA/decarboxylation/aromatization.

Our investigations began by subjecting methyl coumalate (**21**) and 3-chloroindole to 200 ^{o}C in toluene, which generated only a trace amount of methyl carbazole-3-carboxylate (**31**) along with insoluble tars. To avoid the tar formation, we screened other more polar solvents such as $MeNO_2$, DMF, and MeCN, while keeping the other conditions

constant. Unfortunately, changing the solvent did not decrease the tar accumulation during the reaction. Thus, the complications led us to incorporate an alkyl unit or an electron-donating protecting group on the 1-positions of the indole dienophile.

Table 1. Reaction optimization with 1-methyl-3-chloroindole (**57a**)[a]

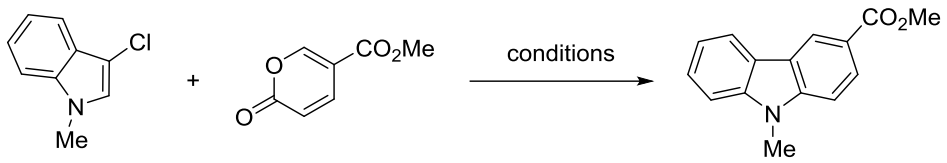

57a **21** **60a**

entry	solvent	concn (M)	temp (°C)	**60a**:**57a** ratio[b]
1	toluene	0.10	200	1:0
2	MeCN	0.05	200	1:1.3
3	MeCN	0.10	165	1:2.9
4	MeCN	0.15	200	1:0.6
5	—	neat	200	complex

[a] All reactions were run for 16 h with 3.0 equivalents of methyl coumalate (**21**).
[b] Ratios were determined by integration of crude ^{1}H NMR.

We then turned our attention to exploring the conditions with the 1-methyl-3-chloroindole (**57a**) dienophile. Pleasingly, the IEDDA reaction proceeded smoothly in toluene at 200 °C to give the corresponding carbazole **60a**, observed by the crude ^{1}H NMR (Table 1, entry 1). Although other trials in MeCN at both 200 °C and 165 °C produced some carbazole **60a**, the conversion of the indole starting material was not complete in 16 hours with altered molar concentrations (Table 1, entries 2-4). Additionally, the reaction

at 200 °C under neat conditions gave a complex mixure (Table 1, entry 5) as seen by the ^{1}H NMR.

Table 2. Lewis acid-mediated IEDDA reaction of **57a** and **21**[a]

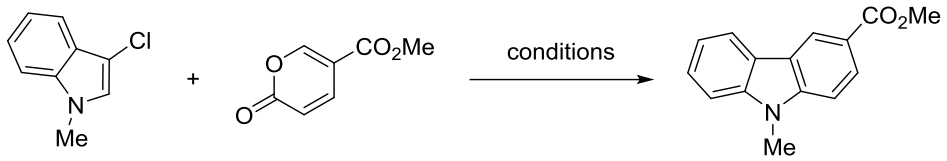

57a **21** **60a**

entry	Lewis acid	Lewis acid equiv	**60a**:**57a** ratio[b]
1	$ZnCl_2$	0.1	1:3.4
2	$ZnCl_2$	1.0	1:1.5[c]
3	$ZnCl_2$	2.0	1:0.2[c]
4	$TiCl_4$	0.1	1:26
5	$SnCl_4$	0.1	1:20

[a] All reactions were run at 150 °C for 16 h in toluene with 3.0 equivalents of methyl coumalate (**21**). The concentration for all reactions was 0.1 M relative to **57a**. Temperatures below 150 °C did not show product formation.
[b] Ratios were determined by integration of crude ^{1}H NMR.
[c] Regioisomers (~ 1:1 ratio) were observed.

Once the heat-mediated IEDDA conditions were set for 1-methyl-3-chloroindole (**57a**), we also wanted to conduct a preliminary study with Lewis acids to lower the reaction temperature. Mild Lewis acids such as $ZnCl_2$ (0.1 equivalent) at 150 °C displayed poor conversion giving a 1:3.4 (carbazole **60a** : indole **57a)** ratio (Table 2, entry 1). Although increasing the Lewis acid amount to one and two equivalents with respect to the indole starting materials improved the conversion, the outcome of the reaction showed poor

regioselectivity. In addition, intractable tar formation was observed, which would possibly be linked to indole oligomerization (Table 2, entries 2 and 3). Switching to $TiCl_4$ and $SnCl_4$ Lewis acids proved ineffective as they presented very low conversions (Table 2, entries 4 and 5). Overall, the Lewis acid conditions were abandoned since no noticeable enhancements towards carbazoles was achieved.

Subsequently, in order to gain access to N-H functionalized carbazoles, we sought an electron-donating protecting group. Our quest for a suitable candidate started with silyl groups. Upon formation, the TMS, TBS, and TIPS-protected 3-chloroindoles were subjected to the IEDDA reaction with methyl coumalate (**21**) in toluene at 200 ^{o}C. After a 16 h time period, crude ^{1}H NMR results showed only trace amounts of desired carbazole products along with significant quantities of starting materials and decomposition byproducts. We then employed the acid-labile and electron-rich methoxymethyl ether protecting group, envisioning a strategy to promote the IEDDA-initiated cascade reaction followed by an *in situ* deprotection of the MOM group through the action of the HCl byproduct to deliver methyl carbazole-3-carboxylate (**31**). Unfortunately, only decomposition products were obtained as a result of the domino process. We were rewarded in protecting group search when 1-benzyl-3-chloroindole (**57b**) proved to be stable at elevated temperatures.

Upon arriving at a good protecting group, we set out to systematically optimize the reaction conditions. We selected 1-benzyl-3-chloroindole (**57b**) as the model system to investigate the parameters of time, equivalence of methyl coumalate (**21**), and

concentration. We settled on 200 °C as the reaction temperature since the lower temperatures did not provide enough activation energy for the system.

As presented in Table 3, generally 16 h was necessary to generate carbazole **60b**, as prolonging the reaction time did not make a significant impact in the product ratio. In fact, undesirable tar formation was observed in entry 11 when the reaction was heated for 48 hours, which accounted for the product loss.

Table 3. Lewis acid-mediated IEDDA reaction of **57b** and **21**[a]

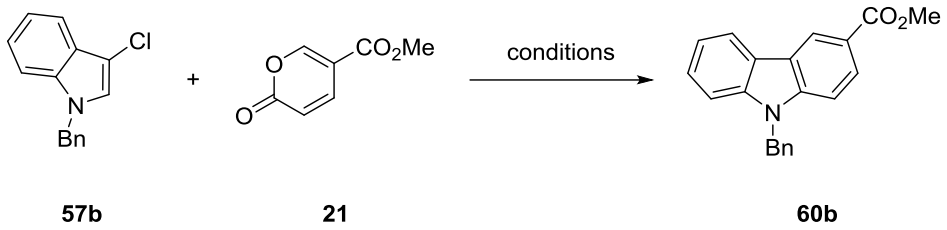

57b **21** **60b**

entry	time (h)	equiv **21**	concn (M)	**60b**:**57b** ratio[b]
1	6	10	0.5	1:5.5
2	16	10	0.2	1:0
3	16	6	0.1	1:0.8
4	**16**	**6**	**0.2**	**1:0**
5	16	5	0.2	1:0.1
6	16	5	0.2	1:0.1
7	16	3	neat	1:2.4
8	16	3	0.2	1:4.0
9	16	3	0.05	1:6.7
10	24	3	0.2	1:0.5
11	48	3	0.2	1:0.4

[a] All reactions were run at 200 °C in toluene.

[b] Ratios were determined by integration of crude ^{1}H NMR.

Furthermore, the relative equivalents of methyl coumalate (**21**) to indole **57b** was investigated. A number of trials showed that excess equivalents of **21** promotes full conversion within 16 h. Overall, the best conditions were achieved when 6 equivalents of **21** reacted with **57b** for in 0.2 M concentration for 16 hours as highlighted in Table 3, entry 4.

After optimizing the reaction conditions according to the model system, the stage was set for exploring the scope and limitations of our methodology. We started with **57a** which cleanly generated **60a** in 90% yield. This was very promising since similar 9-alkylcarbazole-3-carboxylates show antiviral activity. Moreover, 9-benzyl carbazole **60b** was afforded in 65% yield. Incorporation of electron-donating groups on the 5- and 7-position of the indole was effective to improve the efficiency of the IEDDA cascade reaction, as was the case for **60c,** which was isolated in 71% yield. Indoles **57d** and **57e**, empowered by electron-rich methoxy substitutions, gave access to **60d** and **60e** in 80% and 77% yields, respectively. In addition, the methodology successfully produced 3-carbomethoxy-11*H*-benzo[*a*]carbazole **60f** in 67% yield as a single regioisomer.

Our initial success with the electron-donating groups motivated us to investigate the influence of electron-withdrawing groups on the starting indole. We envisioned that the construction of a halogen-substituted carbazole derivative would be a valuable synthon for further functionalization through the transition metal cross-coupling technologies. With that in mind, bromo-substituted carbazoles **60g** and **60h** were produced in 42% and 56% yields, respectively. The lower yields were presumably due to the slower rate of the reaction caused by the inductively electron-withdrawing bromide moiety (Scheme 9).

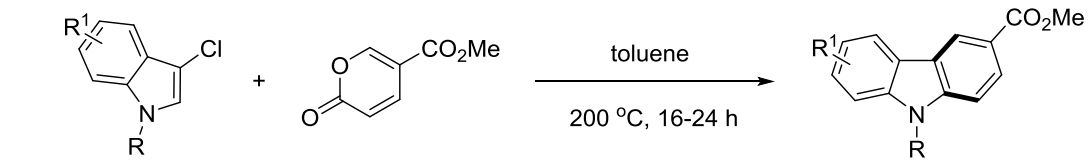

57a-k **21** **60a-k**

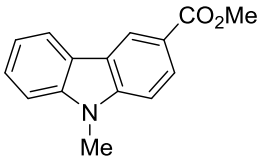

60a, 90%

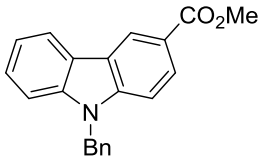

60b, 65%

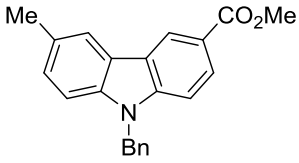

60c, 71%

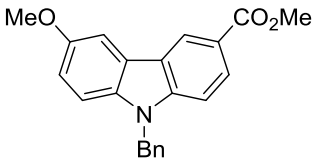

60d, 80%

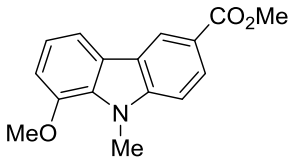

60e, 77%

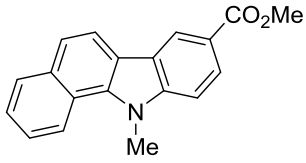

60f, 67%

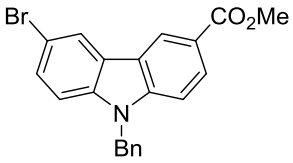

60g, 42%

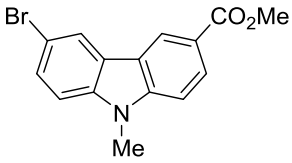

60h, 56%

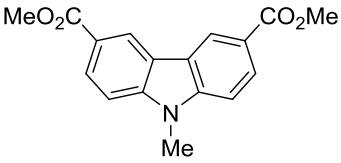

60i, 49%

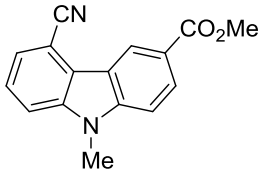

60j, 0%

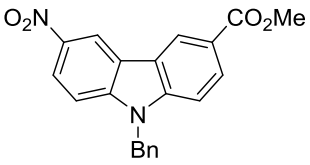

60k, 0%

Scheme 9. Scope and limitations of the methodology[a,b].

[a] Reagents and conditions: **57a–k** (1.0 equiv), **21** (6.0 equiv), toluene (0.2 M). All yields are isolated. Reaction time was 24 h for **60f–i**. [b] Acetonitrile was used as the solvent for **60a**.

Integration of the ester functionality on the indole was conveniently tolerated by the overall electronics of the system, giving rise to the symmetrical carbazole **60i** in 49% yield. Generally, the electron-deficient indoles **57f-i** required longer reaction time frames compared to the parent indoles **57a-b**. However, we did not prolong the reaction times more for than 24 hours from an efficiency standpoint.

Lastly, the cyano- and nitro- substituents were too highly deactivating; thus, the formation of carbazoles **60j** and **60k** were not observed. Nevertheless, these results verified the vital importance of effectively matching the electronics of the diene and the dienophile in IEDDA reactions.

After demonstrating the scope and limitations of our methodology, we attempted to access the naturally occurring carbazoles *via* a trivial deprotection of the benzyl protecting group. As shown in Scheme 10, $AlCl_3$-mediated deprotection of **60b** and **60d** were accomplished in toluene at ambient temperature by altering the literature procedure[35], affording the natural carbazole alkaloids **31** and **38** in 82% and 97% yields, respectively. The characterization data of **31** and **38** matched the previously reported literature values.[28,36,37]

Overall, the successful debenzylation of the representative carbazoles paved the way for our method to potentially allow access to all the other natural carbazoles presented in Figure 2 by straightforward manipulation[38] of the oxidation states.

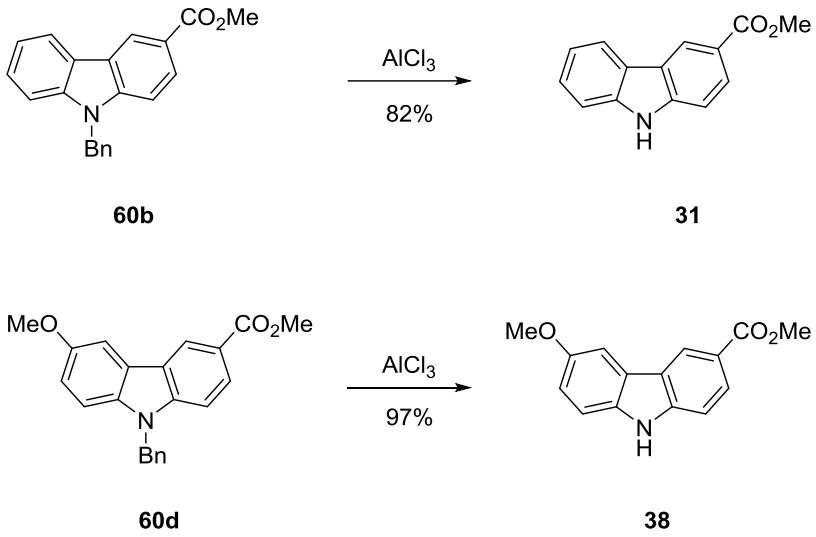

Scheme 10. Synthesis of naturally occurring carbazoles **31** and **38** through deprotection[a].
[a] Reagents and conditions: **60b** and **60d** (1.0 equiv), $AlCl_3$ (6.0 equiv), toluene (0.1 M), 23 °C, 6-24 h.

2.3. Conclusions

The Indole 2,3-carbon–carbon double bond moiety has been successfully exploited in IEDDA reactions to construct biologically active natural products ever since being uncovered by both Seitz and Takahashi. The utility of the indole dienophiles were mostly restricted to electron-poor azadienes, *o*-azaquinones, and *o*-azaxylylenes in IEDDA reactions. Inspired by our group's prior achievements, we expanded the scope of the IEDDA reaction through demonstration of the first successful example of the IEDDA reaction between substituted indoles and a 2-pyrone methyl coumalate to efficiently synthesize carbazole alkaloids. Our new methodology hinged on a thermally-induced, metal-free, single-pot IEDDA/decarboxylation/aromatization cascade sequence to produce carbazoles with exclusive regiospecificity. The key to our success was the use of 1-alkyl-

3-chloroindoles as the electron-rich dienophiles, since the presence of the chloride group was advantageous not only because of its easy introduction to the indole scaffold, but also to prevent ring-opening of the pyrrole component while promoting the aromatization. In summary, this methodology provides a rapid route to natural and synthetic carbazoles in up to 90% yield, and holds potential applicability to complex alkaloids.

2.4. Experimental

General Procedures

All starting materials were purchased from Sigma-Aldrich; solvents were purchased from Fisher Scientific and used without further purification. Sodium hydride (60% in mineral oil) was purchased from TCI America. All reactions were carried out in flame-dried glassware under argon with dry solvents under anhydrous conditions. All yields refer to chromatographically isolated products. Reactions were monitored by thin-layer chromatography (TLC) carried out on 0.20 mm silica gel plates using UV light as a visualizing agent and either potassium permanganate or 5% sulfuric acid in methanol with heat as developing agents. Silica gel 60Å, particle size 0.032 – 0.063 mm, was used for flash column chromatography. ^{1}H and ^{13}C NMR spectra were acquired in $CDCl_3$ on a Varian MR-400 or Bruker Avance III 600 MHz spectrometer. ^{1}H and ^{13}C chemical shifts (δ) are given in ppm relative to the residual protonated solvent peak ($CDCl_3$: δ_H = 7.26 ppm, δ_C = 77.0 ppm; CD_3OD: δ_H = 3.31 ppm, δ_C =49.0 ppm; $(CD_3)_2SO$: δ_H = 2.50 ppm, δ_C = 39.52 ppm; $(CD_3)_2CO$: δ_H = 2.05 ppm, δ_C = 29.84 ppm) as an internal reference. High-

resolution mass spectra (HRMS) were recorded on an Agilent 6540 QTOF (quadrupole time of flight) mass spectrometer using ESI (electrospray ionization) or APCI (atmospheric-pressure chemical ionization), or EI (electron ionization) on an Agilent 6890 GC/MS.

Selected Experimental, Physical, and Spectral Data

Chlorination of indoles:

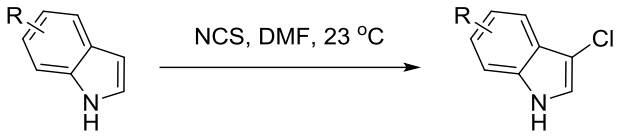

61a-j **62a-j**

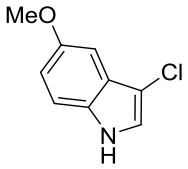

62d

3-Chloro-5-methoxy-1*H*-indole (62d). The preparation of **62d** is representative. Over the course of the reaction, the flask was protected from light. To a solution of 5-methoxyindole **61d** (2.0 g, 13.59 mmol) in DMF (56 mL) at room temperature was added NCS (1.91 g, 14.27 mmol). The reaction was monitored by TLC to determine complete consumption of starting material. (In most cases, the R_f of the starting material and product were very similar but differed when stained with 5% H_2SO_4/MeOH). Afterwards, brine (30 mL) was added to the reaction mixture and the aqueous layer was extracted with ethyl

acetate (3 x 30 mL). The organic layer was washed with water (3 x 30 mL) and brine (30 mL), dried over sodium sulfate, and concentrated *in vacuo*. The crude product was purified by flash column chromatography (silica gel, EtOAc:hexanes 1:9 to 2:8) to afford **62d** (2.08 g, 84% yield) as a white solid. **62d:** R_f = 0.54 (silica gel, EtOAc:hexanes 1:2); ^{1}H NMR ($CDCl_3$, 400 MHz) δ = 7.96 (brs, 1H), 7.25 (d, *J* = 8.0 Hz, 1H), 7.15 (d, *J* = 2.6 Hz, 1H), 7.05 (d, *J* = 2.3 Hz, 1H), 6.90 (dd, *J* = 8.8, 2.3 Hz, 1H), 3.89 (s, 3H) ppm; ^{13}C NMR ($CDCl_3$, 100 MHz) δ = 154.8, 129.9, 125.7, 121.4, 114.0, 112.4, 106.1, 99.2, 55.8 ppm; HRMS (APCI-TOF) calcd for C_9H_9ClNO $[M + H]^+$ 182.0367, found 182.0365.

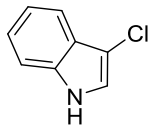

62a/62b

3-Chloroindole (62a = 62b). Both **62a** and **62b** describe the same intermediate, which was prepared according to the literature procedure[39] and all characterization data (^{1}H NMR, ^{13}C NMR, and mass spectrometry) matched those previously reported.

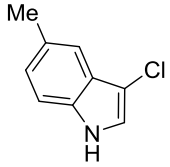

62c

3-Chloro-5-methyl-1*H*-indole (62c): White solid (0.27 g, 86% yield); R_f = 0.76 (silica gel, EtOAc:hexanes 1:1); ^{1}H NMR ($CDCl_3$, 400 MHz) δ = 7.95 (brs, 1H), 7.43 (s, 1H), 7.25

(d, *J* = 8.3 Hz, 1H), 7.14 (d, *J* = 2.6 Hz, 1H), 7.08 (dd, *J* = 8.4, 1.5 Hz, 1H), 2.48 (s, 3H) ppm; ^{13}C NMR ($CDCl_3$, 100 MHz) δ = 133.2, 129.9, 125.5, 124.8, 120.8, 117.7, 111.1, 105.9, 21.4 ppm; HRMS (EI-TOF) calcd for C_9H_9ClN $[M + H]^+$ 166.0423, found 166.0427.

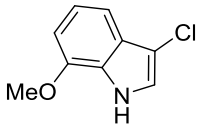

62e

3-Chloro-7-methoxy-1*H*-indole (62e): Brown oil (0.26 g, 70% yield); R_f = 0.38 (silica gel, EtOAc:hexanes 1:3); ^{1}H NMR ($CDCl_3$, 600 MHz) δ = 8.28 (brs, 1H), 7.29 (dt, *J* = 8.1, 0.8 Hz, 1H), 7.16 – 7.13 (m, 2H), 6.71 (dd, *J* = 7.7, 0.8 Hz, 1H), 3.98 (s, 3H) ppm; ^{13}C NMR ($CDCl_3$, 150 MHz) δ = 146.0, 126.6, 125.6, 120.8, 120.4, 110.7, 106.7, 102.6, 55.3 ppm; HRMS (APCI-TOF) calcd for C_9H_9ClNO $[M + H]^+$ 182.0367, found 182.0362.

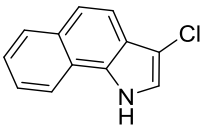

62f

3-Chloro-1*H*-benzo[*g*]indole (62f): White-green solid (0.26 g, 73% yield); R_f = 0.36 (silica gel, EtOAc:hexanes 1:3); ^{1}H NMR ($CDCl_3$, 600 MHz) δ = 8.74 (s, 1H), 7.96 (dd, *J* = 10.9, 8.2 Hz, 2H), 7.72 (d, *J* = 8.7 Hz, 1H), 7.59 (d, *J* = 8.6 Hz, 1H), 7.56 (ddd, *J* = 8.2, 7.0, 1.2 Hz, 1H), 7.48 (ddd, *J* = 8.1, 7.0, 1.2 Hz, 1H), 7.24 (d, *J* = 2.6 Hz, 1H) ppm; ^{13}C NMR ($CDCl_3$, 150 MHz) δ = 130.8, 129.8, 129.1, 125.9, 124.6, 121.5 (2C), 121.4, 119.0,

118.9, 117.7, 108.2 ppm; HRMS (APCI-TOF) calcd for $C_{12}H_8ClN$ [*M* + H]$^+$ 202.0418, found 202.0416.

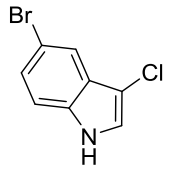

62g/62h

5-Bromo-3-chloro-1*H*-indole (62g = 62h): (Both **62g** and **62h** describe the same intermediate). White-purple solid (2.05 g, 87% yield); R_f = 0.79 (silica gel, EtOAc:hexanes 1:1); ^{1}H NMR ($CDCl_3$, 400 MHz) δ = 8.13 (brs, 1H), 7.78 (d, *J* = 1.8 Hz, 1H), 7.33 (dd, *J* = 8.7, 1.8 Hz, 1H), 7.24 (d, *J* = 8.7 Hz, 1H), 7.19 (d, *J* = 2.6 Hz, 1H) ppm; ^{13}C NMR ($CDCl_3$, 100 MHz) δ = 133.5, 127.0, 126.1, 122.0, 120.9, 113.8, 112.9, 106.0 ppm; HRMS (EI-TOF) calcd for C_8H_6BrClN [*M* + H]$^+$ 229.9372, found 229.9368.

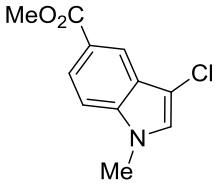

57i

Methyl 3-chloro-1-methylindole-5-carboxylate (57i): White solid (0.44 g, 84% yield); R_f = 0.29 (silica gel, EtOAc:hexanes 1:3); ^{1}H NMR ($CDCl_3$, 400 MHz) δ = 8.38 (d, *J* = 1.4 Hz, 1H), 7.96 (dd, *J* = 8.7, 1.4 Hz, 1H), 7.30 (d, *J* = 8.7 Hz, 1H), 7.07 (s, 1H), 3.95 (s, 3H), 3.78 (s, 3H) ppm; ^{13}C NMR ($CDCl_3$, 100 MHz) δ = 167.8, 138.1, 126.6, 125.3, 123.9, 122.0,

121.4, 109.3, 106.2, 51.9, 33.2 ppm; HRMS (APCI-TOF) calcd for $C_{11}H_{11}ClNO_2$ [*M* + H]$^+$ 224.0473, found 224.0469.

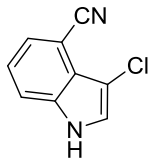

62j

3-Chloro-4-cyano-1*H*-indole (62j): White solid (0.12 g, 97% yield); R_f = 0.07 (silica gel, EtOAc:hexanes 1:3); ^{1}H NMR (CD_3OD, 600 MHz) δ = 7.70 (d, *J* = 8.3 Hz, 1H), 7.52 – 7.51 (m, 2H), 7.28 (t, *J* = 7.8 Hz, 1H) ppm; ^{13}C NMR (CD_3OD, 150 MHz) δ = 137.1, 128.3, 126.7, 125.0, 123.2, 119.0, 118.5, 105.3, 101.9 ppm; HRMS (ESI-TOF) calcd for $C_9H_6ClN_2$ [*M* + H]$^+$ 177.0214, found 177.0211.

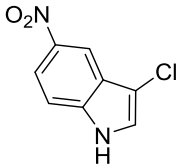

62k

3-Chloro-5-nitro-1*H*-indole (62k). Over the course of the reaction, the flask was protected from light. To a solution of 5-nitroindole (**61k**) (1.00 g, 6.17 mmol) in DMF (10 mL) at room temperature was added NCS (0.82 g, 6.18 mmol) and stirred for 20 hours. The reaction mixture was poured into water (100 mL) to generate a precipitate which was vacuum filtered and rinsed with water, then dried under vacuum to afford **62k** (1.11 g, 91% yield) as a pure yellow solid. **62k:** R_f = 0.53 (silica gel, EtOAc:hexanes 1:1); ^{1}H NMR

($(CD_3)_2CO$, 400 MHz) δ = 11.14 (brs, 1H), 8.47 (d, *J* = 2.2 Hz, 1H), 8.10 (dd, *J* = 9.0, 2.3 Hz, 1H), 7.71 (s, 1H), 7.66 (d, *J* = 9.1 Hz, 1H) ppm; ^{13}C NMR ($(CD_3)_2CO$, 100 MHz) δ = 142.9, 139.1, 126.8, 125.4, 118.6, 115.2, 113.6, 107.7 ppm; HRMS (EI-TOF) calcd for $C_8H_6ClN_2O_2$ $[M + H]^+$ 197.0117, found 197.0120.

Methylation of indoles:

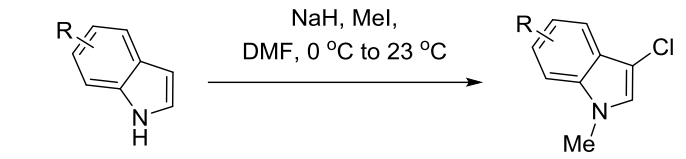

62b, 62e-f, 62h, 62j **57b, 57e-f, 57h, 57j**

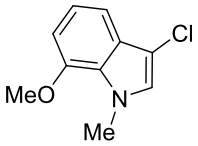

57d

3-Chloro-7-methoxy-1-methylindole (57e). The preparation of **57e** is representative. To a suspension of sodium hydride (62 mg, 60% suspension in mineral oil, 1.55 mmol) in DMF (5 mL) at 0 °C was added a solution of 3-chloro-7-methoxy-1*H*-indole (**62e**) (235 mg, 1.29 mmol) in DMF (3 mL), dropwise. The reaction mixture was warmed to room temperature and stirred for 30 minutes then cooled to 0 °C. Methyl iodide (0.10 mL, 1.68 mmol) was added dropwise at 0 °C, after which the reaction was warmed to room temperature and monitored by TLC. After approximately 1 hour, a saturated ammonium chloride solution (30 mL) was carefully added, and the aqueous layer was extracted with

diethyl ether (3 x 30 mL). The combined organic phases were washed with brine (30 mL), dried over sodium sulfate, and concentrated *in vacuo*. The crude product was purified by flash column chromatography (silica gel, EtOAc:hexanes 1:9 to 2:8) to afford **57e** (226 mg, 89% yield) as a pale tan solid. **57e:** R_f = 0.54 (silica gel, EtOAc:hexanes 1:3); ^{1}H NMR ($CDCl_3$, 400 MHz) δ = 7.21 (d, *J* = 8.0 Hz, 1H), 7.06 (t, *J* = 7.9 Hz, 1H), 6.90 (s, 1H), 6.65 (d, *J* = 7.7 Hz, 1H), 4.02 (s, 3H), 3.93 (s, 3H) ppm; ^{13}C NMR ($CDCl_3$, 100 MHz) δ = 147.8, 127.9, 126.2, 125.6, 120.4, 111.0, 104.1, 103.0, 55.4, 36.6 ppm; HRMS (APCI-TOF) calcd for $C_{10}H_{11}ClNO$ $[M + H]^+$ 196.0524, found 163.0520.

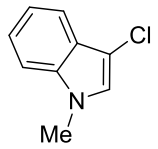

57a

3-Chloro-1-methylindole (57a): 57a was prepared according to the literature procedure[40] and all characterization data (^{1}H NMR, ^{13}C NMR, and mass spectrometry) matched those previously reported.

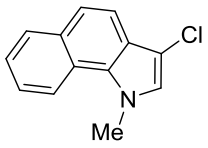

57f

3-Chloro-1-methylbenzo[*g*]indole (57f): Pale yellow solid (0.30 g, 97% yield); R_f = 0.57 (silica gel, EtOAc:hexanes 1:3); ^{1}H NMR ($CDCl_3$, 400 MHz) δ = 8.44 (d, *J* = 8.4 Hz, 1H),

7.97 (d, J = 8.0 Hz, 1H), 7.70 (d, J = 8.6 Hz, 1H), 7.58 – 7.54 (m, 2H), 7.47 (t, J = 8.3, 1H), 7.05 (s, 1H), 4.26 (s, 3H) ppm; ^{13}C NMR ($CDCl_3$, 100 MHz) δ = 131.6, 129.4, 129.3, 125.6, 125.3, 123.9, 123.1, 123.0, 121.6, 120.7, 117.8, 105.3, 38.6 ppm; HRMS (APCI-TOF) calcd for $C_{13}H_{10}ClN$ [M + H]$^+$ 216.0575, found 216.0573.

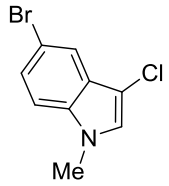

57h

5-Bromo-3-chloro-1-methylindole (57h): Pale yellow solid (0.49 g, 92% yield); R_f = 0.54 (silica gel, EtOAc:hexanes 1:3); ^{1}H NMR ($CDCl_3$, 400 MHz) δ = 7.74 (dd, J = 1.8, 0.6 Hz, 1H), 7.33 (dd, J = 8.7, 1.9 Hz, 1H), 7.16 (dd, J = 8.7, 0.6 Hz, 1H), 7.01 (s, 1H), 3.73 (s, 3H) ppm; ^{13}C NMR ($CDCl_3$, 100 MHz) δ = 134.4, 127.2, 126.3, 125.5, 120.9, 113.3, 111.0, 103.8, 33.1 ppm; HRMS (EI-TOF) calcd for C_9H_8BrClN [M + H]$^+$ 243.9528, found 243.9524.

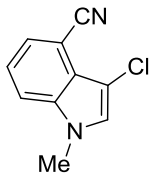

57j

3-Chloro-4-cyano-1-methylindole (57j): Yellow solid (0.10 g, 83% yield); R_f = 0.42 (silica gel, EtOAc:hexanes 1:1); ^{1}H NMR ($CDCl_3$, 600 MHz) δ = 7.52 (d, J = 8.4 Hz, 1H),

7.48 (d, *J* = 7.3 Hz, 1H), 7.26 (t, *J* = 7.9 Hz, 1H), 7.16 (s, 1H), 3.81 (s, 3H) ppm; ^{13}C NMR ($CDCl_3$, 150 MHz) δ = 135.8, 128.4, 127.0, 124.3, 122.0, 117.7, 114.4, 104.0, 101.9, 33.2 ppm; HRMS (ESI-TOF) calcd for $C_{10}H_8ClN_2$ $[M + H]^+$ 191.0371, found 191.0370.

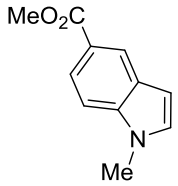

61i

Methyl 1-methylindole-5-carboxylate (61i): To a suspension of sodium hydride (273 mg, 60% suspension in mineral oil, 6.82 mmol) in DMF (9 mL) at 0 °C was added a solution of 1*H*-indole-5-carboxylic acid (500 mg, 3.10 mmol) in DMF (9 mL), dropwise. The reaction mixture was warmed to room temperature and stirred for 30 minutes then cooled to 0 °C. Methyl iodide (0.48 mL, 7.75 mmol) was added dropwise at 0 °C, after which the reaction was warmed to room temperature and monitored by TLC. After approximately 1 hour, a saturated ammonium chloride solution (10 mL) was carefully added, and the aqueous layer was extracted with diethyl ether (3 x 10 mL). The combined organic phases were washed with water (2 x 10 mL), brine (10 mL), dried over sodium sulfate, and concentrated *in vacuo* to afford pure **61i** (0.52 g, 88% yield) as a yellow solid. **61i:** R_f = 0.44 (silica gel, EtOAc:hexanes 1:3); ^{1}H NMR ($CDCl_3$, 400 MHz) δ = 8.40 (s, 1H), 7.93 (d, *J* = 8.7 Hz, 1H), 7.33 (d, *J* = 8.7 Hz, 1H), 7.11 (d, *J* = 3.1 Hz, 1H), 6.59 (d, *J* = 3.4 Hz, 1H), 3.93 (s, 3H), 3.82 (s, 3H) ppm; ^{13}C NMR ($CDCl_3$, 100 MHz) δ = 168.2,

139.1, 130.2, 127.9, 123.9, 122.9, 121.3, 108.8, 102.6, 51.8, 33.0 ppm; HRMS (EI-TOF) calcd for $C_{11}H_{12}NO_2$ [*M* + H]$^+$ 190.0868, found 190.0871.

Benzylation of indoles:

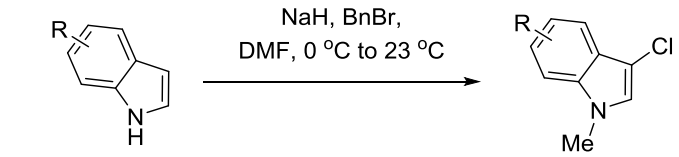

62b, 62c-d, 62g, 62k **57b, 57c-d, 57g, 57k**

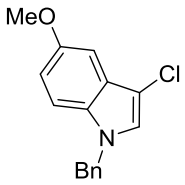

57d

1-Benzyl-3-chloro-5-methoxyindole (57d): The preparation of **57d** is representative. To a solution of 3-chloro-5-methoxy-1*H*-indole (**62d**) (0.71 g, 3.89 mmol) in DMF (4 mL) was added NaH (19 mg, 60% suspension in mineral oil, 4.67 mmol) at 0 °C. The reaction mixture was warmed to room temperature and stirred for 30 minutes then cooled to 0 °C. Benzyl bromide (0.51 mL, 4.28 mmol) was added dropwise at 0 °C, after which the reaction was warmed to room temperature and monitored by TLC. After approximately 1 hour, the reaction was carefully quenched with a saturated ammonium chloride solution (30 mL) was added and the aqueous layer was extracted with diethyl ether (3 x 30 mL). The combined organic layers were washed with brine (30 mL), dried over sodium sulfate, and

concentrated *in vacuo*. The crude product was purified by flash column chromatography (silica gel, EtOAc:hexanes 1:9 to 2:8) to afford **57d** (1.06 g, 94% yield) as a white solid. **57d:** R_f = 0.60 (silica gel, EtOAc:hexanes 1:3); ^{1}H NMR ($CDCl_3$, 400 MHz) δ = 7.34 – 7.27 (m, 3H), 7.16 (d, *J* = 8.9 Hz, 1H), 7.13 – 7.09 (m, 2H), 7.06 (s, 1H), 7.05 (d, *J* = 2.4 Hz, 1H), 6.87 (dd, *J* = 8.9, 2.5 Hz, 1H), 5.24 (s, 2H), 3.88 (s, 3H) ppm; ^{13}C NMR ($CDCl_3$, 100 MHz) δ = 154.6, 136.9, 130.6, 128.8, 127.8, 126.8, 126.3, 125.0, 113.6, 111.0, 104.5, 99.4, 55.7, 50.4 ppm; HRMS (APCI-TOF) calcd for $C_{16}H_{15}ClNO$ $[M + H]^+$ 272.0837, found 272.0840.

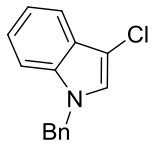

57b

1-Benzyl-3-chloroindole (57b): Yellow solid (1.59 g, 79% yield); R_f = 0.50 (silica gel, EtOAc:hexanes 1:9); ^{1}H NMR ($CDCl_3$, 600 MHz) δ = 7.64 (dd, *J* = 7.6, 1.2 Hz, 1H), 7.33 – 7.28 (m, 4H), 7.23 (t, *J* = 7.2 Hz, 1H), 7.19 (t, *J* = 7.3 Hz, 1H), 7.13 (d, *J* = 7.1 Hz, 2H), 7.09 (s, 1H), 5.28 (s, 2H) ppm; ^{13}C NMR ($CDCl_3$, 150 MHz) δ = 136.8, 135.5, 128.9, 127.9, 126.9, 126.0, 124.6, 122.8, 120.2, 118.5, 109.9, 105.3, 50.2 ppm; HRMS (APCI-TOF) calcd for $C_{15}H_{13}ClN$ $[M + H]^+$ 242.0731, found 242.0731.

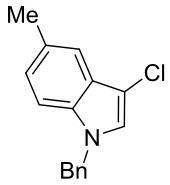

57c

1-Benzyl-3-chloro-5-methylindole (57c): Yellow oil (0.37 g, 88% yield); R_f = 0.74 (silica gel, EtOAc:hexanes 1:3); ^{1}H NMR ($CDCl_3$, 400 MHz) δ = 7.46 (s, 1H), 7.33 – 7.29 (m, 3H), 7.19 (d, *J* = 8.5 Hz, 1H), 7.15 – 7.11 (m, 2H), 7.09 – 7.06 (m, 2H), 5.24 (s, 2H), 2.50 (s, 3H) ppm; ^{13}C NMR ($CDCl_3$, 100 MHz) δ = 136.9, 133.9, 129.6, 128.8, 127.8, 126.8, 126.1, 124.6, 124.5, 118.0, 109.7, 104.6, 50.2, 21.4 ppm; HRMS (APCI-TOF) calcd for $C_{16}H_{15}ClN$ [*M* + H]$^+$ 256.0893, found 256.0888.

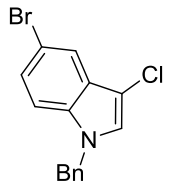

57g

1-Benzyl-5-bromo-3-chloroindole (57g): Yellow solid (1.43 g, 94% yield); R_f = 0.63 (silica gel, EtOAc:hexanes 1:3); ^{1}H NMR ($CDCl_3$, 400 MHz) δ = 7.77 (d, *J* = 1.8 Hz, 1H), 7.32 – 7.28 (m, 4H), 7.14 (d, *J* = 8.8 Hz, 1H), 7.11 – 7.09 (m, 3H), 5.25 (s, 2H) ppm; ^{13}C NMR ($CDCl_3$, 100 MHz) δ = 136.3, 134.1, 128.9, 128.1, 127.5, 126.8, 125.8 (2C), 121.1, 113.6, 111.5, 104.6, 50.4 ppm; HRMS (APCI-TOF) calcd for $C_{15}H_{12}BrClN$ [*M* + H]$^+$ 319.9836, found 319.9835.

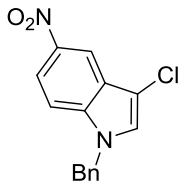

57k

1-Benzyl-3-chloro-5-nitroindole (57k): Yellow-orange solid (0.71 g, 98% yield); R_f = 0.38 (silica gel, EtOAc:hexanes 1:3); ^{1}H NMR ($CDCl_3$, 600 MHz) δ = 8.62 (d, *J* = 2.2 Hz, 1H), 8.13 (dd, *J* = 9.1, 2.3 Hz, 1H), 7.35 – 7.33 (m, 4H), 7.24 (s, 1H), 7.13 (dd, *J* = 7.9, 1.6 Hz, 2H), 5.33 (s, 2H) ppm; ^{13}C NMR ($CDCl_3$, 150 MHz) δ = 142.2, 138.0, 135.4, 129.2, 128.5, 127.7, 126.9, 125.5, 118.4, 116.1, 110.2, 108.1, 50.8 ppm; HRMS (ESI-TOF) calcd for $C_{15}H_{12}ClN_2O_2$ $[M + H]^+$ 287.0583, found 287.0584.

IEDDA/decarboxylation/aromatization reaction to carbazoles:

57a-k **21** **60a-k**

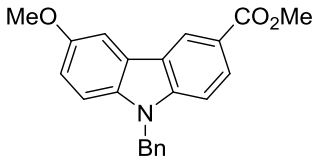

60d

Methyl 9-benzyl-6-methoxycarbazole 3-carboxylate (60d): The preparation of **60d** is representative, with the exception of **60f**-**60i** which were run for 24 hours. To a sealable 65-mL pressure vessel was successively added 1-benzyl-3-chloro-5-methoxyindole **57d** (100 mg, 0.37 mmol), methyl coumalate (**21**) (340 mg, 2.2 mmol), and toluene (1.8 mL) under argon. The solution was heated to 200 °C and stirred for 16 h. Upon completion of the reaction, the sealable pressure vessel was cooled to room temperature. The solution was transferred to another flask, while rinsing with ethyl acetate, after which the solution was concentrated *in vacuo*. The crude product was purified by flash column chromatography (silica gel, EtOAc:hexanes 1:9 to 2:8) to afford **60d** (0.10 g, 80% yield) as a yellow solid. **60d:** R_f = 0.46 (silica gel, EtOAc:hexanes 1:3); ^{1}H NMR ($CDCl_3$, 400 MHz) δ = 8.82 (d, *J* = 1.2 Hz, 1H), 8.12 (dd, *J* = 8.7, 1.7 Hz, 1H), 7.66 (d, *J* = 2.4 Hz, 1H), 7.34 (d, *J* = 8.6 Hz, 1H), 7.29 – 7.23 (m, 4H), 7.13 – 7.07 (m, 3H), 5.50 (s, 2H), 3.97 (s, 3H), 3.94 (s, 3H) ppm; ^{13}C NMR ($CDCl_3$, 100 MHz) δ = 167.8, 154.5, 143.7, 136.6, 136.0,

128.9, 127.6, 127.4, 126.3, 123.6, 122.9, 122.6, 120.6, 115.8, 110.2, 108.5, 103.4, 56.0, 51.9, 46.8 ppm; HRMS (APCI-TOF) calcd for $C_{22}H_{20}NO_3$ $[M + H]^+$ 346.1438, found 346.1441.

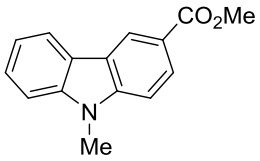

60a

Methyl 9-methylcarbazole-3-carboxylate (60a): White solid (65 mg, 90% yield); R_f = 0.73 (silica gel, EtOAc:hexanes 1:1); ^{1}H NMR ($CDCl_3$, 400 MHz) δ = 8.82 (d, *J* = 1.6 Hz, 1H), 8.18 (dd, *J* = 8.6, 1.7 Hz, 1H), 8.14 (dt, *J* = 7.9, 0.9 Hz, 1H), 7.52 (ddd, *J* = 8.3, 7.2, 1.2 Hz, 1H), 7.42 (d, *J* = 8.2 Hz, 1H), 7.38 (d, *J* = 8.6 Hz, 1H), 7.30 (t, *J* = 7.4 Hz, 1H), 3.98 (s, 3H), 3.85 (s, 3H) ppm; ^{13}C NMR ($CDCl_3$, 100 MHz) δ = 167.9, 143.5, 141.5, 127.3, 126.4, 122.9, 122.8, 122.5, 120.7, 120.6, 119.9, 108.8, 107.9, 51.9, 29.2 ppm; HRMS (ESI-TOF) calcd for $C_{15}H_{14}NO_2$ $[M + H]^+$ 240.1019, found 240.1022.

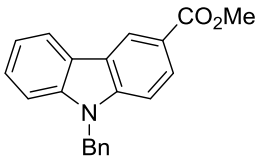

60b

Methyl 9-benzylcarbazole-3-carboxylate (60b): Yellow solid (42 mg, 65% yield); R_f = 0.47 (silica gel, EtOAc:hexanes 1:3); ^{1}H NMR ($CDCl_3$, 400 MHz) δ = 8.87 (dd, *J* = 1.6, 0.6 Hz, 1H), 8.18 (dt, *J* = 8.0, 1.0 Hz, 1H), 8.14 (dd, *J* = 8.6, 1.7 Hz, 1H), 7.47 (ddd, *J* =

8.3, 7.1, 1.2 Hz, 1H), 7.41 – 7.35 (m, 2H), 7.34 – 7.29 (m, 1H), 7.29 – 7.24 (m, 3H), 7.13 (dd, *J* = 7.6, 1.8 Hz, 2H), 5.53 (s, 2H), 3.98 (s, 3H) ppm; ^{13}C NMR ($CDCl_3$, 100 MHz) δ = 167.8, 143.3, 141.2, 136.4, 128.9, 127.7, 127.5, 126.6, 126.3, 123.1, 122.9, 122.8, 121.1, 120.7, 120.2, 109.3, 108.4, 51.9, 46.7 ppm; HRMS (APCI-TOF) calcd for $C_{21}H_{18}NO_2$ [*M* + H]$^+$ 316.1332, found 316.1336.

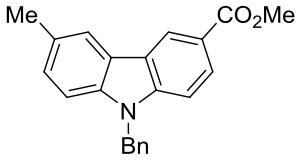

60c

Methyl 9-benzyl-6-methylcarbazole-3-carboxylate (60c): Pale brown solid (45 mg, 71% yield); R_f = 0.51 (silica gel, EtOAc:hexanes 1:3); ^{1}H NMR ($CDCl_3$, 600 MHz) δ = 8.80 (d, *J* = 2.0 Hz, 1H), 8.09 (d, *J* = 8.6 Hz, 1H), 7.95 (s, 1H), 7.29 (d, *J* = 8.6 Hz, 1H), 7.25 – 7.19 (m, 5H), 7.08 (d, *J* = 7.0 Hz, 2H), 5.45 (s, 2H), 3.94 (s, 3H), 2.52 (s, 3H) ppm; ^{13}C NMR ($CDCl_3$, 100 MHz) δ = 167.8, 143.5, 139.4, 136.6, 129.6, 128.8, 127.8, 127.6, 127.3, 126.3, 123.2, 122.8, 122.6, 120.8, 120.6, 109.0, 108.3, 51.9, 46.7, 21.4 ppm; HRMS (APCI-TOF) calcd for $C_{22}H_{20}NO_2$ [*M* + H]$^+$ 330.1489, found 330.1492.

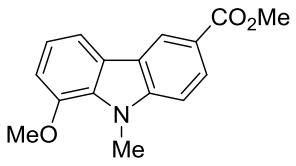

60e

Methyl 8-methoxy-9-methylcarbazole-3-carboxylate (**60e**): Pale yellow solid (53 mg, 77% yield); R_f = 0.43 (silica gel, EtOAc:hexanes 1:3); ^{1}H NMR ($CDCl_3$, 400 MHz) δ = 8.78 (s, 1H), 8.16 (d, *J* = 8.6 Hz, 1H), 7.74 (d, *J* = 7.8 Hz, 1H), 7.36 (d, *J* = 8.7 Hz, 1H), 7.18 (t, *J* = 7.8 Hz, 1H), 6.95 (d, *J* = 7.9 Hz, 1H), 4.17 (s, 3H), 3.99 (s, 3H), 3.98 (s, 3H) ppm; ^{13}C NMR ($CDCl_3$, 100 MHz) δ = 167.9, 147.1, 143.8, 130.7, 127.0, 124.7, 122.8, 122.5, 120.5, 120.3, 113.0, 108.1, 107.7, 55.6, 51.8, 32.4 ppm; HRMS (APCI-TOF) calcd for $C_{16}H_{16}NO_3$ $[M + H]^+$ 270.1125, found 270.1124.

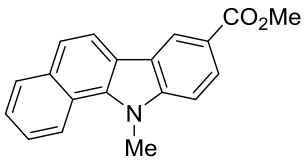

60f

Methyl 11-methylbenzo[*a*]carbazole-8-carboxylate (**60f**): Yellow solid (45 mg, 67% yield); R_f = 0.52 (silica gel, EtOAc:hexanes 1:3); ^{1}H NMR ($CDCl_3$, 600 MHz,) δ = 8.89 (d, *J* = 1.6 Hz, 1H), 8.70 (d, *J* = 8.5 Hz, 1H), 8.22 – 8.19 (m, 2H), 8.06 (d, *J* = 8.0 Hz, 1H), 7.72 (d, *J* = 8.5 Hz, 1H), 7.62 (t, *J* = 8.2 Hz, 1H), 7.57 (d, *J* = 7.9 Hz, 1H), 7.54 (d, *J* = 8.7 Hz, 1H), 4.43 (s, 3H), 4.00 (s, 3H) ppm; ^{13}C NMR ($CDCl_3$, 150 MHz) δ = 167.9, 143.1, 136.2, 133.8, 129.5, 126.1, 125.5, 125.0, 122.6 (2C), 122.4, 121.9, 121.5, 121.4, 119.3,

119.0, 108.6, 52.0, 34.3 ppm; HRMS (ESI-TOF) calcd for $C_{19}H_{16}NO_2$ $[M + H]^+$ 290.1176, found 290.1179.

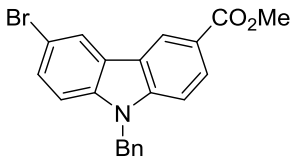

60g

Methyl 9-benzyl-6-bromocarbazole-3-carboxylate (60g): White-orange solid (52 mg, 42% yield); R_f = 0.50 (silica gel, EtOAc:hexanes 1:3); ^{1}H NMR ($CDCl_3$, 400 MHz) δ = 8.75 (d, *J* = 1.7 Hz, 1H), 8.23 (d, *J* = 1.9 Hz, 1H), 8.13 (dd, *J* = 8.6, 1.7 Hz, 1H), 7.50 (dd, *J* = 8.7, 1.8 Hz, 1H), 7.33 (d, *J* = 8.7 Hz, 1H), 7.29 – 7.23 (m, 3H), 7.20 (d, *J* = 8.7 Hz, 1H), 7.09 – 7.05 (m, 2H), 5.44 (s, 2H), 3.96 (s, 3H) ppm; ^{13}C NMR ($CDCl_3$, 100 MHz) δ = 167.5, 143.4, 139.8, 135.9, 129.2, 128.9, 128.1, 127.8, 126.2, 124.8, 123.4, 123.0, 121.7, 121.6, 113.1, 110.8, 108.6, 52.0, 46.8 ppm; HRMS (APCI-TOF) calcd for $C_{21}H_{17}BrNO_2$ $[M + H]^+$ 394.0437, found 394.0438.

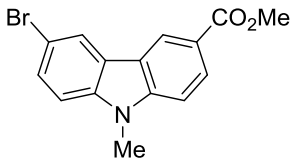

60h

Methyl 6-bromo-9-methylcarbazole-3-carboxylate (60h): Pale tan solid (37 mg, 56% yield); R_f = 0.23 (silica gel, EtOAc:hexanes 1:3); ^{1}H NMR ($CDCl_3$, 600 MHz) δ = 8.77 (d, *J* = 1.3 Hz, 1H), 8.25 (d, *J* = 1.9 Hz, 1H), 8.20 (dd, *J* = 8.6, 1.6 Hz, 1H), 7.60 (dd, *J* = 8.6,

1.9 Hz, 1H), 7.40 (d, *J* = 8.6 Hz, 1H), 7.30 (d, *J* = 8.6 Hz, 1H), 3.98 (s, 3H), 3.86 (s, 3H) ppm; ^{13}C NMR ($CDCl_3$, 150 MHz) δ = 167.6, 143.7, 140.2, 129.0, 127.9, 124.5, 123.3, 123.0, 121.4, 121.2, 112.8, 110.3, 108.2, 52.0, 29.4 ppm; HRMS (APCI-TOF) calcd for $C_{15}H_{13}BrNO_2$ $[M + H]^+$ 318.0124, found 318.0124.

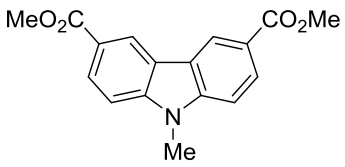

60i

Dimethyl 9-methylcarbazole-3,6-dicarboxylate (60i): Pale yellow solid (33 mg, 49% yield); R_f = 0.61 (silica gel, EtOAc:hexanes 1:1); ^{1}H NMR ($CDCl_3$, 400 MHz) δ = 8.82 (s, 2H), 8.20 (d, *J* = 8.5 Hz, 2H), 7.39 (d, *J* = 8.6 Hz, 2H), 3.98 (s, 6H), 3.86 (s, 3H) ppm; ^{13}C NMR ($CDCl_3$, 100 MHz) δ = 167.5, 144.1, 127.9, 122.9, 122.6, 121.8, 108.4, 52.0, 29.5 ppm; HRMS (APCI-TOF) calcd for $C_{17}H_{16}NO_4$ $[M + H]^+$ 298.1074, found 298.1072.

Deprotection of carbazoles:

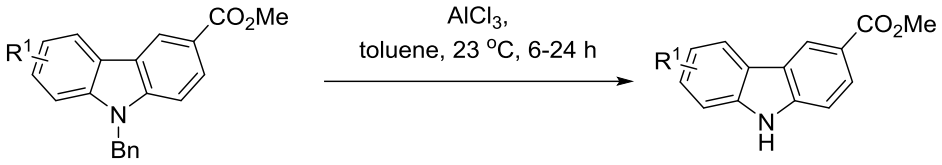

60b, 60d **31, 38**

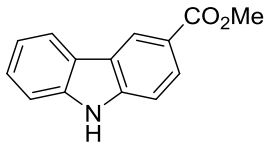

31

Methyl 9*H*-carbazole-3-carboxylate (**31**)**:** The preparation of **31** is representative, but methyl 9-benzyl-6-methoxycarbazole-3-carboxylate (**60d**) only required 6 hours. To a suspension of $AlCl_3$ (80 mg, 0.6 mmol) in toluene (1 mL) at room temperature was added a solution of methyl 9-benzylcarbazole-3-carboxylate (**60b**) (32 mg, 0.1 mmol) in toluene (1 mL), dropwise. The mixture was stirred at room temperature and monitored by TLC for complete consumption of starting material. After 24 hours, the reaction was quenched with saturated sodium bicarbonate (5 mL), diluted with dichloromethane (10 mL), and the organic layer washed with saturated sodium bicarbonate (2 x 5 mL) and brine (5 mL), dried over sodium sulfate, and concentrated *in vacuo*. The crude product was purified by flash column chromatography (silica gel, EtOAc:hexanes 1:3) to afford **31** (19 mg, 82% yield) as pale yellow solid. (The natural product NMR data was reported in both $CDCl_3$ and $(CD_3)_2SO$ to compare the spectra in the same originally reported solvent and to provide another experimentally convenient comparison). **31:** R_f = 0.40 (silica gel, EtOAc:hexanes

1:3); ^{1}H NMR ($CDCl_3$, 400 MHz) δ = 8.83 – 8.82 (m, 1H), 8.36 (s, 1H), 8.13 (ddd, *J* = 7.9, 4.5, 1.3 Hz, 2H), 7.47 – 7.46 (m, 2H), 7.43 (dd, *J* = 8.5, 0.7 Hz, 1H), 7.32 – 7.28 (m, 1H), 3.98 (s, 3H) ppm; ^{13}C NMR ($CDCl_3$, 101 MHz) δ = 167.9, 142.2, 139.9, 127.4, 126.6, 123.3, 123.1, 122.9, 121.4, 120.6, 120.3, 110.9, 110.1, 52.0 ppm; ^{1}H NMR ($(CD_3)_2SO$, 600 MHz) δ = 11.71 (s, 1H), 8.79 (s, 1H), 8.26 (d, *J* = 7.7 Hz, 1H), 8.02 (d, *J* = 8.9 Hz, 1H), 7.55 (t, *J* = 9.4 Hz, 2H), 7.45 (t, *J* = 7.4 Hz, 1H), 7.23 (t, *J* = 7.4 Hz, 1H), 3.89 (s, 3H) ppm; ^{13}C NMR ($(CD_3)_2SO$, 150 MHz) δ = 166.9, 142.6, 140.3, 126.7, 126.4, 122.4, 122.3, 122.2, 120.7, 119.8, 119.5, 111.4, 110.8, 51.7 ppm; HRMS (APCI-TOF) calcd for $C_{14}H_{12}NO_2$ [*M* + H]$^{+}$ 224.0863, found 226.0860.

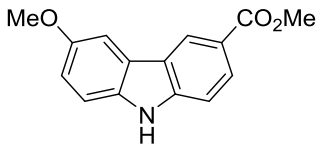

38

Methyl 6-methoxy-9H-carbazole-3-carboxylate (**38**)**:** (The natural product NMR data was reported in both $CDCl_3$ and $(CD_3)_2CO$ to compare the spectra in the same originally reported solvent and to provide another experimentally convenient comparison). Yellow solid (21 mg, 97% yield); R_f = 0.55 (silica gel, EtOAc:hexanes 1:1); ^{1}H NMR ($CDCl_3$, 600 MHz) δ = 8.78 – 8.77 (m, 1H), 8.21 (s, 1H), 8.11 (dd, *J* = 8.5, 1.7 Hz, 1H), 7.60 (d, *J* = 2.4 Hz, 1H), 7.38 (dd, *J* = 26.8, 8.6 Hz, 2H), 7.10 (dd, *J* = 8.7, 2.5 Hz, 1H), 3.98 (s, 3H), 3.94 (s, 3H) ppm; ^{13}C NMR ($CDCl_3$, 150 MHz) δ = 167.9, 154.5, 142.9, 134.6, 127.3, 123.8, 123.1, 122.9, 121.0, 115.9, 111.6, 110.2, 103.2, 56.0, 51.9 ppm; ^{1}H NMR ($(CD_3)_2CO$, 600 MHz) δ = 10.55 (s, 1H), 8.80 (s, 1H), 8.04 (d, *J* = 8.5 Hz, 1H), 7.84 (s, 1H), 7.54 (d, *J* =

8.5 Hz, 1H), 7.47 (d, *J* = 8.7 Hz, 1H), 7.09 (d, *J* = 8.7 Hz, 1H), 3.93 (s, 3H), 3.91 (s, 3H) ppm; ^{13}C NMR ($(CD_3)_2CO$, 150 MHz) δ = 168.0, 155.4, 144.3, 136.2, 127.6, 124.5, 123.8, 123.4, 121.3, 116.8, 112.9, 111.4, 103.8, 56.1, 51.9 ppm; HRMS (ESI-TOF) calcd for $C_{15}H_{14}NO_3$ $[M + H]^+$ 256.0968, found 256.0965.

2.5. References

1. Huisgen, R., *Angew. Chem. Int. Ed. Engl.* **1968,** *7*, 321-328.

2. (a) Nicolaou, K. C.; Snyder, S. A.; Montagnon, T.; Vassilikogiannakis, G., *Angew. Chem., Int. Ed.* **2002,** *41*, 1668-1698. (b) Corey, E. J., *Angew. Chem., Int. Ed.* **2002,** *41*, 1650-1667. (c) Jorgensen, K. A., *Eur. J. Org. Chem.* **2004,** 2093-2102. (d) Takao, K.; Munakata, R.; Tadano, K., *Chem. Rev.* **2005,** *105*, 4779-4807. (e) Funel, J.-A.; Abele, S., *Angew. Chem., Int. Ed.* **2013,** *52*, 3822-3863.

3. Diels, O.; Alder, K., *Justus Liebigs Ann. Chem.* **1928,** *460*, 98-122.

4. (a) Trost, B. M., *Science* **1991,** *254*, 1471-1477. (b) Trost, B. M., *Angew. Chem., Int. Ed. Engl.* **1995,** *34*, 259-281.

5. Carboni, R. A.; Lindsey, R. V., Jr., *J. Am. Chem. Soc.* **1959,** *81*, 4342-4346.

6. (a) Pirovano, V.; Abbiati, G.; Dell'Acqua, M.; Facoetti, D.; Giordano, M.; Rossi, E., *Synlett* **2012,** *23*, 2913-2918. (b) Pindur, U., *Adv. Nitrogen Heterocycl.* **1995,** *1*, 121-172. (c) Pindur, U., *Heterocycles* **1988,** *27*, 1253-1268. (d) Kester, R. F.; Berthel, S. J.; Firooznia, F. In *Heterocyclic Scaffolds II: Reactions and Applications of Indoles*; Gribble, G. W., Ed.; Topics in Heterocyclic Chemistry Series 26; Springer-Verlag: Berlin, 2010.

7. Seitz, G.; Kampchen, T., *Arch. Pharm. (Weinheim)* **1976,** *309*, 679-681.

8. Takahashi, M.; Ishida, H.; Kohmoto, M., *Bull. Chem. Soc. Jpn.* **1976,** *49*, 1725-1726.

9. Lee, L.; Snyder, J. K., *Adv. Cycloaddit.* **1999,** *6*, 119-171.

10. Kester, R. F.; Berthel, S. J.; Firooznia, F., *Top. Heterocycl. Chem.* **2010,** *26*, 327-396.

11. (a) Kraus, G. A.; Raggon, J.; Thomas, P. J.; Bougie, D., *Tetrahedron Lett.* **1988,** *29*, 5605-5608. (b) Kraus, G. A.; Bougie, D.; Jacobson, R. A.; Su, Y., *J. Org. Chem.* **1989,** *54*, 2425-2428.

12. May, J. A.; Zeidan, R. K.; Stoltz, B. M., *Tetrahedron Lett.* **2003,** *44*, 1203-1205.

13. Steinhagen, H.; Corey, E. J., *Angew. Chem., Int. Ed.* **1999,** *38*, 1928-1931.

14. Bodwell, G. J.; Li, J., *Angew. Chem., Int. Ed.* **2002,** *41*, 3261-3262.

15. Zhang, H.; Boonsombat, J.; Padwa, A., *Org. Lett.* **2007,** *9*, 279-282.

16. Martin, D. B. C.; Vanderwal, C. D., *Chem. Sci.* **2011,** *2*, 649-651.

17. Noland, W. E.; Kedrowski, B. L., *J. Org. Chem.* **1999,** *64*, 596-603.

18. Blattes, E.; Fleury, M.-B.; Largeron, M., *J. Org. Chem.* **2004,** *69*, 882-890.

19. Crawley, S. L.; Funk, R. L., *Org. Lett.* **2006,** *8*, 3995-3998.

20. (a) Posner, G. H.; Bull, D. S., *Recent Res. Dev. Org. Chem.* **1997,** *1*, 259-271. (b) Woodard, B. T.; Posner, G. H., *Adv. Cycloaddit.* **1999,** *5*, 47-83. (c) Jung, Y.-G.; Lee, S.-C.; Cho, H.-K.; Darvatkar, N. B.; Song, J.-Y.; Cho, C.-G., *Org. Lett.* **2013,** *15*, 132-135. (d) Smith, M. W.; Snyder, S. A., *J. Am. Chem. Soc.* **2013,** *135*, 12964-12967.

21. Benson, S. C.; Palabrica, C. A.; Snyder, J. K., *J. Org. Chem.* **1987,** *52*, 4610-4614.

22. Kraus, G. A.; Riley, S.; Cordes, T., *Green Chem.* **2011,** *13*, 2734-2736.

23. Lee, J. J.; Kraus, G. A., *Green Chem.* **2014,** *16*, 2111-2116.

24. Lee, J. J.; Kraus, G. A., *Tetrahedron Lett.* **2013,** *54*, 2366-2368.

25. (a) Roy, J.; Jana, A. K.; Mal, D., *Tetrahedron* **2012,** *68*, 6099-6121. (b) Knoelker, H.-J.; Reddy, K. R., *Chem. Rev.* **2002,** *102*, 4303-4427. (c) Knölker, H. J.; Reddy, K. R., Chemistry and biology of carbazole alkaloids. In *The Alkaloids: Chemistry and Biology* Academic Press: San Diego, 2008; Vol. 65, p 1-430.

26. Schmidt, A. W.; Reddy, K. R.; Knoelker, H.-J., *Chem. Rev.* **2012,** *112*, 3193-3328.

27. Domanski, A.; Kyziol, J. B., *Pol. J. Chem.* **1985,** *59*, 613-20.

28. Li, W. S.; McChesney, J. D.; El-Feraly, F. S., *Phytochemistry* **1991,** *30*, 343-6.

29. Witulski, B.; Alayrac, C., *Angew. Chem., Int. Ed.* **2002,** *41*, 3281-3284.

30. Back, T. G.; Pandyra, A.; Wulff, J. E., *J. Org. Chem.* **2003,** *68*, 3299-3302.

31. (a) Liu, Z.; Larock, R. C., *Tetrahedron* **2007,** *63*, 347-355. (b) Liu, Z.; Larock, R. C., *Org. Lett.* **2004,** *6*, 3739-3741.

32. Ozaki, K.; Zhang, H.; Ito, H.; Lei, A.; Itami, K., *Chem. Sci.* **2013,** *4*, 3416-3420.

33. Sundberg, R. J., The chemistry of indoles. In *Organic Chemistry, a Series of Monographs*, Academic Press: New York, 1970; pp 1-489.

34. Guney, T.; Lee, J. J.; Kraus, G. A., *Org. Lett.* **2014,** *16*, 1124-1127.

35. Watanabe, T.; Kobayashi, A.; Nishiura, M.; Takahashi, H.; Usui, T.; Kamiyama, I.; Mochizuki, N.; Noritake, K.; Yokoyama, Y.; Murakami, Y., *Chem. Pharm. Bull.* **1991,** *39*, 1152-6.

36. Bergman, J.; Johnson, A.-L., *Org. Prep. Proced. Int.* **2006,** *38*, 593-599.

37. Forke, R.; Krahl, M. P.; Krause, T.; Schlechtingen, G.; Knolker, H.-J., *Synlett* **2007,** 268-272.

38. (a) Kikugawa, Y.; Aoki, Y.; Sakamoto, T., *J. Org. Chem.* **2001,** *66*, 8612-8615. (b) Bringmann, G.; Tasler, S.; Endress, H.; Peters, K.; Peters, E.-M., *Synthesis* **1998,** 1501-1505.

39. Kuttruff, C. A.; Zipse, H.; Trauner, D., *Angew. Chem., Int. Ed.* **2011,** *50*, 1402-1405.

40. Yang, J.; Liu, S.; Zheng, J.-F.; Zhou, J., *Eur. J. Org. Chem.* **2012,** 6248-6259.

CHAPTER 3.

CONCISE SYNTHESIS OF FLUORESCENT ROSAMINE PROBES FOR CELLULAR IMAGING[†]

3.1. Introduction

Live-cell imaging has become one of the most indispensable tools in biochemistry and biology to visualize a broad spectrum of phenomena from the way proteins in cells translate signals in their intracellular networks to the dynamics of cell-cell interactions that are responsible for life.[1] Live-cell imaging technologies have been synergistically supported by continued advancements in fluorescent microscopy, identification of natural and synthetic fluorescent probes, and the development of biomolecule labelling methods.[2,3]

In particular, driven by the growing interest in cellular imaging applications, designing diverse fluorophores has been an active research area to facilitate the labelling of a broader range of intracellular biomolecules including RNA. These probes are generally categorized into two main groups. The first group is defined as the labelling agent, which can be florescent dyes or radionuclides. They are employed to show the localization and/or concentration of their covalently-attached specific biomolecules. The second group of imaging probes contains sensors that generate a luminescence signal only after their recognition of specific target biomolecules.[4]

[†] Adapted with permission from Kraus, G. A.; Guney, T.; Kempema, A.; Hyman, J. M.; Parvin, B., *Tetrahedron Lett.* **2014**, *55*, 1549-1551. Copyright © 2014 Elsevier.

Organic synthesis has been instrumental in providing the flexibility to tailor the desired imaging probes with diverse properties necessary to address various biological questions through live-cell imaging.[5] Some of the desired properties of these probes involve being bright and photostable, nontoxic, permeable across membranes, and accommodating for adequate contrast between the biomolecule of interest and the background noise.[3]

Two major complementary synthetic technologies have been used in the probe development process. The target-oriented synthetic approach has been selected when a particular biological system, which was either *in vitro* or *in vivo*, was sufficiently defined or a previous library screening method identified imaging probe candidates. Therefore, the necessary fluorophores can be synthesized based upon a rational design procedure. However, in most cases, the lack of understanding of biological actions at the molecular level has hindered the strategy of creating probes in a rational manner.

An alternative, diversity-oriented synthetic approach, has recently emerged, which is built on a rapid and systematic diversification of the chemical space through organic synthesis. The high throughput screening of the combinatorial imaging probe libraries that was made accessible by the diversity-oriented synthesis has led to the discovery of numerous new probes for particular biomolecular targets.[6]

Through the use of recently advanced novel synthetic routes as well as the further optimization of known syntheses, small-molecule florescent probe libraries have significantly been expanded as representative structures are shown in Figure 1. These fluorescent molecules **1**-**9** display emission spectra from the blue to near-infrared region.[7]

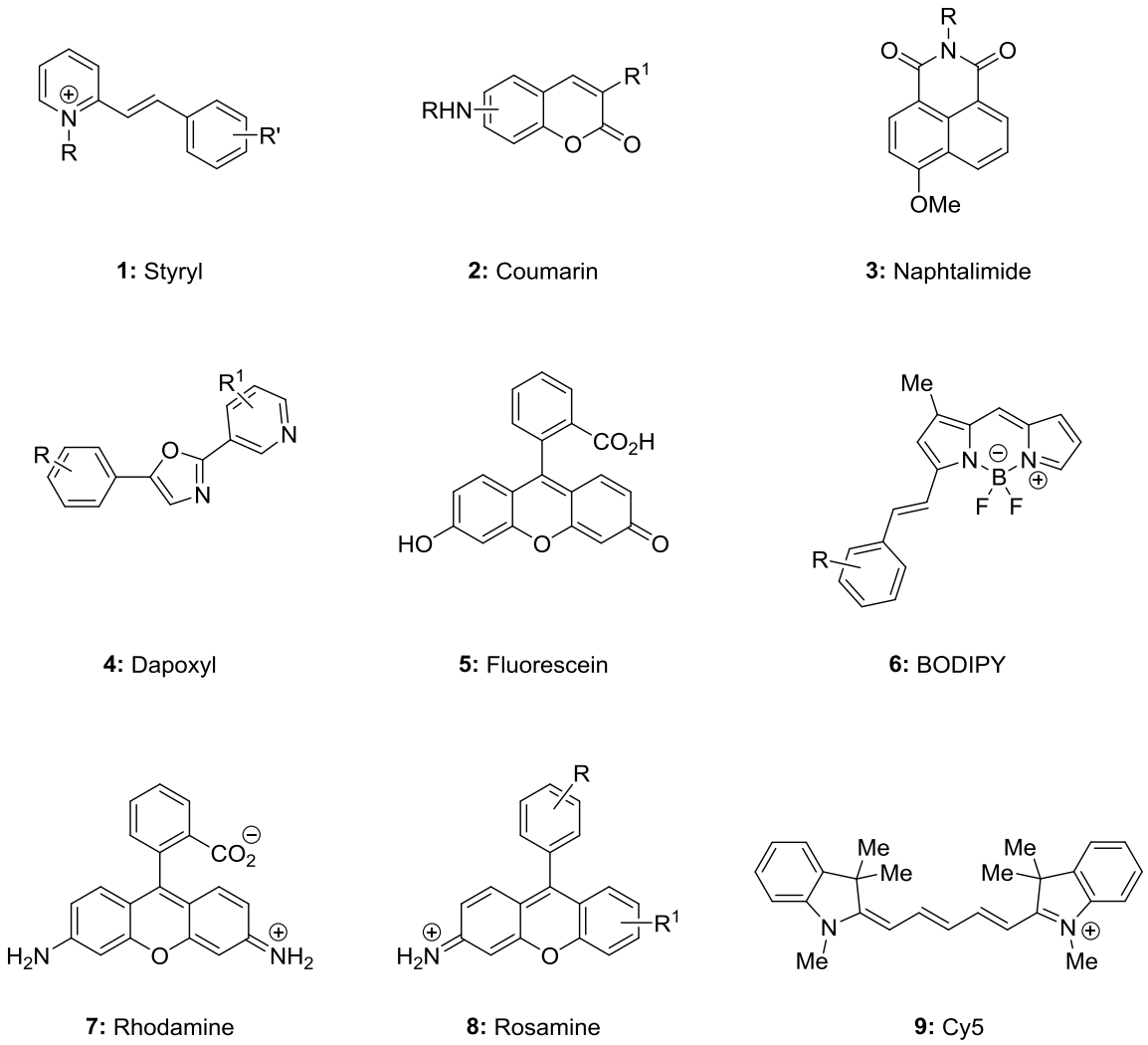

Figure 1. Representative common structures of small-molecule fluorescent probes.

An important class of fluorescent probes are embodied by the tricyclic xanthene scaffold **10**, such as fluorescein (**5**), rhodamine **7**, and rosamine **8**. Because of their exceptional photophysical properties coupled with their high photostability and high quantum yield, xanthylium-based fluorophores are widely employed in imaging applications.[8] For instance, as one of the few fluorescent molecules that is approved by

the U.S. Food and Drug Administration, fluorescein (**5**) has been used in clinical angiographic applications for over 50 years to diagnose and treat retinal disorders.[9] In addition, rhodamine B (**11**) has been utilized as a fluorescence quantum yield standard, a histology stain, a chemosensor for metal ions, as well as a pH indicator.[10] Similarly, rosamines can be used as photosensitizers and stains in biological applications.[11] For example, rosamine CDy1 (**12**) has been described as the first selective biomarker for both embryonic and induced pluripotent stem cells as the structures shown in Figure 2.[12]

In terms of the structural features, both fluorescein (**5**) and rhodamine B (**11**) are substituted with a carboxylic acid functionality on the 2'-position, which regulates the fluorescence level by restraining the free rotation of the 9-phenyl ring. In contrast, rosamine **12** lacks the 2'-carboxylic acid moiety. Moreover, rhodamines and rosamines are distinguished from fluorescein (**5**) by the alkylamino substututions on the 3- and 6-positions of the xanthylium core.

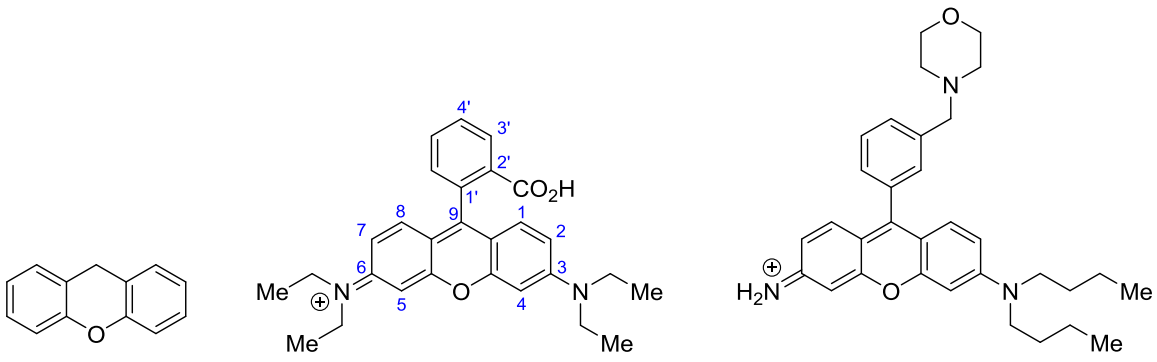

10: Xanthene **11:** Rhodamine B **12:** Rosamine CDy1

Figure 2. Structures of xanthene (**10**), rhodamine B (**11**) and rosamine CDy1 (**12**).

In particular, rosamines have gained considerable interest in the areas of cancer[13], stem-cell[14], and most recently, neurodegenerative disorder research including the investigations of therapeutic strategies for Alzheimer's disease.[15] Preparation of the first combinatorial rosamine library by Chang and co-workers made a notable impact to unlock the undervalued potential of rosamines in biomedical research.[16]

Historically, rosamine dyes were first discovered by Heumann and Rey in 1889.[17] The synthesis of tetramethylrosamine chloride (**13**) was achieved when 3-(dimethylamino)phenol (**14**) was condensed with benzotrichloride (**15**) in benzene as shown in Scheme 1. They also reported that rosamine **13** was very soluble in both water and alcohols, possessed a purplish color in visible light, as well as produced an intense orange fluorescence. Numerous rosamines have since been prepared through the manipulation of not only the functional groups substituted on the 3-, 6-, and 9-positions of the xanthylium scaffold but also the counterions to explore the fluorescence characteristics to be able to exploit various applications.

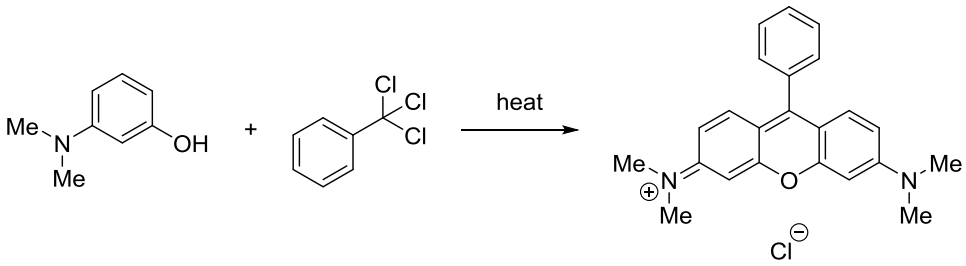

14 **15** **13**

Scheme 1. First synthesis of rosamines by Heumann and Rey.[17]

To date, three distinct synthetic strategies have been effective for the formation of rosamines coupled with either a solution or a solid-phase approach. The condensation route, which was the first reported protocol, has been further extended to incorporate a number of aromatic aldehydes **16** and 3-aminophenols **17** in the presence of an acid catalyst or an oxidant to efficiently access various rosamine dyes **18** as shown in Scheme 2. Although the solution-based condensation methodology is one of the well-established paths to rosamines, it often requires high temperatures that results in complex mixtures. Recently, Burgess and co-workers introduced a microwave-assisted condensation procedure which cleanly produced rosamines in minutes rather than hours as was the case with conventional thermal heating.[18] Their significant achievement with microwaves could be broadened to other xanthene-based fluorophores, as they also projected.

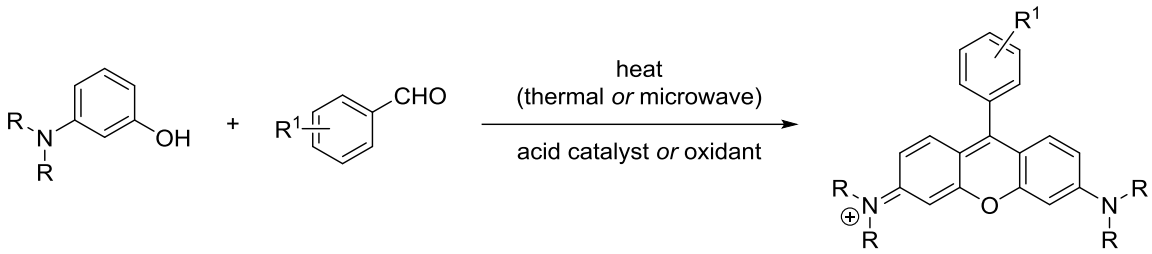

17 **16** **18**

Scheme 2. The condensation approach to rosamines.

Secondly, solution-phase organometallic additions to 3,6-diaminoxanthones or 3,6-diaminochalcogenoxanthones have been heavily utilized for the formation of rosamine species described by Detty and co-workers.[19,20] Many rosamine analogues have been

synthesized through this method, enabling researchers to investigate their properties in photodynamic therapy as newly developed photosensitizers. For example, the synthesis of the first, sulfur-, selenium-, and tellurium-containing rosamine species **19** was reported *via* the key addition of phenylmagnesium bromide (**20**) to tetramethylchalcogenoxanthones **21** as shown in Scheme 3.

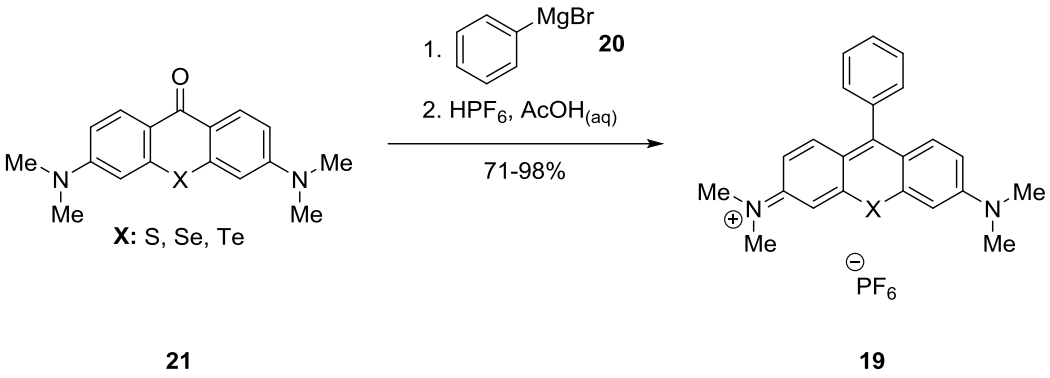

21 **19**

Scheme 3. Synthesis of chalcogenorosamines by Detty.[19]

The Burgess group further modified the xanthone framework by incorporating cyclic amines **22** through the nucleophilic aromatic substitution reactions of easily obtainable 3,6-dihydroxyxanthone ditriflate **23**, which were then systematically reacted with many arylmagnesium bromides **24** to furnish rosamines **25** in good yields after subsequent acid-catalyzed dehydration as outlined in Scheme 4.[21]

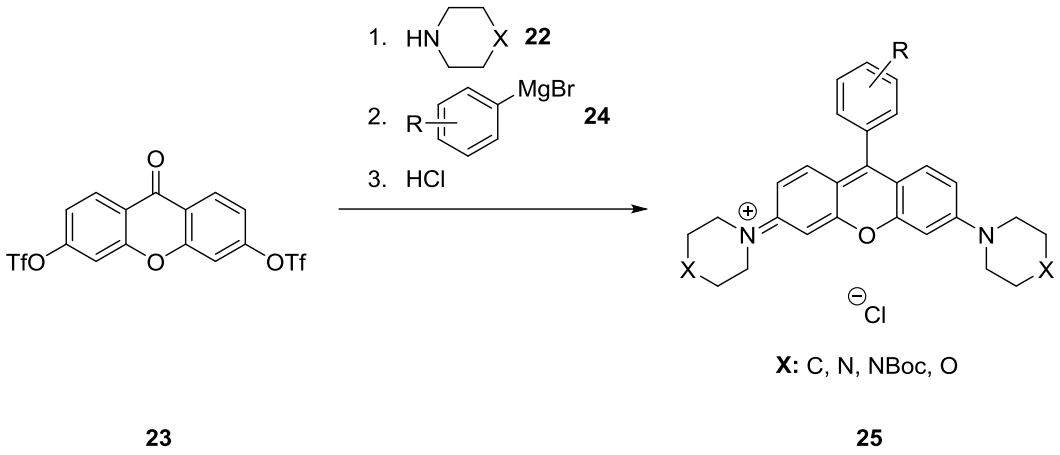

Scheme 4. Synthesis of cyclic amine substituted rosamines by Burgess.[21]

In 2007, Chang and co-workers[16] successfully demonstrated the solid-phase synthesis of the first combinatorial library of rosamines, taking advantage of the pivotal Grignard addition to resin-bound xanthones. Their synthesis commenced with the construction of 3-amino-6-nitroxanthones **26** through the copper-mediated coupling of 2-chloro-4-nitrobenzoic acid (**27**) with 3-acetamidophenol, 3-acetamidothiophenol, and 3-acetamidoaniline building blocks **28** and the consequent acid-mediated condensations under thermal conditions. After the derivatization of the 3-amino groups of xanthones **26**, the 6-nitro component was first reduced to a primary amine functionality, which was linked to a 2-chlorotrityl resin-support to afford twelve different xanthones **29**. A diverse array of 240 rosamine probes **30** were obtained *via* the two-step successive reactions of 33 distinct arylmagnesium bromides and the acid-catalyzed dehydration/resin cleavage sequence, as shown in Scheme 5.

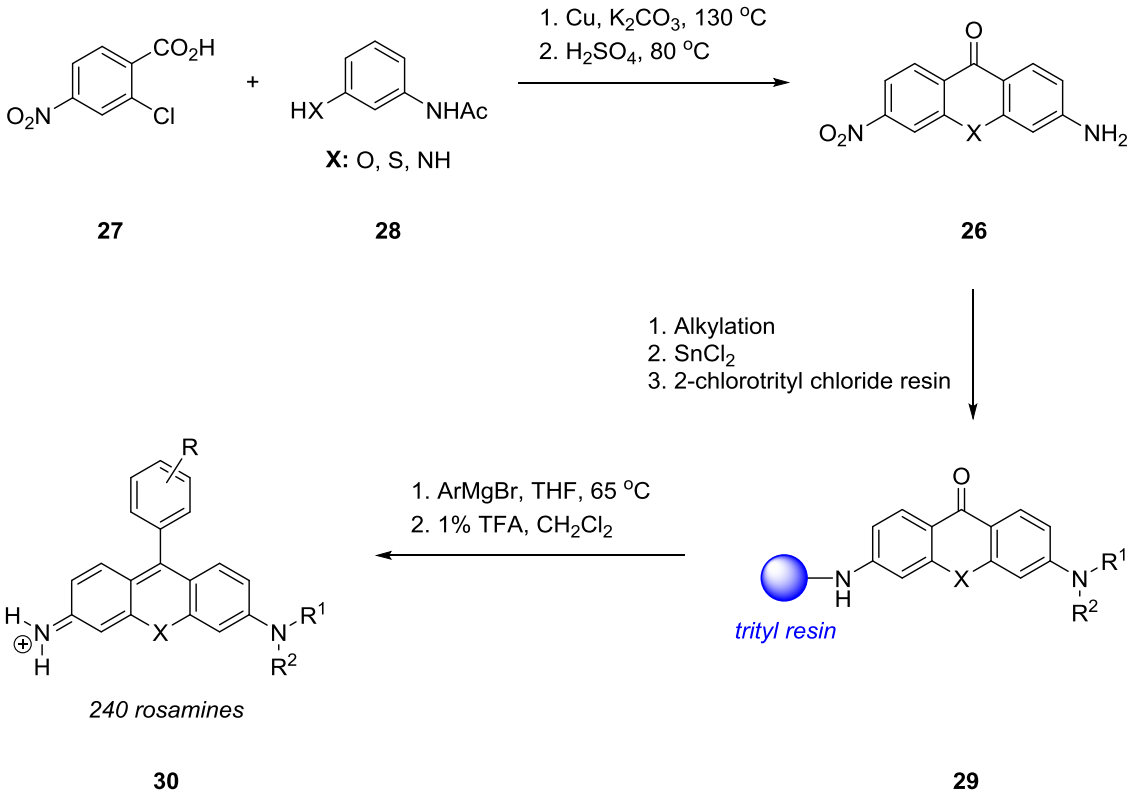

Scheme 5. Combinatorial synthesis of rosamine probes by Chang.[16]

Most recently, the Detty[22] group demonstrated a novel synthesis of rosamines in a third approach, capitalizing on a Suzuki-coupling strategy. According to this one-pot method, chalcogenoxanthones **31** were first treated with triflic anhydride in anhydrous acetonitrile to generate the corresponding triflated xanthones **32** *in situ* in quantitative yields. The triflates **32** were then subsequently reacted with pre-dehydrated boroxin species **33** in the presence of catalytic $PdCl_2(PPh_3)_2$ and quenched with either an aqueous solution of HPF_6 or HCl to form rosamines **34** in 49-79% isolated yields as shown in Scheme 6.

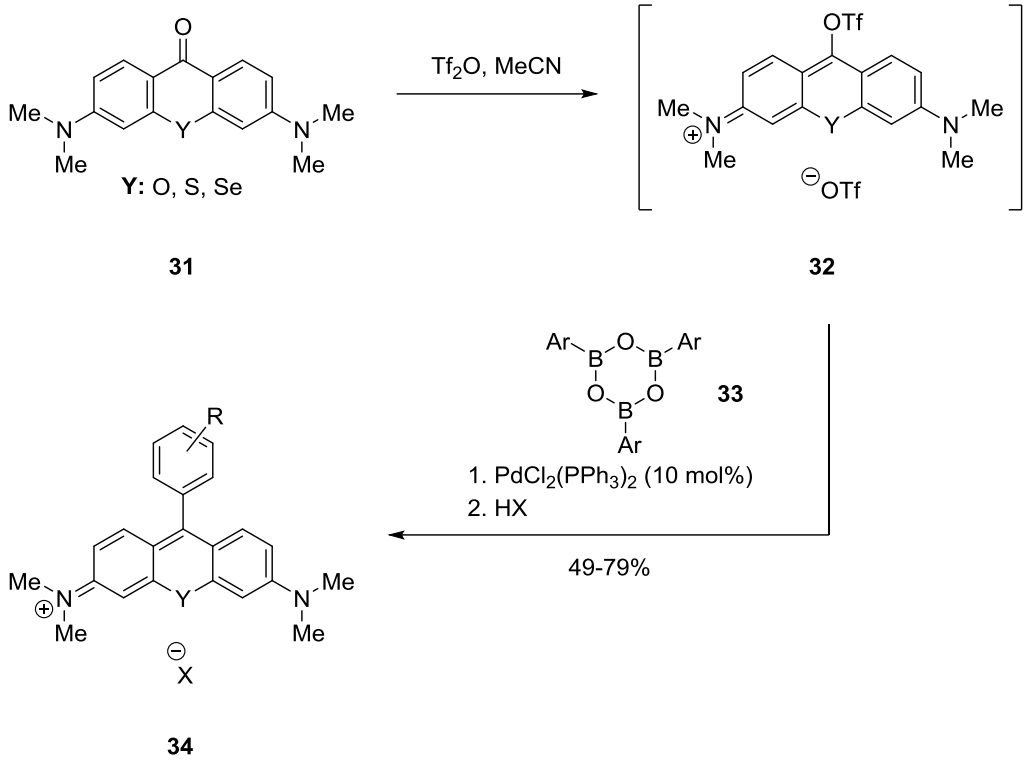

Scheme 6. Synthesis of rosamines via Suzuki coupling.[22]

3.2. Results and Discussion

Our collaborative multidisciplinary project involved the identification and the synthesis of rosamine probes that show low non-specific binding properties and have the characteristics of "non-stickiness" which mirrors the balance between intracellular influx and efflux activities.[23] These are some of the highly preferred properties of fluorescent tags in live-cell imaging to gain a high signal/noise ratio for targeted receptors within a cell. A systematic high throughput screening of rosamines was performed to determine

molecules that possessed such characteristics in mammalian cells as an early-screening method. The identified compounds in the mammalian system were hypothesized to assist the cellular tracking studies in plant and bacterial systems. Ultimately, the *in situ* proliferation of rhizosphere microorganisms that account for a variety of effects from influencing plant growth to human diseases could be examined with the identified probes.[24]

Recently, the Nilsen-Hamilton and Parvin groups utilized Chang's combinatorial rosamine library to screen and quantitatively measure the intracellular influx and efflux properties of the fluorescent probes in three different mammalian cancer cell lines, which were chosen from both human and mouse samples. As a result, several hits were determined that had the desired property of greater non-stickiness and were subsequently validated in plant root hair systems. Comparison of the uptake and retention values measured for each one of the 240-member rosamine library revealed the lead rosamine scaffold **35** as the structure as shown in Figure 3.

With the lead target in hand, we envisioned a novel synthetic strategy to not only access rosamine **35**, but also several other rosamine analogues that would have potential radiolabelling capability such as rosamine **36** (Figure 3) to provide a multifunctional platform for live-cell imaging that is traceable by both fluorescence microscopy and autoradiography.[25]

Our synthetic planning began by recognizing a need for a concise route towards a primary amine-functionalized rosamine scaffold. The previous route developed by Chang and co-workers[16] used 3-nitro-6-aminoxanthone **37**. The 3-nitro moiety of **37** was first reduced to the primary amine that was connected to a solid support before the

organometallic addition. Subsequently, the final cleavage of the resin with trifluoroacetic acid delivered rosamine **38**.

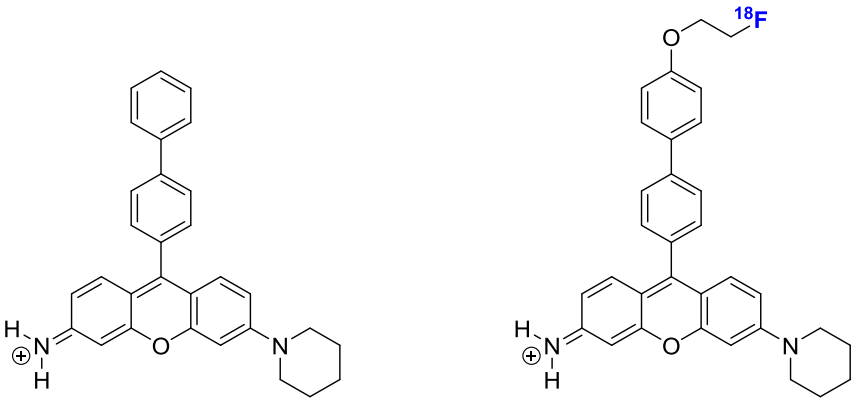

35 **36**

Figure 3. Representative structures of the targeted rosamines.

Even though Chang's diversity-oriented rosamine synthesis proved very effective to generate a large collection of fluorescent library, our solution-phase synthetic design was intended to be shorter and scalable for targeted rosamines. Specifically, capitalizing on xanthone **39** which was substituted with a benzophenone imine as the primary amine equivalent would allow facile introduction to the highly desirable class of rosamines **38** though the organometallic addition and the consequential acidic workup as outlined in Scheme 7.

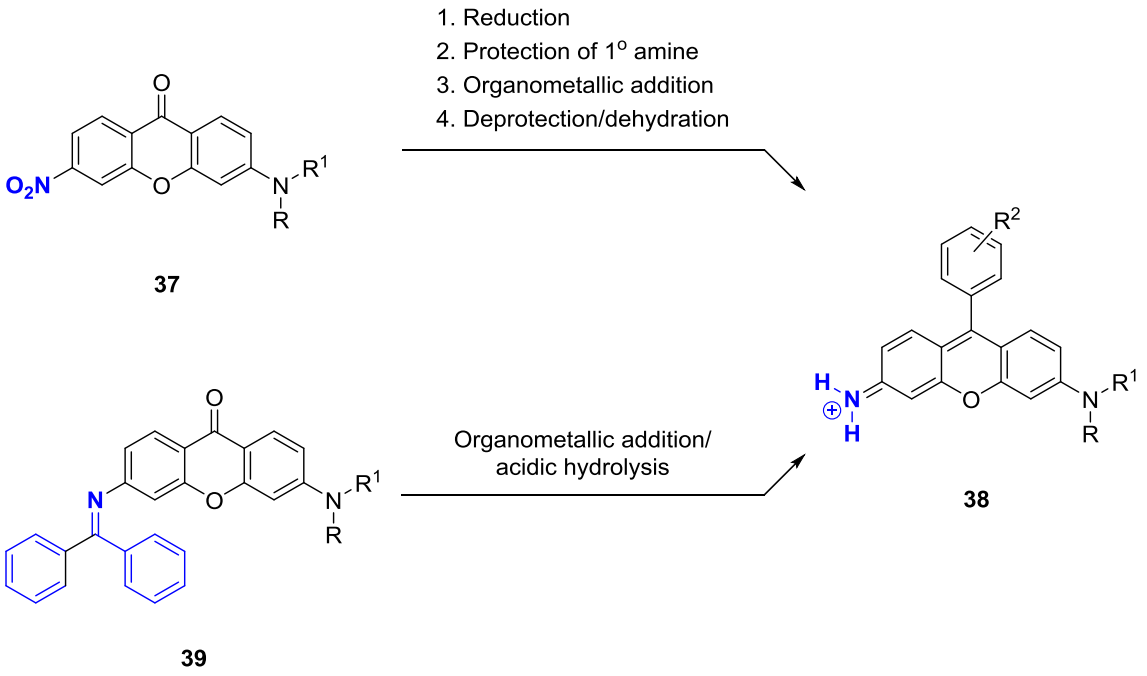

Scheme 7. Comparison of synthetic strategies to primary amine functionalized rosamines.

Our synthesis commenced with the preparation of known 3,6-dihydroxyxanthone (**40**) from 2,2′,4,4′-tetrahydroxybenzophenone (**41**) according to the literature procedure.[26] The suspension of **41** in water was heated to 180 °C in a sealed tube for 72 h to produce **40** in nearly quantitative yield. Xanthone **40** was then converted to 3,6-dihydroxyxanthone ditriflate **23** by the action of triflic anhydride and pyridine.[27] After recrystallization, xanthone **23** was isolated in 89% yield. Subsequently, the transformation of **23** to piperidine-substituted xanthone **42** smoothly proceeded, following recent work from the Burgess[21] lab as shown in Scheme 8.

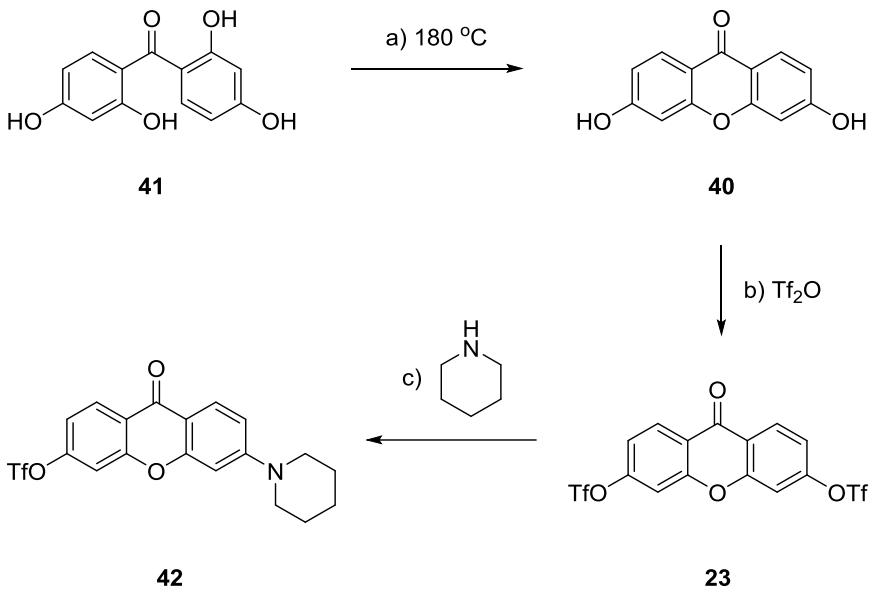

Scheme 8. Synthesis of piperidine substituted xanthone (**42**)[a].
[a] Reagents and conditions: a) H_2O, 180 °C, 72 h, 98%; b) **40** (1.0 equiv), Tf_2O (3.0 equiv), Pyridine (10.0 equiv), CH_2Cl_2, 0 °C to 23 °C, 24 h, 89%; c) **23** (1.0 equiv), piperidine (5.0 equiv), DMSO, 23 °C, 1.5 h, 87%.

We were inspired by the Buchwald[28] group's innovative work of generating aniline derivatives from aryl halides and triflates *via* palladium-catalyzed amination reactions. Similarly, we envisioned coupling the readily hydrolyzable and commercially available benzophenone imine (**43**) moiety onto xanthone **42**, which, to the best of our knowledge, represents the first application of its kind. The imine that is substituted onto xanthone **44** would then function as the primary amine equivalent that is essential for our rosamine scaffolds in imaging applications.

As shown in Scheme 9, the amination of xanthone **42** was carried out in the presence of palladium(II) acetate and a catalytic amount of *rac*-BINAP in dry THF. The imine adduct **44** was cleanly obtained in 84% yield, adapting the conditions developed by Buchwald.

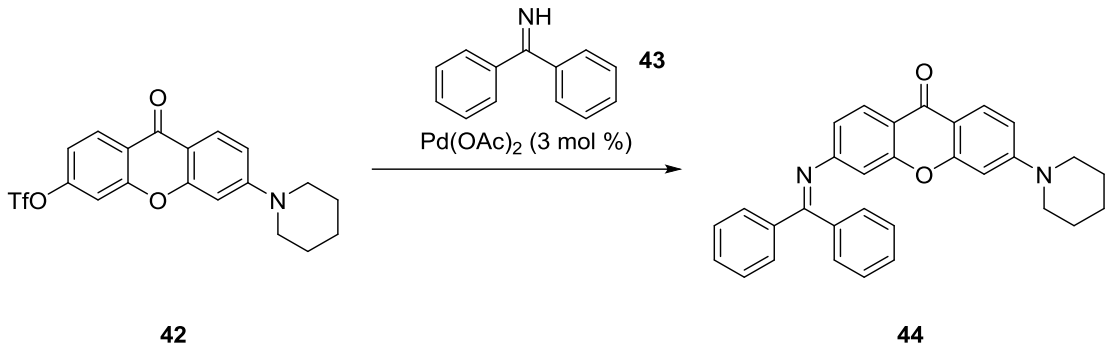

42 44

Scheme 9. Synthesis of xanthone **44** *via* palladium-catalyzed amination[a].
[a] Reagents and conditions: a) **42** (1.0 equiv), **43** (1.2 equiv), $Pd(OAc)_2$ (3 mol %), *rac*-BINAP (4.5 mol %), Cs_2CO_3 (1.4 equiv), THF, 65 °C, 16 h, 84%.

Subsequently, the diversification platform **44** was ready for reactions with aryllithium building blocks to furnish rosamines. Our initial studies for the key transformation started with the lithiation of *tert*-butyldimethylsilyl-protected 4′-bromo-(1,1′-biphenyl)-4-ol **45** and its ensuing reaction with xanthone **44**. After 16 hours of stirring at room temperature, the acidification of the reaction mixture with aqueous hydrochloric acid formed rosamine **46** as shown in Scheme 10. TBS deprotection was attempted with either tetrabutylammonium fluoride or hydrogen fluoride-pyridine systems but was unproductive. The isolation of rosamine **47** was challenging through chromatographic methods because of the charged nature of both the deprotection reagents and **47**; thus, the synthesis of rosamines using protecting groups was abandoned.

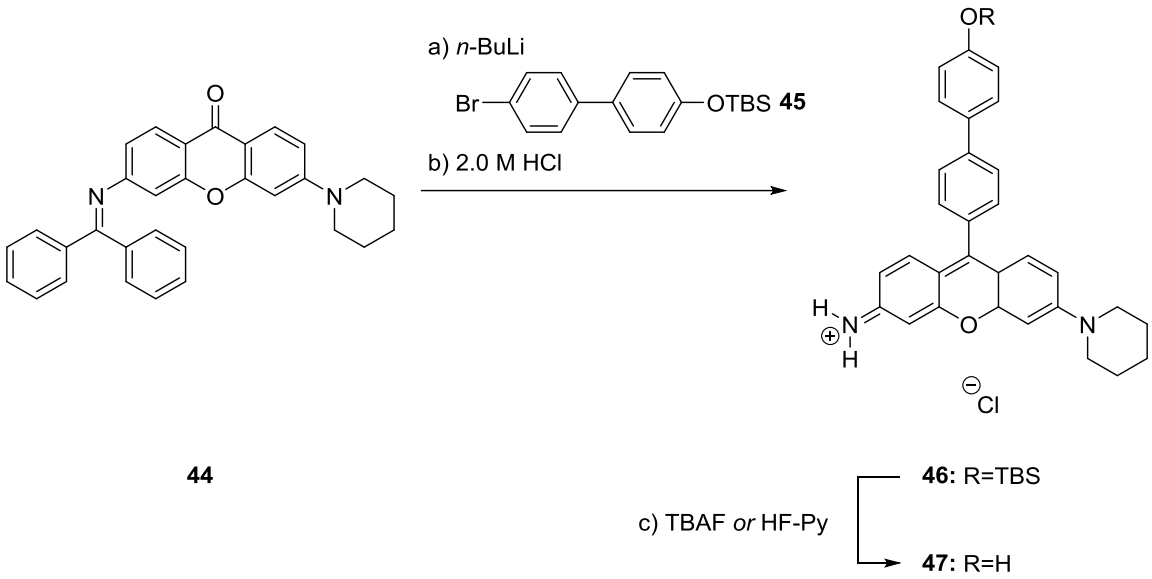

Scheme 10. Synthesis of rosamine **47** using TBS-protected aryllithium **45**.

Our second generation attempt to access rosamine **47** featured the *in situ* generation of the dianion from 4′-bromo-(1,1′-biphenyl)-4-ol (**48**), which rendered the previous protecting group unnecessary. Accordingly, the dianion of **48**, formed by the addition of two equivalents of *n*-BuLi, was combined with xanthone **44**. Afterwards, the acid-catalyzed hydrolysis of the resulting intermediate pleasingly gave rosamine **47** in 95% isolated yield as shown in Scheme 11. Rosamine **47** is particularly important since it can be potentially converted to radiolabelled rosamine **36** (Figure 3) by reacting it with [^{18}F]2-fluoroethyl arylsulfonates.[29]

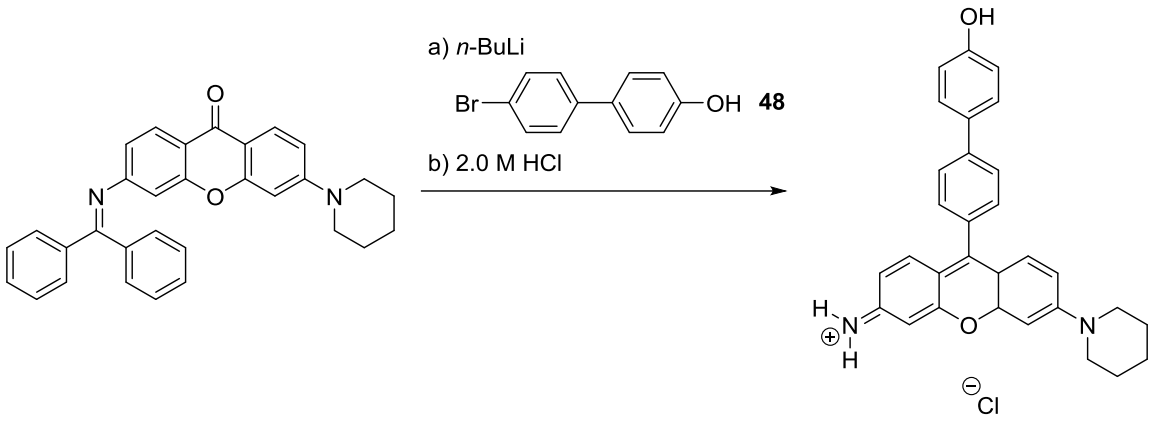

44 **47**

Scheme 11. Efficient synthesis of rosamine **47** *via* the dianion of **48**[a].
[a] Reagents and conditions: a) **44** (1.0 equiv), **48** (5.0 equiv), *n*-BuLi (10.0 equiv), THF, -78 °C to 23 °C, 24 h; b) HCl (2.0 M), 95%.

Once the conditions were optimized for the aryllithium additions, we looked at a few more rosamine analogues that might be useful for imaging applications. To begin with, biphenyls **49**-**51** were synthesized by the electrophilic substitution of 4′-bromo-(1,1′-biphenyl)-4-ol (**48**) with dichloroethane, 1,2-bis(tosyloxy)ethane, and 2-fluoroethyltosylate, accordingly. The treatment of biphenyls with a single equivalent of *n*-BuLi, efficiently produced aryllithiated species, which were exposed to xanthone **44** to construct rosamine analogues **52**, **53**, and **54** in 78%, 54%, and 82%, respectively, as shown in Scheme 12. Rosamines **52** and **53** are potential candidates for conversion into rosamine **36** by the fluorine-18 nucleophile.

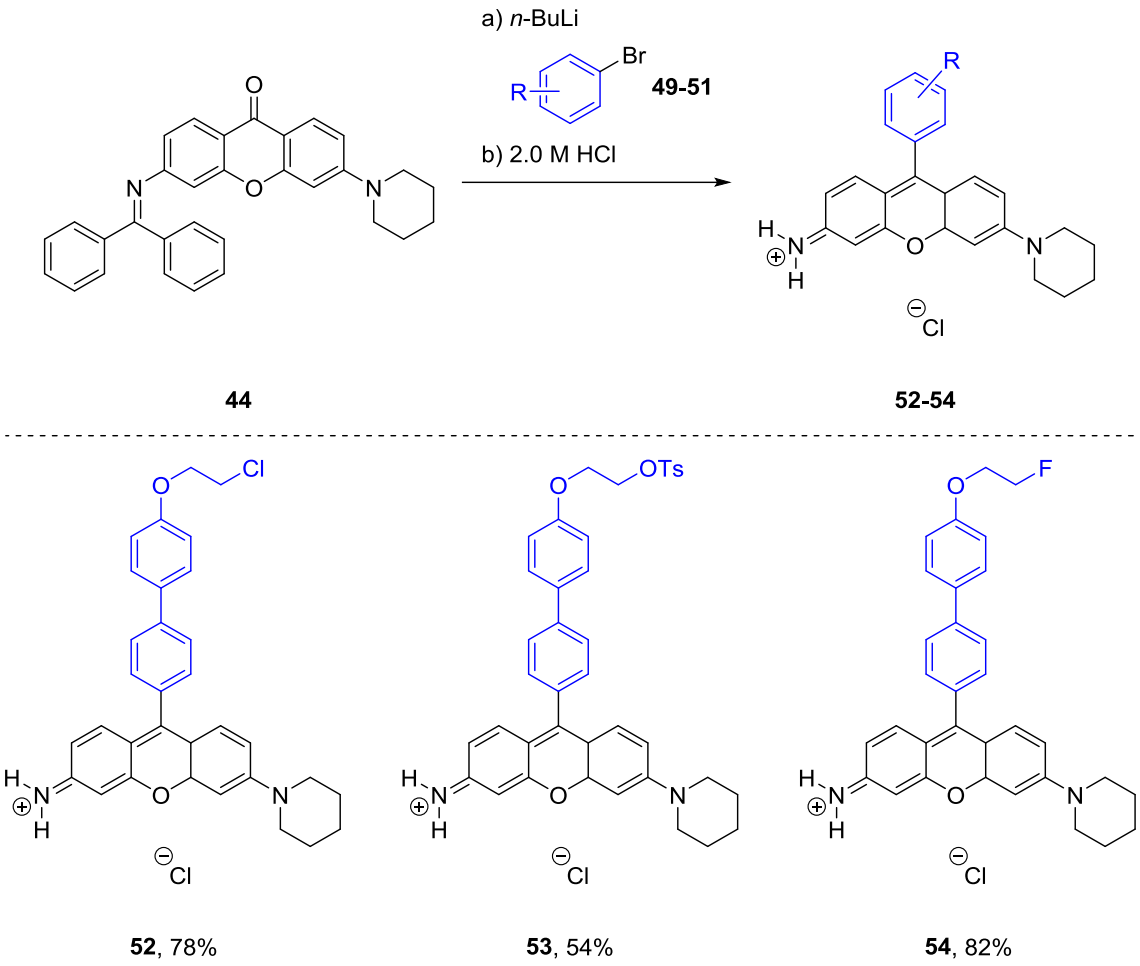

Scheme 12. Synthesis of rosamines **52-54**[a,b].

[a] Reagents and conditions: a) **44** (1.0 equiv), **49-51** (4.0 equiv), *n*-BuLi (4.0 equiv), THF, -78 °C to 23 °C, 16 h; b) HCl (2.0 M). [b] **53** was isolated as an inseparable mixture (**53**:⁻OTs, 2:1).

3.3. Conclusions

Rosamines have been assembled via three main strategies: (i) The condensation of aminophenols and aryl aldehydes, (ii) the 1,2-addition of aromatic organometallic reagents to xanthone carbonyls and the subsequent acid-catalyzed dehydration reaction, as well as (iii) Suzuki coupling of triflated xanthones and arylboronic acids. As part of our

collaborative project which set out to synthesize the novel rosamine probes that possess a primary amine group on the 3-position and a biphenyl unit on the 9-position of the rosamine scaffold, we disclosed an efficient route that allowed a rapid and scalable realization of the desired rosamines. Our synthetic design utilized the benzophenone imine subunit attached onto the xanthone framework to mask the amine functionality during the organometallic addition and unmask it during the acidic workup, which also assisted in the dehydration process towards the formation of fluorescent rosamine dyes. This newly developed method shortened the overall protocol compared to the previous methodologies and provided a flexible synthesis of important rosamines analogues for cellular imaging.

3.4. Experimental

General Procedures

All starting materials were purchased from Sigma-Aldrich or TCI America; solvents were purchased from Fisher Scientific and used without further purification. All reactions were carried out in flame-dried glassware under argon with dry solvents under anhydrous conditions. All yields refer to chromatographically isolated products. Reactions were monitored by thin-layer chromatography (TLC) carried out on 0.20 mm silica gel plates using UV light as a visualizing agent. Silica gel 60Å, particle size 0.032 – 0.063 mm, was used for flash column chromatography. ^{1}H and ^{13}C NMR spectra were acquired on a Varian MR-400 or Bruker Avance III 600 MHz spectrometer. ^{1}H and ^{13}C chemical shifts (δ) are given in ppm relative to the residual protonated solvent peaks ($CDCl_3$: δ_H =

7.26 ppm, δ_C = 77.0 ppm; CD_3OD: δ_H = 3.31 ppm, δ_C = 49.0 ppm; $(CD_3)_2SO$: δ_H = 2.50 ppm, δ_C = 39.52 ppm) as an internal reference. High-resolution mass spectra (HRMS) were recorded on an Agilent 6540 QTOF (quadrupole time of flight) mass spectrometer using ESI (electrospray ionization) or APCI (atmospheric-pressure chemical ionization), or EI (electron ionization) on an Agilent 6890 GC/MS. Melting points are uncorrected and were analyzed on a Melt-Temp II capillary melting point apparatus.

Compounds **23**[27], **40**[26], and **42**[21] were prepared according to literature procedures and all obtained NMR data matched the reported values. Melting points of the rosamines **47**, **52**, and **54** could not be accurately determined since the samples decomposed as they were monitored up to 300 °C.

Selected Experimental, Physical, and Spectral Data

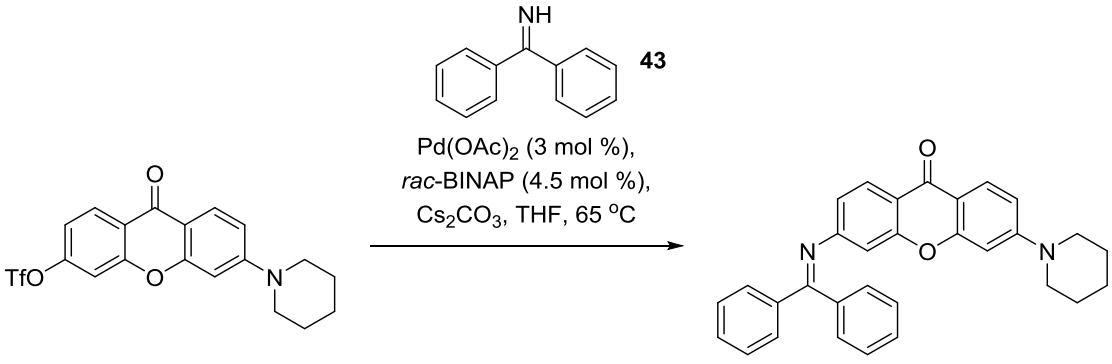

42 **44**

Xanthone 44. The title compound was prepared according to the following procedure, adapted from Buchwald et al.[28] To a flask was added $Pd(OAc)_2$ (10 mg, 0.046 mmol), *rac*-BINAP (43 mg, 0.068 mmol), **42** (0.65 g, 1.52 mmol), benzophenone imine (**43**) (0.33 g, 1.82 mmol), Cs_2CO_3 (0.69 g, 2.13 mmol), and THF (10 mL). The reaction mixture was

heated to 65 °C for 16 h, after which it was cooled to room temperature and diluted with CH_2Cl_2 (100 mL). The reaction mixture was filtered after which it was washed with water and brine, dried over sodium sulfate, and concentrated *in vacuo*. The crude product was purified by flash column chromatography (silica gel, 10% to 25% EtOAc-hexanes) to afford **44** (0.70 g, 84% yield) as a yellow solid. **44:** m.p. 180-181 °C; R_f = 0.70 (silica gel, EtOAc:hexanes 1:1); ^{1}H NMR (600 MHz, DMSO-d_6) δ 7.87 (t, J = 9.2 Hz, 1H), 7.70 (d, J = 7.2 Hz, 1H), 7.59 – 7.53 (m, 1H), 7.48 (t, J = 6.9 Hz, 2H), 7.31 (d, J = 6.9 Hz, 2H), 7.23 (d, J = 6.2 Hz, 1H), 6.96 (d, J = 9.1 Hz, 1H), 6.79 (s, 1H), 6.76 (d, J = 8.7 Hz, 1H), 6.72 (s, 1H), 3.40 (t, J = 5.0 Hz, 3H), 1.60 – 1.50 (m, 6H) ppm; ^{13}C NMR (150 MHz, DMSO-d_6) δ 173.4, 168.5, 157.7, 156.9, 156.0, 155.0, 138.0, 135.2, 131.5, 129.1, 128.9, 128.7, 128.4, 128.1, 127.0, 126.2, 117.1, 116.8, 111.5, 111.2, 107.6, 98.6, 47.7, 24.8, 23.9 ppm; HRMS (ESI-QTOF) calcd for $C_{31}H_{27}N_2O_2$ $[M + H]^+$ 459.2067, found 459.2057.

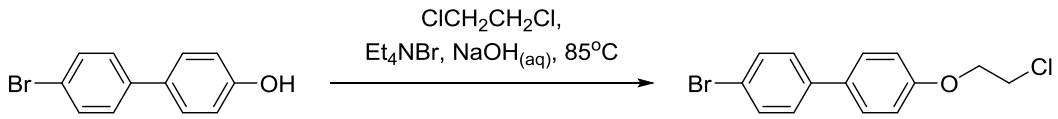

48 **49**

Biphenyl 49. To a solution of 4′-bromo-(1,1′-biphenyl)-4-ol (**48**) (2.00 g, 8.03 mmol) in dichloroethane (20 mL) at room temperature was added tetra-*n*-butylammonium bromide (52 mg, 0.16 mmol), followed by 5.0 M NaOH (8.30 mL). The resulting slurry was heated to 85 °C over 16 hours after which the mixture was cooled to room temperature. The solution was diluted with dichloroethane (40 mL), washed with water and brine, dried over sodium sulfate, and concentrated *in vacuo*. The crude mixture was purified by flash

column chromatography (silica gel, 5% to 20% EtOAc-Hexanes) to afford **49** (1.3 g, 52% yield) as a white solid. **49:** R_f = 0.85 (silica gel, EtOAc:Hexanes 1:1); ^{1}H NMR (600 MHz, $CDCl_3$) δ 7.54 (d, *J* = 8.5 Hz, 2H), 7.49 (d, *J* = 8.7 Hz, 2H), 7.41 (d, *J* = 8.5 Hz, 2H), 6.99 (d, *J* = 8.7 Hz, 2H), 4.28 (t, *J* = 5.9 Hz, 2H), 3.84 (t, *J* = 5.9 Hz, 2H) ppm; ^{13}C NMR (150 MHz, $CDCl_3$) δ 158.0, 139.6, 133.3, 131.8, 128.3, 128.1, 121.0, 115.1, 68.1, 41.8 ppm; HRMS (EI-GC/MS) calcd for $C_{14}H_{12}BrClO$ $[M+H]^+$ 310.9838, found 310.9842.

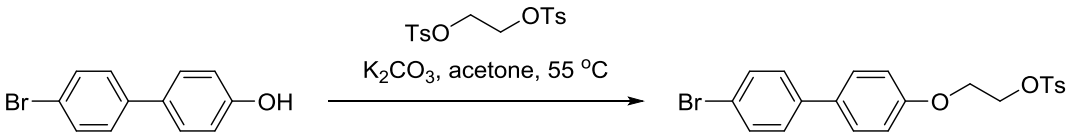

48 **50**

Biphenyl 50. To a solution of 4′-bromo-(1,1′-biphenyl)-4-ol (**48**) (1.00 g, 4.01 mmol) in acetone (30 mL) was added 1,2-bis(tosyloxy)ethane (2.02 g, 5.46 mmol) and potassium carbonate (0.88 g, 6.42 mmol) which was then heated to 55 °C for 24 hours. After dilution with water (30 mL), the reaction mixture was extracted with CH_2Cl_2 (3 x 30 mL). The combined organic layers were dried over sodium sulfate and concentrated *in vacuo*. The crude mixture was purified by flash column chromatography (silica gel, 5% to 30% EtOAc-hexanes) to afford **50** (0.79 g, 44% yield) as a white solid. **50:** R_f = 0.81 (silica gel, EtOAc:Hexanes 1:1); ^{1}H NMR (400 MHz, $CDCl_3$) δ 7.83 (d, *J* = 8.3 Hz, 2H), 7.53 (d, *J* = 8.6 Hz, 2H), 7.44 (d, *J* = 8.9 Hz, 2H), 7.41 – 7.37 (m, 2H), 7.36 – 7.33 (m, 2H), 6.85 (d, *J* = 8.7 Hz, 2H), 4.43 – 4.35 (m, 2H), 4.24 – 4.14 (m, 2H), 2.45 (s, 3H) ppm; ^{13}C NMR (150 MHz, $CDCl_3$) δ 157.8, 145.0, 139.5, 133.2, 132.9, 131.8, 129.8, 128.3, 128.0, 128.0, 121.0,

115.0, 68.0, 65.5, 21.7 ppm; HRMS (APCI-QTOF) calcd for $C_{21}H_{19}BrO_4S$ $[M+H]^+$ 447.0265, found 447.0264.

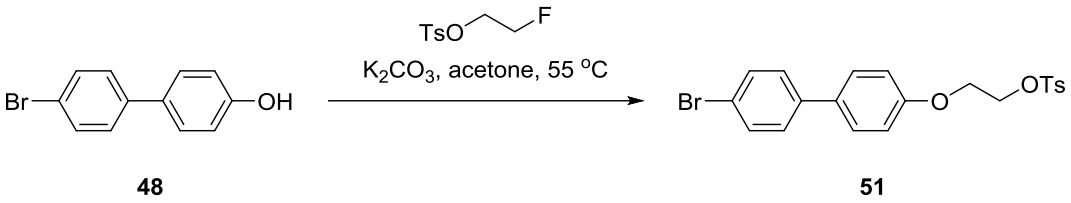

Biphenyl 51. To a solution of 4′-bromo-(1,1′-biphenyl)-4-ol (**48**) (2.00 g, 8.03 mmol) in acetone (60 mL) was added 2-fluoroethyltosylate[30] (2.45 g, 11.24 mmol) and potassium carbonate (1.77 g, 12.85 mmol) which was then heated to 55 °C for 24 hours. After filtration through Celite, the solution diluted with water (30 mL), the reaction mixture was extracted with CH_2Cl_2 (2 x 30 mL). The combined organic layers washed with brine, dried over sodium sulfate and concentrated *in vacuo*. The crude mixture was purified by flash column chromatography (silica gel, 0% to 10% EtOAc-hexanes) to afford **51** (1.41g, 60% yield) as a white solid. **51:** R_f = 0.93 (silica gel, EtOAc:Hexanes 1:1); ^{1}H NMR (400 MHz, $CDCl_3$) δ 7.53 (d, *J* = 8.5 Hz, 2H), 7.49 (d, *J* = 8.7 Hz, 2H), 7.41 (d, *J* = 8.5 Hz, 2H), 7.00 (d, *J* = 8.7 Hz, 2H), 4.87 – 4.70 (m, 2H), 4.32 – 4.20 (m, 2H) ppm; ^{13}C NMR (100 MHz, $CDCl_3$) δ 158.2, 139.6, 133.1, 131.8, 128.3, 128.0, 120.9, 115.0, 82.7, 81.0, 67.3, 67.1 ppm; HRMS (EI-GC/MS) calcd for $C_{14}H_{12}BrFO$ $[M+H]^+$ 295.0133, found 295.0137.

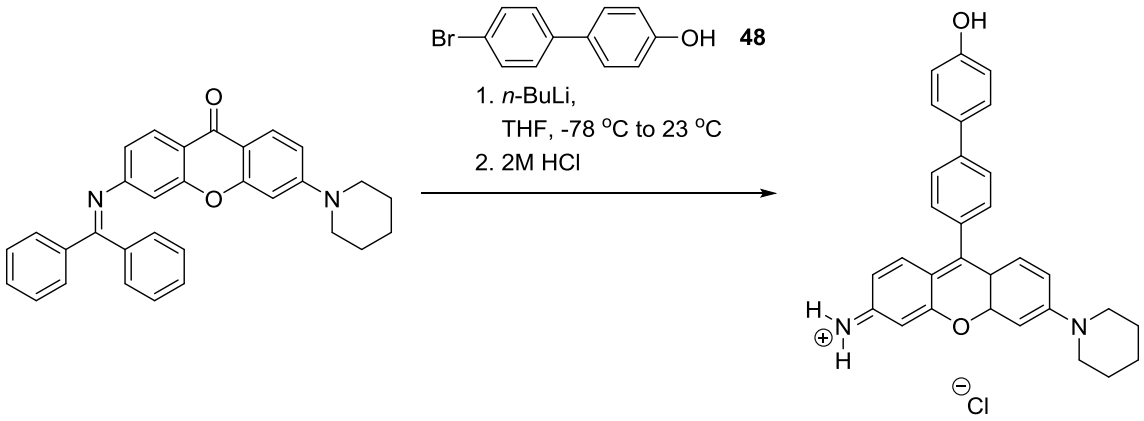

44 **47**

Rosamine 47. To a solution of 4′-bromo-(1,1′-biphenyl)-4-ol (**48**) (0.27 g, 1.09 mmol) in THF (10 mL) at -78 °C was added *n*-BuLi (2.5M in hexanes, 0.88 mL, 2.18 mmol), dropwise over 5 minutes. The resulting solution was stirred for 25 minutes during which time the consistency resembled a thick slurry. To this solution was added a cooled solution of **44** (0.10 g, 0.22 mmol) in THF (6 mL), dropwise over 5 minutes. The reaction mixture was slowly allowed to warm to room temperature over 24 h, after which 2.0 M HCl (2 mL) was added dropwise, during which the color changed from cloudy yellow to red-purple upon complete addition of the acid. The resulting solution was then stirred for 30 minutes at room temperature. Utilizing a standard aqueous workup procedure caused product loss presumably due to the low solubility of **47** in EtOAc or CH_2Cl_2. Therefore, the crude solution was directly loaded onto silica gel for purification by flash column chromatography (silica gel, 0% to 10% MeOH-CH_2Cl_2) to afford **47** (100 mg, 95% yield) as a purple solid. **47:** R_f = 0.14 (silica gel, MeOH:CH_2Cl_2 1:9); ^{1}H NMR (600 MHz, CD_3OD) δ 7.86 (d, *J* = 8.1 Hz, 2H), 7.61 (d, *J* = 8.5 Hz, 2H), 7.50 (d, *J* = 8.2 Hz, 2H), 7.47 (d, *J* = 9.6 Hz, 1H), 7.42 (d, *J* = 9.2 Hz, 1H), 7.22 (dd, *J* = 9.7, 2.3 Hz, 1H), 7.13 (d, *J* =

2.3 Hz, 1H), 6.93 (d, *J* = 8.5 Hz, 2H), 6.87 (dd, *J* = 9.2, 1.9 Hz, 1H), 6.83 (d, *J* = 1.9 Hz, 1H), 3.77 (t, *J* = 5.4 Hz, 4H), 1.84 – 1.78 (m, 2H), 1.78 – 1.72 (m, 4H) ppm; ^{13}C NMR (150 MHz, CD_3OD) δ 161.3, 160.1, 159.8, 159.4, 159.2, 158.1, 144.5, 133.6, 133.3, 132.1, 131.4, 131.3, 129.3, 127.7, 117.9, 117.0, 115.9, 114.9, 114.5, 98.6, 98.2, 49.9, 27.1, 25.3 ppm; HRMS (ESI-QTOF) calcd for $C_{30}H_{27}N_2O_2$ [*M* - Cl]$^+$ 446.1994, found 447.2065.

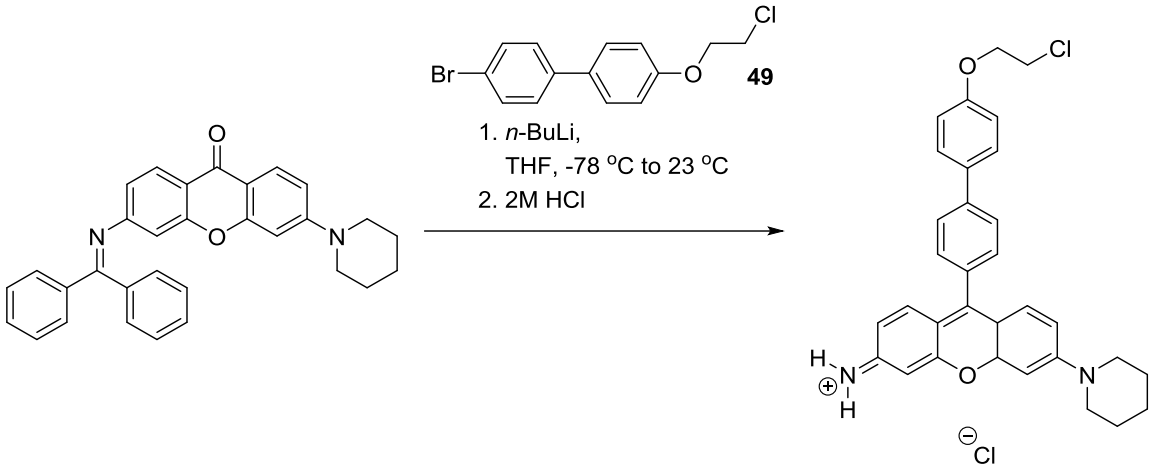

44 **52**

Rosamine 52. To a solution of **49** (0.28 g, 0.89 mmol) in THF (10 mL) at -78 °C was added *n*-BuLi (2.5M in hexanes, 0.35 mL, 0.89 mmol), dropwise over 5 minutes. The resulting solution was stirred for 30 minutes after which a cooled solution of **44** (0.10 g, 0.22 mmol) in THF (5 mL) was added dropwise over 5 minutes. The reaction mixture was slowly allowed to warm to room temperature over 16 h, after which 2.0 M HCl (2 mL) was added dropwise, during which the color changed from cloudy yellow to red-purple upon complete addition of the acid. The resulting solution was then stirred for 30 minutes at room temperature. The solution was diluted with EtOAc (100 mL), washed with water (2

x 10 mL), and dried over sodium sulfate (utilizing magnesium sulfate caused product loss) and concentrated *in vacuo*. The crude mixture was purified by flash column chromatography (silica gel, 2% to 10% MeOH-CH_2Cl_2) to afford **52** (93 mg, 78% yield) as a purple solid. **52:** R_f = 0.15 (silica gel, MeOH:CH_2Cl_2 1:9); ^{1}H NMR (400 MHz, $CDCl_3$) δ 8.38 (s, 2H), 7.76 (d, *J* = 8.1 Hz, 2H), 7.64 (d, *J* = 8.7 Hz, 2H), 7.47 – 7.33 (m, 3H), 7.30 (d, *J* = 2.4 Hz, 2H), 7.16 (d, *J* = 9.3 Hz, 1H), 7.06 (d, *J* = 8.7 Hz, 2H), 6.93 (dd, *J* = 9.6, 2.1 Hz, 1H), 6.85 (d, *J* = 2.2 Hz, 1H), 4.32 (t, *J* = 5.8 Hz, 2H), 3.87 (t, *J* = 5.8 Hz, 2H), 3.64 (s, 4H), 1.77 (s, 6H) ppm; ^{13}C NMR (150 MHz, $CDCl_3$) δ 160.7, 158.5, 158.4, 157.7, 156.7, 155.8, 142.6, 132.8, 131.9, 131.6, 130.3, 130.1, 128.4, 126.9, 118.9, 115.3, 114.4, 113.6, 112.6, 98.9, 97.7, 68.2, 48.7, 41.9, 25.7, 24.2 ppm; HRMS (ESI-QTOF) calcd for $C_{32}H_{30}ClN_2O_2$ [*M* - Cl]$^+$ 509.1996, found 509.2002.

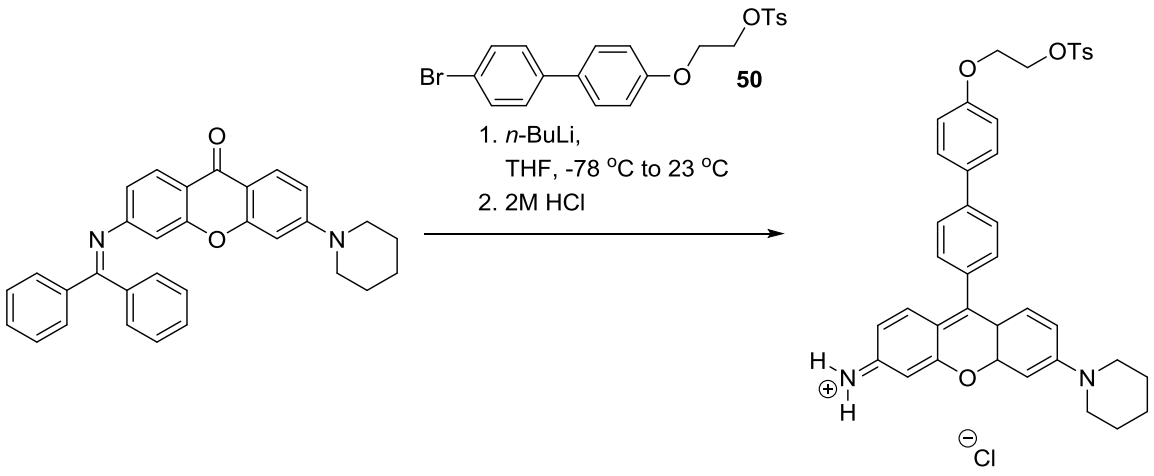

44 **53**

Rosamine 53. To a solution of **50** (0.40 g, 0.89 mmol) in THF (10 mL) at -78 °C was added *n*-BuLi (2.5M in hexanes, 0.35 mL, 0.89 mmol), dropwise over 5 minutes. The

resulting solution was stirred for 30 minutes, after which a cooled solution of **44** (0.10 g, 0.22 mmol) in THF (10 mL) was added dropwise over 5 minutes. The reaction mixture was slowly allowed to warm to room temperature over 16 h, after which 2.0 M HCl (2 mL) was added dropwise, during which the color changed from cloudy yellow to red-purple upon complete addition of the acid. The resulting solution was then stirred for 30 minutes at room temperature. The solution was diluted with CH_2Cl_2 (100 mL), washed with water (2 x 10 mL), and dried over sodium sulfate and concentrated *in vacuo*. The crude mixture was purified by flash column chromatography (silica gel, 2% to 10% MeOH-CH_2Cl_2) to afford purple solid **53** (87 mg, ca. 54% yield) as an inseparable 2:1 mixture of **53** to tosylate impurity (based on ^{1}H NMR analysis). **53:** R_f = 0.29 (silica gel, MeOH:DCM 1:9); ^{1}H NMR (600 MHz, $CDCl_3$) δ 8.30 (s, 2H), 7.87 (d, *J* = 7.8 Hz, 1H, CHx2 on $^-$OTs), 7.83 (d, *J* = 7.8 Hz, 2H), 7.69 (d, *J* = 7.8 Hz, 2H), 7.56 (d, *J* = 8.1 Hz, 2H), 7.36 (d, *J* = 7.8 Hz, 2H), 7.32 – 7.27 (m, 2H and 1H, CHx2 on $^-$OTs), 7.16 – 7.12 (m, 3H), 7.10 (d, *J* = 7.8 Hz, 1H), 6.91 (d, *J* = 8.4 Hz, 2H), 6.75 (s, 1H), 4.40 (t, *J* = 4.6 Hz, 2H), 4.22 (t, *J* = 4.5 Hz, 2H), 3.60 (s, 4H), 2.45 (s, 3H), 2.27 (s, 1.5H, CH_3 on $^-$OTs), 1.71 (d, *J* = 23.5 Hz, 6H) ppm; ^{13}C NMR (150 MHz, $CDCl_3$) δ 160.7, 158.3, 158.3, 157.6, 156.4, 155.7, 145.0, 143.6 (2C on $^-$OTs), 142.5, 139.0 (2C on $^-$OTs), 132.8, 132.7, 131.8, 131.5, 130.2 (2C on $^-$OTs), 130.1, 129.9, 128.5, 128.3, 128.0, 126.9, 126.1 (2C on $^-$OTs), 118.9, 115.1, 114.2, 113.6, 112.5, 98.9, 97.6, 68.1, 65.6, 48.7, 25.7, 24.1, 21.7, 21.3 (C on $^-$OTs) ppm; HRMS (ESI-QTOF) calcd for $C_{39}H_{37}N_2O_5S$ [*M* - Cl]$^+$ 645.2418, found 645.2417.

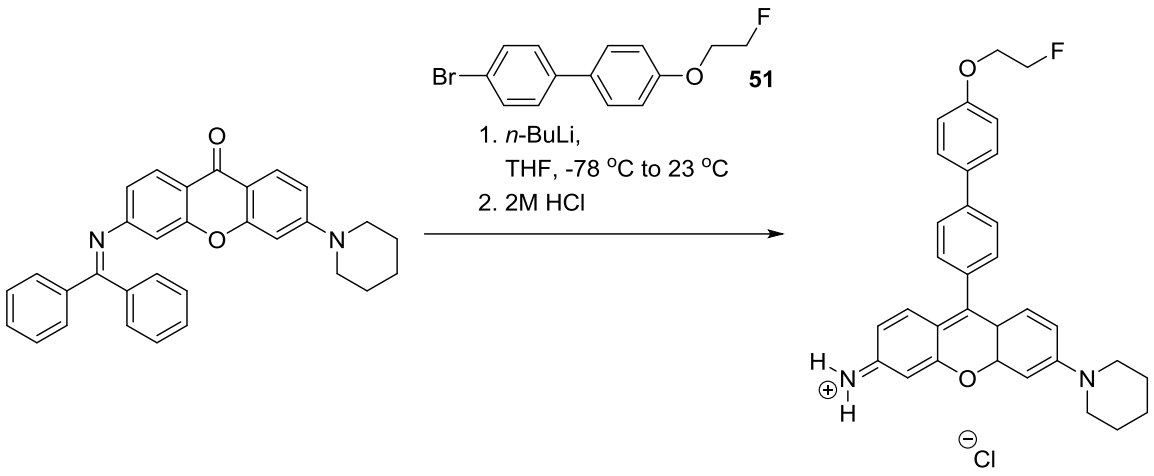

Rosamine 54. To a solution of **51** (0.26 g, 0.89 mmol) in THF (10 mL) at -78 ºC was added *n*-BuLi (2.5M in hexanes, 0.35 mL, 0.89 mmol), dropwise over 5 minutes. The resulting solution was stirred for 30 minutes, after which a cooled solution of **44** (0.10 g, 0.22 mmol) in THF (5 mL) was added dropwise over 5 minutes. The reaction mixture was slowly allowed to warm to room temperature over 16 h, after which 2.0 M HCl (2 mL) was added dropwise, during which the color changed from cloudy yellow to red-purple upon complete addition of the acid. The resulting solution was then stirred for 30 minutes at room temperature. The solution was diluted with CH_2Cl_2 (100 mL), washed with water (2 x 10 mL), brine (10 mL), dried over sodium sulfate and concentrated *in vacuo*. The crude mixture was purified by flash column chromatography (silica gel, 2% to 10% MeOH-CH_2Cl_2) to afford **54** (94 mg, 82% yield) as a purple solid. **54:** R_f = 0.12 (silica gel, MeOH: CH_2Cl_2 1:9); ^{1}H NMR (600 MHz, CD_3OD) δ 7.88 (d, *J* = 7.5 Hz, 2H), 7.71 (d, *J* = 7.8 Hz, 2H), 7.50 (d, *J* = 7.5 Hz, 2H), 7.44 (d, *J* = 9.5 Hz, 1H), 7.39 (d, *J* = 9.0 Hz, 1H), 7.21 (d, *J* = 9.2 Hz, 1H), 7.10 (d, *J* = 8.8 Hz, 3H), 6.87 (d, *J* = 9.2 Hz, 1H), 6.82 (s, 1H), 4.77 (d, *J* =

45.3 Hz, 2H), 4.30 (d, J = 28.8 Hz, 2H), 3.76 (s, 4H), 1.84 – 1.70 (m, 6H) ppm; ^{13}C NMR (150 MHz, CD_3OD) δ 161.3, 160.4, 160.0, 159.7, 159.2, 158.0, 144.1, 133.8, 133.6, 133.2, 131.6, 131.5, 129.3, 127.9, 117.9, 116.3, 115.9, 114.9, 114.4, 98.7, 98.2, 82.6, 82.6, 68.8, 68.7, 49.9, 27.1, 25.3 ppm; HRMS (ESI-QTOF) calcd for $C_{32}H_{30}FN_2O_2$ [M - Cl]$^+$ 493.2291, found 493.2290.

3.5. References

1. (a) de Silva, A. P.; Gunaratne, H. Q. N.; Gunnlaugsson, T.; Huxley, A. J. M.; McCoy, C. P.; Rademacher, J. T.; Rice, T. E., *Chem. Rev.* **1997,** *97*, 1515-1566. (b) Tsien, R. Y.; Miyawaki, A., *Science* **1998,** *280*, 1954-1955. (c) Crivat, G.; Taraska, J. W., *Trends Biotechnol.* **2012,** *30*, 8-16. (d) Jensen, E. C., *Anat. Rec.* **2013,** *296*, 1-8.

2. (a) Zhang, J.; Campbell, R. E.; Ting, A. Y.; Tsien, R. Y., *Nat. Rev. Mol. Cell Biol.* **2002,** *3*, 906-918. (b) Fernandez-Suarez, M.; Ting, A. Y., *Nat. Rev. Mol. Cell Biol.* **2008,** *9*, 929-943. (c) Zhang, G.; Wu, G.; Zhu, T.; Kurtan, T.; Mandi, A.; Jiao, J.; Li, J.; Qi, X.; Gu, Q.; Li, D., *J. Nat. Prod.* **2013,** *76*, 1946-1957.

3. Dean, K. M.; Palmer, A. E., *Nat. Chem. Biol.* **2014,** *10*, 512-523.

4. Lee, J.-S.; Vendrell, M.; Chang, Y.-T., *Curr. Opin. Chem. Biol.* **2011,** *15*, 760-767.

5. Lee, J.-S.; Kim, Y. K.; Vendrell, M.; Chang, Y.-T., *Mol. BioSyst.* **2009,** *5*, 411-421.

6. (a) Vendrell, M.; Zhai, D.; Er, J. C.; Chang, Y.-T., *Chem. Rev.* **2012,** *112*, 4391-4420. (b) Yun, S.-W.; Kang, N.-Y.; Park, S.-J.; Ha, H.-H.; Kim, Y. K.; Lee, J.-S.; Chang, Y.-T., *Acc. Chem. Res.* **2014,** *47*, 1277-1286.

7. Vendrell, M.; Ha, H. H.; Lee, S. C.; Chang, Y. T. In *Solid-Phase Organic Synthesis: Concepts, Strategies, And Applications*. Toy, P. H., Lam, Y., Eds.; John Wiley & Sons: New Jersey, 2012; p 536.

8. Wainwright, M. In *Photosensitizers in Biomedicine*. John Wiley & Sons: New Jersey, 2009; pp 81-108.

9. Kobayashi, H.; Ogawa, M.; Alford, R.; Choyke, P. L.; Urano, Y., *Chem. Rev.* **2010,** *110*, 2620-2640.

10. (a) Kim, H. N.; Lee, M. H.; Kim, H. J.; Kim, J. S.; Yoon, J., *Chem. Soc. Rev.* **2008,** *37*, 1465-1472. (b) Beija, M.; Afonso, C. A. M.; Martinho, J. M. G., *Chem. Soc. Rev.* **2009,** *38*, 2410-2433.

11. Sun, R.; Liu, X.-D.; Xun, Z.; Lu, J.-M.; Xu, Y.-J.; Ge, J.-F., *Sens. Actuators, B* **2014,** *201*, 426-432.

12. Im, C.-N.; Kang, N.-Y.; Ha, H.-H.; Bi, X.; Lee, J. J.; Park, S.-J.; Lee, S. Y.; Vendrell, M.; Kim, Y. K.; Lee, J.-S.; Li, J.; Ahn, Y.-H.; Feng, B.; Ng, H.-H.; Yun, S.-W.; Chang, Y.-T., *Angew. Chem., Int. Ed.* **2010,** *49*, 7497-500.

13. Lim, S. H.; Wu, L.; Burgess, K.; Kiew, L. V.; Chung, L. Y.; Lee, H. B., *PLoS One* **2014,** *9*, e82934.

14. Vendrell, M.; Park, S.-J.; Chandran, Y.; Lee, C.-L. K.; Ha, H.-H.; Kang, N.-Y.; Yun, S.-W.; Chang, Y.-T., *Stem Cell Res.* **2012,** *9*, 185-191.

15. Haque, M. M.; Kim, D.; Yu, Y. H.; Lim, S.; Kim, D. J.; Chang, Y.-T.; Ha, H.-H.; Kim, Y. K., *Amyloid* **2014**, 1-7.

16. Ahn, Y.-H.; Lee, J.-S.; Chang, Y.-T., *J. Am. Chem. Soc.* **2007,** *129*, 4510-4511.

17. Heumann, K.; Rey, H., *Ber. Dtsch. Chem. Ges.* **1889,** *22*, 3001-3004.

18. Jiao, G.-S.; Castro, J. C.; Thoresen, L. H.; Burgess, K., *Org. Lett.* **2003,** *5*, 3675-3677.

19. Detty, M. R.; Prasad, P. N.; Donnelly, D. J.; Ohulchanskyy, T.; Gibson, S. L.; Hilf, R., *Bioorg. Med. Chem.* **2004,** *12*, 2537-2544.

20. (a) Calitree, B.; Donnelly, D. J.; Holt, J. J.; Gannon, M. K.; Nygren, C. L.; Sukumaran, D. K.; Autschbach, J.; Detty, M. R., *Organometallics* **2007,** *26*, 6248-6257. (b) Gannon, M. K., II; Detty, M. R., *J. Org. Chem.* **2007,** *72*, 2647-2650.

21. Wu, L.; Burgess, K., *J. Org. Chem.* **2008,** *73*, 8711-8718.

22. Calitree, B. D.; Detty, M. R., *Synlett* **2010,** 89-92.

23. Nath, S.; Spencer, V. A.; Han, J.; Chang, H.; Zhang, K.; Fontenay, G. V.; Anderson, C.; Hyman, J. M.; Nilsen-Hamilton, M.; Chang, Y.-T.; Parvin, B., *PLoS One* **2012,** *7*, e28802.

24. (a) Berg, G.; Eberl, L.; Hartmann, A., *Environ. Microbiol.* **2005,** *7*, 1673-1685. (b) Opelt, K.; Berg, C.; Berg, G., *FEMS Microbiol. Ecol.* **2007,** *61*, 38-53.

25. Kraus, G. A.; Guney, T.; Kempema, A.; Hyman, J. M.; Parvin, B., *Tetrahedron Lett.* **2014,** *55*, 1549-1551.

26. Shieh, P.; Hangauer, M. J.; Bertozzi, C. R., *J. Am. Chem. Soc.* **2012,** *134*, 17428-17431.

27. Stacko, P.; Sebej, P.; Veetil, A. T.; Klan, P., *Org. Lett.* **2012,** *14*, 4918-4921.

28. Wolfe, J. P.; Ahman, J.; Sadighi, J. P.; Singer, R. A.; Buchwald, S. L., *Tetrahedron Lett.* **1997,** *38*, 6367-6370.

29. Musachio, J. L.; Shah, J.; Pike, V. W., *J. Labelled Compd. Radiopharm.* **2005,** *48*, 735-747.

30. Parenty, A. D. C.; Smith, L. V.; Pickering, A. L.; Long, D.-L.; Cronin, L., *J. Org. Chem.* **2004,** *69*, 5934-5946.

CHAPTER 4.

GENERAL CONCLUSIONS

In the first chapter of this dissertation the total synthesis of (±)-paracaseolide A was described. The naturally-occurring meroterpenoid was constructed *via* a series of synthetic manipulations featuring the introduction of phenylsulfenyl groups to the symmetrical bis-lactone moiety. The resultant intermediate was then desymmetrized *via* the controlled single-sulfide oxidation and elimination, followed by the key tandem 1,4-addition/aldol reaction to introduce the alkyl and alkenyl subunits of the natural scaffold. Subsequently, the final sulfoxide elimination provided (±)-paracaseolide A in 8 steps and 6.6% overall yield. Upon comparison of this work against the other methods reported in the literature, our method offers strong potential for the diverse functionalization of analogues to enhance the already displayed anti-cancer activity.

The second chapter outlined the first inverse electron-demand Diels–Alder (IEDDA) reaction between 3-chloroindoles and methyl coumalate to form carbazole alkaloids. The novel methodology delivered natural and synthetic carbazole scaffolds through the one-pot IEDDA/decarboxylation/aromatization cascade in a regioselective manner in up to 90% yield. Investigation of the scope and limitations of the present methodology revealed that the electron-rich indoles provided high yields of the corresponding carbazoles, whereas highly electron poor indoles did not proceed though the reaction cascade as expected.

The final chapter disclosed the details of an efficient synthesis of rosamine probes that possess a primary amine group for applications in cellular imaging. The synthetic methodology took advantage of the benzophenone imine moiety which was substituted on the xanthone scaffold during the organometallic addition. Ensuing acidic workup not only unmasked the primary amine group but also facilitated the formation of highly conjugated rosamines *via* the final dehydration of the intermediate. Overall, the newly developed method rapidly furnished fluorescent rosamines that also have radiolabelling capability upon treatment of either [^{18}F]2-fluoroethyl arylsulfonates or a fluorine-18 nucleophile.